Understanding Disposition of Efavirenz and Application in Solid Drug Nanoparticle Development

Thesis submitted in accordance with requirements of the University of Liverpool for the degree of Doctor of Philosophy

By Paul Curley

September 2015

This thesis is the result of my own work. The material contained within the thesis has not been presented, either wholly or in part, for any other degree or qualification.

Paul Curley

This research was carried out in the

Department of Molecular and Clinical Pharmacology

University of Liverpool, UK

Table of Contents

Acknowledgements

Firstly, I would like to thank Professor Andrew Owen for his guidance and supervision. Your inspired and often inventive motivational prompts have proved effective and entertaining. I would also like to thank you for your continued faith, for giving me the opportunity of not only my PhD but also my first post doc. I would also like to thank Professor David Back and Professor Saye Khoo. Your advice and support have been invaluable to the completion of my PhD.

I would like to thank Dr Marco Siccardi for your help and guidance, particularly your help with bio-analytical method development and PBPK modelling. Perhaps most significantly I would like to thank you for hosting games nights and providing a modern equivalent to the 1980s games of Dr Muschio!

My thanks go to Dr Neill (2 Ts in Liptrott) Liptrott. Your continued friendship and support has helped me through not only my scientific life but also my personal life. Having someone to talk to about the pressures of a PhD and fatherhood has been incredibly important to me. You of course give me hope for the future. If you can get to the stage in your career and barely be able to operate a mobile phone or PC, I might just be ok.

Where does one begin with Dr James (Sir Bantzalot) Hobson? Your window side chats setting the world to writes are sorely missed. My thanks for your introduction to such things as juxtaposed learning, evolution of the Hobsonese language and of course Apple based products. Many thanks for your friendship and being an incredibly good sport when I decided to play the occasional practical joke!

Dr Darren (have you heard of raltegravir?) Moss, you have been invaluable both for your scientific guidance but also your friendship. Many thanks for hosting games nights on your cutting edge high def projector coupled with a ZX Spectrum, demonstrating the negative impact of a caffeine overdose and generally being the most disruptive force known to man.

My thanks to everyone in H Block and the BAF Lee, Alessandro, Laura D, Henry, Sara, Helen, Justin (the life saver), Laura L, Alieu, Deirdre, Sujan, Niyi, Chris (Neill v2.0), Rajith (Hershey addict!!!), Christina, Louise, Rohan, Megan, Owain, Ana, Sharon, Rana and Josh. Thank you all for your assistance and sharing your scientific life with me.

I would like to thank my Mum, Dad and Sister for their love and support not only over the course of my PhD but throughout my life.

Finally I would like to thank my amazing fiancée, Adele. To say I would not be here without you is an understatement. You have been there when things looked bleakest and helped me find the strength to carry on. Thank you seems insufficient for everything you have done for me over the past 11 years. Having said that, thank you for all your love and support. I only hope one day I can repay you.

I would like to dedicate this thesis to my daughter, Hannah. All the work presented here will hopefully give you a better start in life. All my love, Dad.

Abbreviations

5-HT2A	5-hydroxytryptamine 2A
Å	Angstrom
ACN	Acetonitrile
ADR	Adverse Drug Reactions
ATP	Adenosine Triphosphate
AUC	Area Under the Curve
BBB	Blood Brain Barrier
BCRP	Breast Cancer Resistance Protein
BCS	Biopharmaceutics Classification System
CAR	Constitutive Androstane Receptor
CAR	Cellular Accumulation Ratio
CCR5	C-C Chemokine Receptor 5
Cl	Clearence
CM	Cisterna Magna
C_{max}	Maximum Plasma Concentration
C_{min}	Minimum Plasma Concentration
CNS	Central Nervous System
COX-2	Cyclo-oxygenase 2
CSF	Cerebrospinal Fluid
CTL	Cytotoxic T-lymphocytes
CXCR4	C-X-C Chemokine Receptor 4
CYP	Cytochrome P450
dH_2O	Distilled Water

DiD	1,1’-dioctadecyl-3,3,3’,3’-tetramethylindodi- carbocyanine perchlorate
DNA	Deoxyribonucleic Acid
dNTP	Deoxynucleotide triphosphates
DPM	Disintergrations per Minute
env	Envelope Glycoprotein
EPM	Elevated Plus Maze
ER	Endoplasmic Reticulum
Fa	Fraction Absorbed
FBS	Fetal Bovine Serum
FDA	Food and Drug Administration
fu	Fraction Unbound
FRET	Fluorescence Resonance Energy Transfer
GABA	Gamma Aminobutyric Acid
GI	Gastrointestinal
gp	Glycoprotein
GTP	Guanosine-5'-triphosphate
HAND	HIV-Associated Neurocognitive Disorder
HBSS	Hanks Balanced Salt Solution
HIV	Human Immunodeficiency Virus
HSR	Hypersensitivity Reactions
IC_{50}	Concentration Producing 50% Inhibition
IN	Integrase
IQR	Inter Quartile Range
IS	Internal Standard
Ka	Absorption Constant

kg	Kilogram
Ki	Inhibition Constant
Km	Michaelis Constant
LA	Long-acting
LC-MS/MS	Liquid Chromatography Tandem Mass Spectrometer
Log D	Oil/water distribution
LogP	Octanol/Water Partition Coefficient at pH 7.4
LV	Left Ventricle
MeOH	Methanol
mg	Milligram
ml	Millilitre
mRNA	Messenger RNA
MRP	Multidrug Resistance Proteins
NCE	New Chemical Entities
ng	Nanogram
NNRTI	Non-Nucleoside Reverse Transcriptase Inhibitors
NRTI	Nucleoside Reverse Transcriptase Inhibitors
OAT	Organic Anion Transporter
OATP	Organic Anion-Transporting Polypeptide
ºC	Degrees Centigrade
OCT	Organic Cation Transporter
OH efavirenz	Hydroxylated Efavirenz
P-gp	P-glycoprotein
PBPK	Physiologically Based Pharmacokinetic
PBS	Phosphate Buffered Saline

PCR	Polymerase Chain Reaction
PI	Protease Inhibitor
popPK	Population Pharmacokinetics
PR	Protease
QC	Quality Control
qPCR	Quantitative Polymerase Chain Reaction
QSAR	Quantitative Structure–Activity Relationship
R	Blood to Plasma Ratio
RED	Rapid Equilibrium Dialysis
RFU	Relative Fluorescence Units
RNA	Ribonucleic Acid
RT	Reverse Transcriptase
SAS	Subarachnoid Space
SC	Subcutaneous
SDN	Solid Drug Nanoparticle
SLCO	Solute Carrier Organic Anion Transporter
SNP	Single Nucleotide Polymorphism
SRM	Selected Reaction Monitoring
$t_{1/2}$	Plasma Half Life
TAR	Transactivation Responsive Element
TAT	Transactivator of Transcription
TFV	Third and Fourth Ventricle
T_{max}	Time to Reach Maximum Plasma Concentration
TPSA	Van der Waals Polar Surface Area
tRNA	Transfer RNA

UNAIDS	United Nations Programme on HIV/AIDS
vasbase	Van der Waals Surface Area of the Basic Atoms
Vmax	Maximum Velocity
vs	Versus
Vss	Volume of Distribution
W/V	Weight per Volume
WHO	World Health Organisation
µCi	Microcurie(s)
µg	Microgram(s)
µl	Microlitre(s)
µM	Micromolar

Publications

Peer Reviewed Publications

Ana Alfirevic, Jill Durocher, Anisa Elati, Wilfrido León, David Dickens, Steffen Rädisch, Helen Box, Marco Siccardi, **Paul Curley**, George Xinarianos, Arjun Ardeshana, Andrew Owen, J Eunice Zhang, Munir Pirmohamed, Zarko Alfirevic, Andrew Weeks and Beverly Winikoff. **Misoprostol-induced fever and genetic polymorphisms in drug transporters SLCO1B1 and ABCC4 in women of Latin American and European ancestry.** Pharmacogenomics, June 30th 2015, volume 16, issue 9, pages 919-28.

Moss, D.M, **Curley, P**, Shone, A, Siccardi, M and Owen, A. **A multi-system investigation of raltegravir association with intestinal tissue: implications for PreP and eradication**. Journal of Antimicrobial Chemotherapy, August 11th 2014, volume 69, issue 12, pages 3275-81.

Moss, D. M, Liptrott, N. J, **Curley, P**, Siccardi, M, Back, D. J and Owen, A. **Rilpivirine inhibits drug transporters ABCB1, SLC22A1 and SLC22A2 *in vitro***. Antimicrobial Agents and Chemotherapy, November 2013. Volume 57, issue 11, pages 5612-8.

Liptrott, N. J, Curley, P, Moss, D, Back, D. J, Khoo, S. H and Owen, A. **Interactions between Tenofovir and Nevirapine in CD4+ T cells and Monocyte Derived Macrophages restrict their intracellular accumulation**. Journal of Antimicrobial Chemotherapy, November 2013. Volume 68, issue 11, pages 2545-9.

McDonald, T. O, Giardiello, M, Martin, P, Siccardi, M, Liptrott, N. J, Smith, D, Roberts, P, **Curley, P**, Schipani, A, Khoo, S. H, Long, J, Foster, A. J, Rannard, S. P and Owen, A. **Antiretroviral Solid Drug Nanoparticles with Enhanced Oral Bioavailability: Production, Characterization, and *In Vitro– In Vivo* Correlation**. Advanced Healthcare Materials, September 1st 2013, volume 3, issue 3, pages 400-11.

Siccardi, M Rajoli, R. K. R, **Curley, P**, Olagunju, A, Moss, D and Owen, A. **Physiologically based pharmacokinetic models for the optimization of antiretroviral therapy: recent progress and future perspective**. Future Virology, September 2013. Volume 8, issue 9, pages 871-890.

Conference Presentations:

Highlights of research at the University of Liverpool and activity of the British Society for Nanomedicine (7th CLINAM conference and exhibition, Basel, Switzerland) **Paul Curley**, Neill Liptrott, Lee Tatham, Marco Siccardi, and Andrew Owen

The *in vivo* effects of solid drug nanoparticle and conventional efavirenz on anxiogenesis in rodents (21st Conference on Retroviruses and Opportunistic Infections, Boston, USA) **Paul Curley**, Marco Giardiello, Neill Liptrott, Phil Martin, Tom McDonald, Marco Siccardi, Juliet McAdams, Steve Rannard, Tim Kirkham and Andrew Owen

Multi-system investigation of the mechanisms for raltegravir association with intestinal tissue after oral administration (21st Conference on Retroviruses and Opportunistic Infections, Boston, USA) Darren Moss, **Paul Curley**, Alison Shone, Marco Siccardi and Andrew Owen

Investigation of the potential interactions of efavirenz and the GABAa receptor utilising an *in silico* approach (Manchester Life Sciences PhD Conference, Manchester, UK) **Paul Curley**, Alessandro Schippani, Marco Siccardi and Andrew Owen

Utilising *In Vitro-In Vivo* extrapolation to investigate efavirenz penetration into the central nervous system (14th International Workshop on Clinical Pharmacology of HIV Therapy, Amsterdam, NL) **Paul Curley**, Philip Martin, Neill Liptrott, David Back, Andrew Owen and Marco Siccardi

Prediction of Etravirine Pharmacogenetics using a Physiologically Based Pharmacokinetic approach (20th Conference on Retroviruses and Opportunistic Infections, Atlanta, USA) Marco Siccardi, Adeniyi Olagunju, **Paul Curley**, James Hobson, Saye Khoo, David Back, Andrew Owen

Enhanced Pharmacological Properties of Efavirenz Formulated as Solid Drug Nanoparticles (20th Conference on Retroviruses and Opportunistic Infections, Atlanta, USA) Philip Martin, NJ Liptrott, T McDonald, M Giardiello, P Roberts, **P Curley**, D Smith, M Siccardi, S Rannard, and A Owen

Investigation of the potential interactions of efavirenz with the GABAa receptor (British Pharmacology Society Winter meeting, London, UK) **P A Curley**, A Schipani, D Egan, M Siccardi, C Wyen, G Fätkenheuer and A Owen

An Investigation of the expression of cytochrome P450 3A7 and cytochrome P450 3A4 during stem cell differentiation for use as markers of emerging hepatic phenotype (British Pharmacology Society Winter meeting, London, UK) **Paul Curley**, Lorna Kelly, Rowena Shaw, Neil R Kitteringham, Rosalind E Jenkins, Jane E Alder, Cliff Rowe, Laura Randle, Chris E P Goldring and B Kevin Park

Oral Presentations:

Utilising *In Vitro-In Vivo* extrapolation to investigate efavirenz penetration into the central nervous system (14th International Workshop on Clinical Pharmacology of HIV Therapy, Amsterdam, NL)

Assessment of aqueous and nanoparticle antiretroviral drug transport in the blood brain barrier (2nd UK & Ireland Early Career Blood-Brain Barrier Symposium, Liverpool, UK)

Book Chapters

Liptrott, N.J., **Curley, P**., Tatham, L.T. and Owen, A. **"Opportunities and Challenges in Nanotechnology-enabled antiretroviral Drug Delivery"**, 2nd Edition, Handbook of Immunological Properties of Engineered Nanomaterials

Andrew Owen And **Paul Curley**, **"Species Similarities and Differences in Pharmacokinetics and Distribution of Antiretroviral Drugs"**, 1st edition, Humanized Mice for HIV Research

Abstract

Efavirenz displays many desirable pharmacokinetic properties such as a long half-life allowing once daily dosing and potency against HIV. Despite these favourable properties efavirenz-containing therapy is associated with the development of central nervous system (CNS) toxicities. Current investigations indicate that high plasma concentrations of efavirenz play a putative role in the development of CNS side effects, but there is a current paucity of data relating to the underlying mechanisms of toxicity. Various nanotechnologies have been explored in attempts to mitigate some of the limitations with efavirenz. While there has been progress in increasing the bioavailability of efavirenz there has been no attempt to assess the impact of increased exposure to efavirenz on CNS toxicity. The body of work presented in this thesis aimed firstly to investigate the underlying mechanism of efavirenz CNS toxicity and secondly to assess uptake and CNS toxicity of efavirenz and a novel solid drug nanoformulation (SDN) of efavirenz.

The work presented in this thesis utilised a variety of *in vitro*, *in vivo* and *in silico* methodologies. Chapter 2 utilised allelic discrimination polymerase chain reaction in order to investigate the association of single nucleotide polymorphism (SNPs) in the gamma aminobutyric acid receptor with early treatment discontinuation of efavirenz. In order to assess the effects of SDN efavirenz on the occurrence of CNS toxicities, an *in vivo* model of anxiety (elevated plus maze) was employed (chapter 3). Chapter 4 detailed the development of a robust and sensitive liquid chromatography tandem mass spectrometer assay for the detection of efavirenz in multiple matrices. The uptake of efavirenz and SDN efavirenz in the CNS was investigated utilising cellular uptake and inhibition studies (chapter 5). Physiologically based pharmacokinetic (PBPK) simulations were used to investigate the distribution of efavirenz in plasma, cerebrospinal fluid (CSF) and brain tissue (chapter 6).

Despite an initial trend with Rs211014 and Rs6556547 (univariate analysis) of the training cohort, these SNPs were not found to be significant in the multivariate analysis or in either analysis of the test cohort. Following multiple doses rats treated with efavirenz, but not SDN efavirenz, exhibited anxiety-like behaviour in the EPM. The profile of changes indicated some clear behavioural effects that are likely to be linked to drug-related CNS effects. In particular, a tendency of efavirenz to increase time spent on the central platform may be indicative of anxiogenesis. Cellular accumulation of efavirenz was reduced significantly by montelukast and amantadine, with the reduction in accumulation by prazosin bordering on significance (indicating efavirenz may be a substrate for OCT1 and an SLCO transporter). Additionally, cellular accumulation of SDN efavirenz particles was reduced by dynasore, indicating dynamin-mediated uptake. PBPK simulations predicted efavirenz accumulation in brain tissue, with a tissue to plasma ratio 15.8.

The natural occurrence of conditions such as depression involves a complex interplay of factors influencing neurotransmission. This makes identifying single predictors of efavirenz CNS toxicity more difficult. The data presented in this thesis may be built upon to understand the mechanisms governing efavirenz disposition in the CNS and factors influencing the occurrence of CNS toxicity.

Chapter 1

General Introduction

Contents

1.1 Human Immunodeficiency Virus

The human immunodeficiency virus (HIV) pandemic has been a global issue for over 30 years; at the end of 2013, 35 million people were estimated (by the World Health Organisation [WHO]) to be HIV positive worldwide with approximately 2.1 million new infections and 1.5 million deaths reported (1). Although organisations such as the United Nations Programme on HIV/AIDS (UNAIDS) show a declining trend in HIV infection (50% decline in the number of HIV infections in 26 countries between 2002 and 2012), HIV still represents a significant global health burden (2).

1.2 Replication Cycle of HIV

HIV infection is characterised by infection and subsequent depletion of $CD4^+$ T cells (3). The $CD4^+$ T cells play a crucial role in the adaptive immune response to exogenous pathogens (4). Antigen presenting cells, such as dendritic cells, interact with naïve $CD4^+$ T cells leading to cellular proliferation and differentiation into $CD4^+$ subsets (5). The differentiated effector cells are involved in multiple aspects of immune response, including elimination of extracellular and intracellular pathogens, mediation of humoral immune response, recognition of self and foreign antigens (5). The loss of $CD4^+$ T cells has a dramatic impact on the host immune system, rendering the host vulnerable to opportunistic infections, such as tuberculosis and other bacterial and fungal infections (6). The following sections will discuss the progression of viral infection including attachment, fusion, reverse transcription, integration,

transcription, ribonucleic acid (RNA) export, assembly and finally release of mature virions.

1.2.1 Viral Attachment

Following the introduction of HIV to the host system, the first stage of the viral lifecycle is attachment of the virion to the host cell (Figure 1). Most frequently, HIV recognises and binds to the CD4 glycoprotein (gp) and co-receptors C-C chemokine receptor 5 (CCR5) or C-X-C chemokine receptor 4 (CXCR4) via a trimeric envelope glycoprotein (env), with each subunit formed from an exterior (gp120) and a transmembrane (gp41) region (7). However, CD4 is not the only means of viral attachment. CD4 independent attachment has been demonstrated in monocyte-derived dendritic cells via gp120 binding to a number of C-type lectin receptors (8).

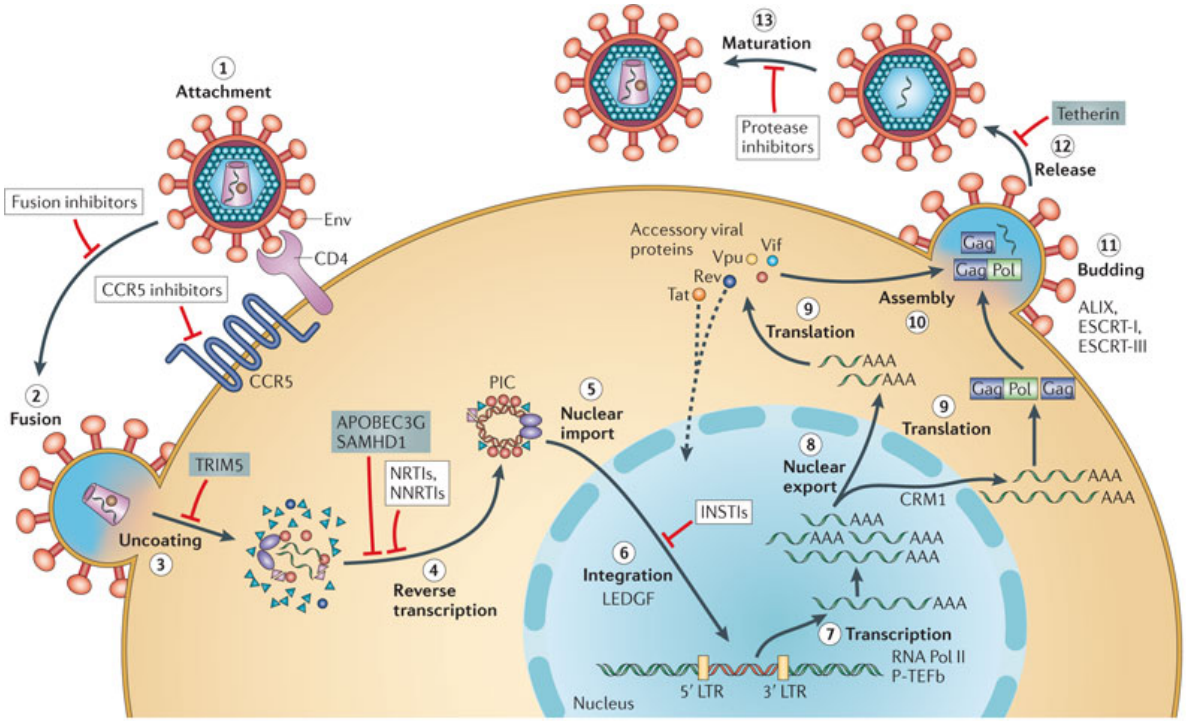

Figure 1. The life cycle HIV detailing viral attachment (1), fusion (2), uncoating (3), reverse transcription (4), nuclear import (5), integration (6), transcription (7), nuclear export (8), translation (9), assembly (10), budding (11), release (12) and maturation (13). Also indicated are the sites of action of nucleoside reverse transcriptase inhibitors (NRTI), non-nucleoside reverse transcriptase inhibitors (NNRTI), protease inhibitors, entry inhibitors (CCR5 and fusion inhibitors) and integrase strand transfer inhibitors (INSTI's). Figure source Engleman and Cherepanov 2012 (9).

1.2.2 Fusion

Following attachment, the virus enters the host cell via membrane fusion. Binding of gp120 to CD4 and co-receptor (either CCR5 or CXCR4 are engaged, dependent on viral tropism) induces a series of conformational changes in the env protein leading to the exposure of the core gp41 N-terminal fusion peptide (10). The resulting interaction induces fusion between the viral capsid cell membrane followed by infection of the host cell (7, 11).

Following viral entry to the host cell the process of uncoating occurs to release the contents of the viral capsid into the cellular cytoplasm (12). The core of the HIV virion consists of the viral genome and associated proteins, including gag (proteolytically cleaved to produce matrix, capsid, nucleocapsid and p6 proteins), pol (proteolytically cleaved to produce the reverse transcriptase [RT], integrase [IN] and protease [PR]) and env contained within a conical capsid (12, 13).

1.2.3 Reverse transcription

As a retrovirus, the genome of HIV is RNA and requires transcription to double-stranded deoxyribonucleic acid (DNA) prior to integration into the host genome. DNA is produced via reverse transcription, accomplished by the enzyme RT (14). Initiation of reverse transcription is achieved by annealing of host transfer RNA (tRNA) to viral RNA. This complex is recognised by RT and reverse transcription may commence via elongation of the 3′ end of the tRNA/RNA complex. As the DNA is transcribed to form a RNA/DNA hybrid, the RNA is

degraded via RNase activity of RT producing newly synthesised DNA (15). The production of DNA via RT is highly error prone due to the lack of exonucleolytic proofreading, leading to a high error rate of 1/1700 and in certain mutational hotspots 1/70 (16). This lack of fidelity can lead to the emergence of HIV strains capable of drug resistance and immune escape (17).

1.2.4 Integration

The next stage in the viral life cycle is integration of the viral DNA with the host DNA. The newly synthesised viral DNA forms a stable complex with the IN enzyme that is transported to the nucleus. The DNA is then processed for integration. Two nucleotides are first removed from 3′ ends of the viral DNA. The free 3′ ends are now able to "attack" phosphodiester bonds in the host DNA, resulting in covalent linkage between the 3′ end of the viral DNA and the 5′ end of the host DNA. The remaining viral 5′ ends are repaired via host enzymes resulting in complete integration of the viral DNA (18).

1.2.5 Transcription

The transcription of new viral RNA is produced by partial subversion of host enzymes. Transcription is initiated by host RNA polymerase II but full transcription is not possible, resulting in short viral transcripts (19). To circumvent this limitation, HIV transcription is facilitated by transactivator of transcription (TAT). The binding of TAT to transactivation responsive element (TAR) and the recruitment of positive transcription elongation factor b lead to ~

100-fold increase in the production of viral RNA, primarily via enhancement of transcription elongation (13, 20, 21).

1.2.6 RNA Export

Transcription yields both spliced and unspliced messenger RNA (mRNA), resulting in more than 40 different splice products. Eukaryotic cells typically degrade unspliced and incompletely spliced mRNA in the nucleus (22, 23). Completely spliced mRNA (1.8kb mRNA coding for TAT, REV and Nef) is transported by endogenous transport mechanisms. Unspliced and incompletely spliced mRNA (9kb and 4kb mRNA coding for gag, pol and env) require the viral protein REV for transport to the cytoplasm (22). Bound REV is able to interact with chromosome region maintenance 1 (also known as exportin 1) in the presence of guanosine-5'-triphosphate (GTP), in the form of Ran GTPase (22, 23). The complex is transported to the cytoplasm, via nuclear pore complexes, where hydrolysis of GTP leads to instability of the complex and the release of viral mRNA to the cytoplasm where translation can occur. Rev is then transported back to the nucleus via importin β (22).

1.2.7 Assembly and Release

The process of assembly occurs at the plasma membrane (in the majority of cells), where key viral components (including the RNA genome, env, RT and PR) are packaged into immature virions (24). As with many viral processes, packaging relies on both viral proteins and the subversion of host systems. The

various processes involved in packaging (including creation of spherical viral particles, concentration of env and packaging of RNA) are mediated by Gag-Pro-Pol. Although Gag-Pro-Pol is able to assemble the virions, release is accomplished via host endosomal sorting complexes required for transport (25). Viral maturation begins simultaneously with release of the virions, beginning with proteolytic cleavage of Gag-Pro-Pol via PR. Maturation continues with the products of Gag-Pro-Pol rearranging to form mature viral particles (25).

1.3 Current Antiretroviral Therapy: Mechanisms of Action

Over the past 30 years there have been remarkable advances in HIV therapy. Treatment has evolved from simple monotherapy to a complex regimen comprised of multiple drugs from numerous classes. Currently, the US Food and Drug Administration (FDA) has approved 27 drugs for the treatment of HIV, which include 9 nucleoside/nucleotide reverse transcriptase inhibitors (NRTI), 5 non-nucleoside reverse transcriptase inhibitors (NNRTI), 9 protease inhibitors (PI), 1 fusion inhibitor, 1 chemokine receptor antagonist and 2 IN inhibitors (Figure 2) (26). As of 2013, of these 7 are recommended by the WHO for treatment of antiretroviral-naïve patients (Table 1) (27). As previously discussed, HIV is highly error prone (17), enabling the virus to quickly adapt to antiretroviral agents through acquisition and selection of resistance mutations via a similar general mechanism to that of cytotoxic T-lymphocytes (CTL) escape (17, 28). Resistance to monotherapy arises extremely quickly and so effective therapy requires at least three drugs in combination to simultaneous target multiple viral targets (29). Through prolonged viral suppression and increased

CD4+ T-cell counts, modern antiretroviral therapy has improved patient survival and transformed HIV into a manageable but chronic infection.

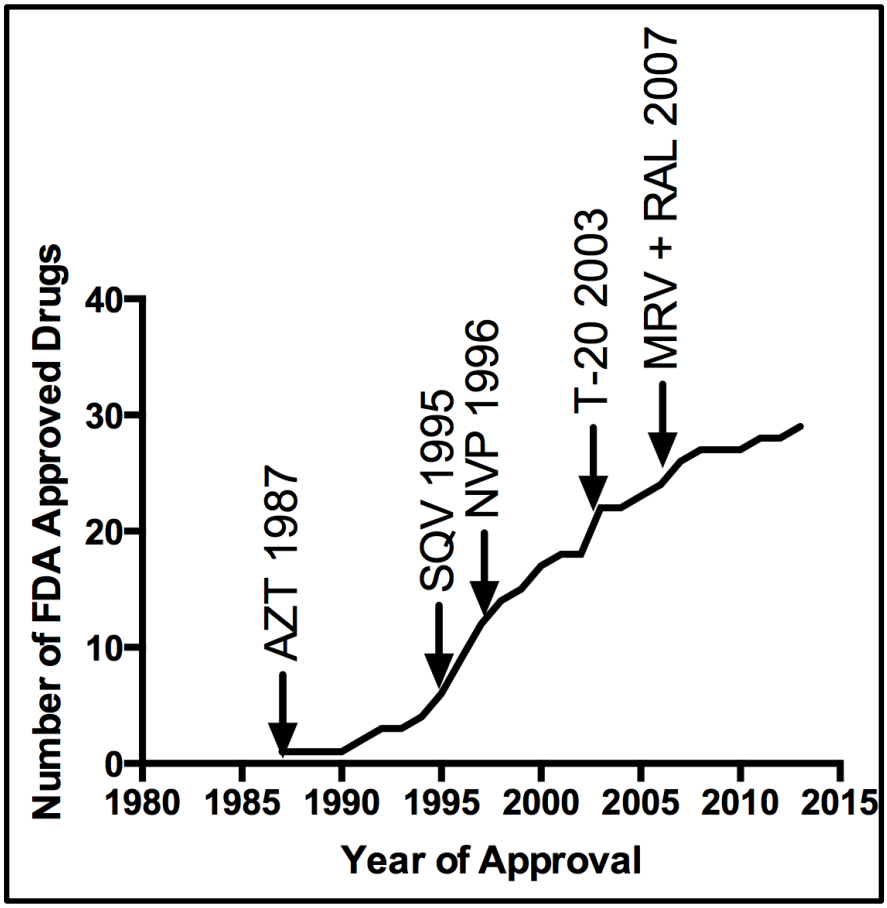

Figure 2. The graph above shows the number of FDA approved antiretrovirals and the year of approval. Also highlighted are the first in class antiretrovirals zidovudine (AZT NRTI), saquinavir (SQV PI), nevirapine (NNRTI NVP), enfuvirtide (entry inhibitor T-20) maraviroc (entry inhibitor MRV) and raltegravir (integrase inhibitor RAL). Data extracted from (26).

	NNRTI or boosted PI	NRTI Backbone
First Line Therapy	Efavirenz (NNRTI)	Tenofovir Emtricitabine
Alternative	Efavirenz (NNRTI)	Zidovudine Emtricitabine
	Nevirapine (NNRTI)	Zidovudine Emtricitabine
	Nevirapine (NNRTI)	Tenofovir Emtricitabine
Second Line Therapy	Atazanavir (PI) Ritonavir (PI)	Tenofovir Emtricitabine
Alternative	Lopinavir (PI) Ritonavir (PI)	Tenofovir Emtricitabine

Table 1. The table above shows the World Health Organisations current recommendations for antiretroviral therapy. First line therapy consists of a NNRTI supported by a NRTI backbone. When this option is unsuitable (due to viral rebound or patient toxicity), second line therapy consists of a PI (boosted by ritonavir) supported by a NRTI backbone (27).

1.3.1 Nucleoside Reverse Transcriptase Inhibitors

The enzyme RT catalyses a key step in the HIV life cycle. As shown in Figure 1, reverse transcriptase translates the viral genome from RNA to DNA. The NRTI class of antiretroviral drugs (e.g. zidovudine, tenofovir disoproxil fumarate and emtricitabine) are analogues of endogenous nucleosides with one significant difference (30). Endogenous nucleosides are incorporated into DNA via phosphodiester bonds. NRTIs are incorporated into the viral DNA however; they are incapable of binding to other nucleosides. NRTIs lack a hydroxyl group at the 3′ position, this is essential for the incorporation of further nucleosides (31).

The incorporation of an NRTI prevents further synthesis of the DNA chain, leading to non-functional DNA that cannot be incorporated into the host DNA.

1.3.2 Non-Nucleoside Reverse Transcriptase Inhibitors

NNRTI's act on the same viral target as NRTI's but the mechanism of action is significantly different. NNRTI's inhibit reverse transcriptase via allosteric modulation, acting via non-competitive inhibition. Binding of NNRTI's to a hydrophobic pocket (approximately 10Å from the active site) induces the side chains of tyrosine 181 and 188 in the active site of reverse transcriptase to invert orientation. This conformational change leads to a decrease in the binding affinity of endogenous nucleosides, disrupting reverse transcription (14). Due to the different mechanisms of action, NNRTI's can be used in conjunction with NRTI's acting synergistically. Currently there are 5 NNRTIs available (efavirenz, nevirapine, delavirdine, rilpivirine and etravirine). The work presented in this thesis focuses on efavirenz and a novel nanoformulation of efavirenz, discussed in section 1.4.1 and 1.5.3, respectively.

1.3.3 Protease Inhibitors

The viral enzyme PR is responsible for the proteolytic cleavage of the Gag-Pol polyprotein to produce functional viral proteins (32). Inhibition of this process (via PI's, such as lopinavir, atazanavir and darunavir) leads to incomplete viral maturation resulting in the formation of incomplete, non-infectious virions (32, 33). Viral PR targets phenylalanine-proline and tyrosine-proline bonds found in

Gag-Pol. As host protease does not usually target these bonds, PIs are able to target the viral PR active site whilst minimising activity against host proteases (34). The prescription of PI's supported by an NRTI backbone may be recommended as an alternative when NNRTIs are unsuitable (e.g. due to viral resistance or patient intolerance).

1.3.4 Integrase Inhibitors

Following the production of viral DNA, the viral genome is fused into the host DNA via the viral enzyme IN. The first stage of this process is the formation of an IN-viral DNA complex. Following complex formation the 3′ end of the viral DNA is processed, producing reactive hydroxyl groups. The complex is transported to the host cell nucleus (35). This complex then targets host DNA, where the reactive 3′ hydroxyl groups attack the phosphodiester bond and are covalently linked to the host DNA. This is followed by full integration of the viral genome as host repair mechanisms integrate the viral DNA (35, 36). Inhibitors of IN (such as dolutegravir, elvitegravir and raltegravir) act via competitive antagonism of the IN active site, via chelation of the divalent metals of the IN active site (35). By preventing the binding of the IN-viral DNA complex to the host DNA, IN inhibitors prevent the incorporation of the viral genome halting the viral life cycle (36).

1.3.5 Entry Inhibitors

All the previously discussed classes of antiretroviral drugs act by ceasing the propagation of the virus within cells that are already infected by HIV. Entry inhibitors aim to prevent the virus from penetrating the cell, thus preventing the infection of new cells. There are a number of strategies currently at various stages of development (e.g. ibalizumab, a monoclonal antibody that targets CD4 is currently in phase II). However, there are only 2 drugs currently approved by the FDA, maraviroc and enfuvirtide (also known as T20) (37-39).

In order for cell entry to take place, the virus must bind to CD4 receptor and a coreceptor. A polymorphism in CCR5 (CCR5-Δ32) leads to the production of a non-functional protein and has been shown to confer resistance to HIV infection and disease progression (40), but carriers are otherwise healthy. This was the basis for development of CCR5 inhibitors and the first in class, maraviroc, prevents viral entry via inhibition of the coreceptor CCR5 (41). Limitations of maraviroc include poor and variable pharmacokinetics and the necessity for viral tropism tests prior to initiation of therapy. Only HIV that utilises CCR5 is inhibited by maraviroc, which has no effect on HIV that utilises CXCR4 as a co-receptor (39, 42).

Another approach to preventing viral entry is to inhibit fusion of the viral capsid with the cell membrane. Enfuvirtide is a synthetic peptide that binds to gp41 preventing it from interacting with the cell membrane and halting fusion (39). As

enfuvirtide is a peptide, oral administration is problematic. The presence of peptidases in the GI rapidly degrades enfuvirtide resulting in very poor bioavailability, thus parenteral administration is required to bypass the GI.(43). Given the high dosing frequency (twice daily) and the route of administration (subcutaneous [SC]), prescription of enfuvirtide is usually reserved for when other therapeutics have failed (44). Recent studies have sought to address this issue via a polylactic-co-glycolic acid microparticle formulation to provide sustained release (sustained *in vitro* release over 18 days) (44).

1.4 The Central Nervous System in HIV

The central nervous system (CNS) is a key anatomical region in HIV therapy as the CNS is separated from systemic circulation by the blood brain barrier (BBB) (45). The BBB is comprised of a complex interplay of multiple cell types that produce an effective barrier limiting the entry of both endogenous and exogenous molecules (Figure 3). The BBB is characterised by the presence of tight cellular junctions, formed by interactions between key proteins (including claudins, occludin and junction adhesion molecule) expressed by the endothelial cells of the BBB (46, 47). Endothelial cells are supported by a number of other cells, providing processes necessary for the formation of the BBB, capillary basement membrane, astrocyte foot processes and pericytes (46).

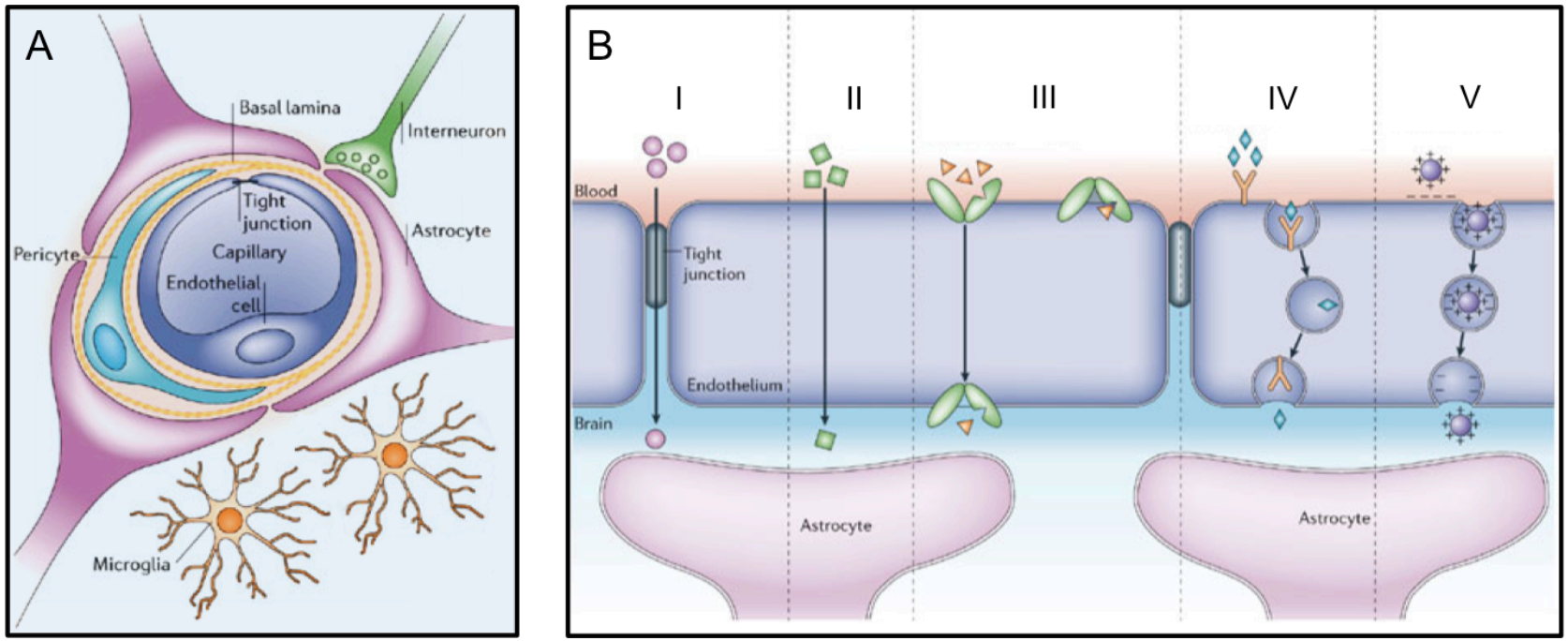

Figure 3 A. Shows the cellular organisation of the BBB including endothelial cells, pericytes, astrocyte end feet and microglia. **Figure 3 B** shows the most common methods of passage across the BBB paracellular (I), transcellular (II), via transport proteins both influx and efflux (III), receptor mediated trancytosis (IV) and absorptive trancytosis (V). Figures adapted from source (48).

In addition to the presence of tight junctions, limiting paracellular diffusion, endothelial cells highly express metabolising enzymes, efflux transporters and possess a large amount of mitochondria (required for active transport and metabolism), all of which limit access of antiretrovirals to the CNS (49, 50). Understanding the mechanisms the BBB employs to defend the CNS enables identification of physicochemical properties effecting CNS penetration.

Molecular weight has been identified as a key factor determining BBB penetration. Low molecular weight chemicals have been shown to more readily pass the BBB than those with a higher molecular weight. According to Lipinski's "rule of five" (Table 2) the molecular weight cut off for good permeability is ≤500 KDa. However, for BBB penetration it has been suggested an even lower molecular weight needs to be applied (≤ 400 KDa) (51, 52). The lipophilicity of a compound has also been shown to play a significant role in BBB penetration, with an oil/water distribution (LogP) of ≤5 indicating good permeability. In addition to the physicochemical properties, there are a number of pharmacological considerations that may affect BBB permeability. Highly protein bound antiretrovirals are unlikely to readily pass the BBB as only the free drug is available for permeation. The endothelial cells of the BBB have been shown to express many cytochrome P450 (CYP) enzymes (both CYP2B6 and CYP3A4 mRNA were expressed in primary brain endothelial cultures) and drug transporters (e.g P-glycoprotein [P-gp] and breast cancer resistance protein [BCRP]) (47, 53). The expression of metabolic enzymes and drug transporters provide an effective barrier to antiretroviral penetration across the BBB.

Physicochemical Property	Value for good permeability	Value for good BBB permeability
Number of Hydrogen Bond Donors	≤ 5	≤ 5
Number of Hydrogen Bond Acceptors	≤ 10	≤ 5
Molecular Weight	≤ 500	≤ 400
Log P	≤ 5	1.5-2.7
Number of Rotatable Bonds	≤ 10	≤ 5

Table 2. Lipinski's rule of 5 shows the desired physicochemical properties of orally available to predict good absorption or permeability across a biological membrane and specifically the BBB. These rules only apply to drugs utilising passive permeation. Permeability of transporter proteins substrates is dependant of the type of transporter (influx or efflux), affinity and abundance of the transporter. Data extracted from (51, 52)

The BBB is highly effective at preventing the penetration of many antiretrovirals into the CNS. Using current technology CNS penetration is assessed using cerebrospinal fluid (CSF) as a surrogate marker. However, it is currently being debated as to how accurate a marker CSF concentrations are for brain concentrations when determining drug exposure (54-56). It has been demonstrated in guinea pigs that brain tissue concentrations of nevirapine not only differ from those in the CSF but also vary between brain regions (54). Nevirapine uptake was shown to be 0.32 ml/g in the CSF whereas nevirapine uptake was lower in the choroid plexus (0.25 ml/g) and higher in the pituitary (1.61 ml/g) when compared to the CSF (54) . These data indicate that predicting brain tissue concentrations from CSF is problematic. Indeed, concentrations within CSF have been shown to vary depending on where the sample was taken. Lamivudine (a nucleoside reverse transcriptase inhibitor) has been shown to be

5-fold higher in CSF sampled from the lumbar region compared to ventricular CSF in rhesus monkeys (55).

Antiretrovirals display wide variation in CSF penetration (considered by CSF sampling). For example CSF concentrations of efavirenz, nevirapine and lopinavir were determined to be lower than plasma concentrations, 0.5%, 63% and 0.23%, respectively (57-59). Despite lower concentrations in the CSF, antiretroviral concentrations maybe sufficient to display antiretroviral activity, exceeding the concentration producing 50% inhibition (IC_{50}) (57, 59). However, this is not always the case and tenofovir CSF concentrations were shown to be 5% of plasma concentrations with 77% of patients (cohort of 183 patients) having CSF concentrations below the IC_{50} (60).

A significant limitation of current antiretroviral treatment is that while the BBB limits the penetration of many antiretrovirals, HIV is able to infect the CNS and replicate (47). HIV crosses the BBB via infected peripheral blood lymphocytes and monocytes, which migrate to the brain (61, 62). Although the mechanism of HIV passage across the BBB has not been fully elucidated, it has been demonstrated that infection of CD14+ and CD16+ monocytes results in an increase in migration across to the brain in response to CCL2 (a chemoattractant) when compared to uninfected cells (62). It is postulated that continued viral replication in the CNS is a contributor to viral rebound. Currently, HIV is incurable and upon termination of therapy the virus is able to re-infect biological

compartments previously showing suppression of viral growth (63). A further concern is the development of resistant strains of HIV.

In addition to the risk of viral rebound, viral replication in the CNS can lead to the development of HIV-associated neurocognitive disorder (HAND). Once released, HIV is able to infect brain parenchyma triggering a signalling cascade resulting in increased concentrations of neurotoxins (61). The increase in neurotoxins eventually leads to neuronal damage and cognitive impairment. HAND can be subdivided into asymptomatic neurocognitive impairment, mild neurocognitive disorder and HIV-associated dementia. Symptoms present in a range of psychological disturbances (including sleep disorders, depression and mania) (61).

1.4.1 Efavirenz Associated Central Nervous System Side Effects

Currently the WHO recommends global treatment of HIV should consist of 1 NNRTI supported by an NRTI backbone (64). The most frequent combination administered is efavirenz combined with tenofovir and emtricitabine. This combination is co-formulated into a single tablet administered once daily (Atripla) (26).

Patients receiving efavirenz-containing therapy frequently report CNS disturbances. Symptoms occur with a high frequency and can include depression, anxiety, abnormal dreams and hallucinations (65). The majority of patients report

development of CNS disorders shortly after commencing efavirenz with symptoms dissipating during the initial months of therapy. A minority of patients continue to experience symptoms for the duration of receiving efavirenz-containing therapy (66). More recently however, efavirenz CNS toxicities have been shown to have more long-term effects. Leutscher *et al* demonstrated a 60% discontinuation rate of efavirenz versus 3% receiving non-efavirenz-containing therapy. It was further shown that half of the patients discontinuing efavirenz did so ≥ 12 months (67).

In addition to the negative impact on the quality of the patient's life, CNS toxicities may also lead to a decrease in patient adherence. Poor patient adherence to antiretroviral medication is a major concern with regards to HIV therapy but in particular efavirenz therapy. Exposure to sub-therapeutic concentrations can lead to therapeutic failure and the development of viral mutations and resistant strains of HIV (sometimes class-resistant). NNRTI's are considered to have a low genetic barrier to the development of resistance; a single mutation (such as K103N) can confer resistance to multiple NNRTI's (68). The impact of CNS side effects on patient adherence is not clearly defined. Previous studies imply patients demonstrate tolerance to CNS side effects, resulting in little or no impact on patient adherence (69, 70).

Many studies have attempted to elucidate the relationship between CNS adverse effects and variability in plasma concentrations of efavirenz. Efavirenz is metabolised primarily by CYP2B6 and to a lesser extent CYP2A6, CYP3A4 and

uridine 5'-diphospho-glucuronosyltransferase isoform 2B7 (UGT2B7) (71). Higher plasma concentrations of efavirenz have been shown to be associated with polymorphisms in these enzymes, in particular polymorphisms in *CYP2B6*, such as 516G>T, *CYP2B6*6* (constituted by 516G>T and 785A>G polymorphisms) and *CYP2B6*16* (containing 983T>C and the 785A>G polymorphisms) (72, 73).

The relationship between patient polymorphisms and plasma concentrations of efavirenz has been clearly demonstrated. However, the association of higher pharmacokinetic exposure to efavirenz and CNS toxicities remains unclear. Polymorphisms in *CYP2B6* have been shown to be associated with increased incidence of CNS side effects in some studies. Marzolini *et al* reported plasma concentrations of >4000 μg/l are associated with a 3-fold increase in CNS side effects (Figure 4) (74). Conversely; Haas *et al* described a higher frequency of the *CYP2B6* 516G>T polymorphism in African-Americans than European-Americans but no significant difference in the occurrence of neuropsychiatric adverse effects, while Takahashi *et al* concluded that there was no correlation with efavirenz plasma concentrations and CNS side effects in Japanese patients (75, 76). Our current understanding leads to the conclusion that increased plasma concentrations of efavirenz play a putative role in the development of CNS side effects, but there is a current paucity of data relating to the underlying mechanisms of toxicity.

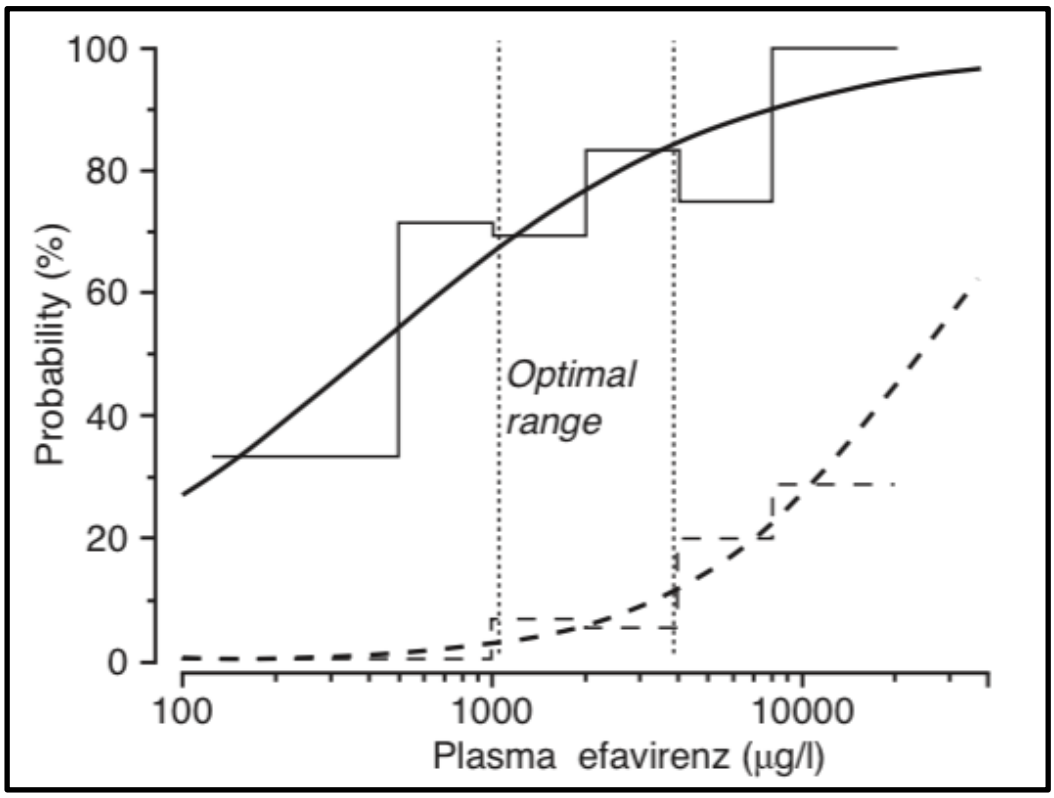

Figure 4. The graph above shows the association with probability of either viral suppression (solid line) or occurrence of CNS toxicity (broken line) with concentration of efavienz. The optimal range highlights efavirenz concentrations of 1000 µg/l and 4000 µg/l where viral suppression is maintained with acceptable occurrence of CNS toxicity. Figure source (74).

1.5 Limitations of Current Antiretroviral Therapeutics

Currently all licensed antiretroviral drugs (except enfuvirtide) are prescribed as solid formulations for oral administration. The pharmacokinetics of orally administered drugs are subject to the first pass effect, poor absorption and the hostile environment of the gastrointestinal (GI) tract (77). Before reaching the site of action, antiretroviral drugs have to first enter the GI tract and be absorbed. The extreme pH environment and the presence of digestive enzymes degrade some drugs prior to absorption. Bioavailability is also influenced by poor solubility and the presence of drug transporters in enterocytes of the GI tract (78). Following absorption, many of the drugs undergo extensive hepatic

metabolism (79). The factors governing absorption have a significant impact on bioavailability and pharmacokinetics, with huge inter-individual variability being a hallmark for most antiretroviral drugs.

The major aim of HIV therapy is to maintain sufficient concentrations of antiretrovirals to enable sustained virological suppression. Sub-therapeutic concentrations of antiretroviral drugs can allow continued viral replication and facilitate development of resistance (80). Particular classes of antiretroviral drug are more susceptible to emergence of resistance than others (81). As discussed above, NNRTIs have a low genetic barrier to resistance, and class-wide resistance can compromises multiple agents in one event (82).

Poor penetration into certain anatomical sites enables continued viral replication, and is a major limitation to antiretroviral therapy. Areas such as the CNS, genital tract and the lymphatic system have been shown to have low concentrations (termed sanctuary sites), which may be involved in viral rebound and resistance (83). Recently, it has been demonstrated that despite viral suppression in the blood (the current marker of successful treatment) there is incomplete suppression and in some cases higher viral replication in lymphoid tissue of patients receiving key antiretroviral drugs (84).

There are currently limited paediatric formulations of antiretrovirals. Significant differences are apparent in children due to the changes during development. For

example, neonates (children below 6 months) show increased clearance of lopinavir and children below 6 years old show increased renal excretion of lamivudine (85). Gastric pH is higher during the first 2 years of life, and plasma protein, water content and expression of CYPs vary significantly from adults (85). Therefore, difficulties in treating children in resource-limited settings are exacerbated by the limited availability of paediatric formulations, cost and issues with stability and storage.

The efficacy of combination antiretroviral therapy for HIV patients who take their medications appropriately is approximately 90% with the main factors that distinguish one regimen from another being simplicity (dose, format, size) and toxicity (86). A number of toxicities have been reported clinically across the various classes of antiretrovirals and have been extensively reviewed (86-88). Currently, efavirenz and nevirapine are the two most frequently prescribed NNRTIs. This is because both drugs are highly potent (efavirenz inhibition constant of the reverse transcriptase enzyme [K_i] = 2.9 nM, nevirapine K_i = 7.0 nM) and generally well tolerated (89, 90). However, both drugs are associated with distinct toxicity profiles. Efavirenz is associated with a series of neuropsychiatric adverse effects such as anxiety, depression, hallucinations, paranoia and suicide ideation, as discussed in section 1.4.1 (91).

Some nanotechnologies are being applied to extend the pharmacokinetic exposure of drug for long-acting (LA) delivery (see below). Clearly, the presence of hypersensitivity reactions (HSRs) means care must be taken in selection of

drugs for this approach. Moreover, since the low frequency of HSRs mean they are not usually detected until late in development (or routine use) the application of these types of approach to new chemical entities (NCE) requires careful consideration.

1.5.1 Utilisation of Nanomedicine to Address The Limitations of Current Antiretroviral Therapeutics

Collectively, the major drivers for the application of nanotechnology to improve the pharmacology of antiretroviral drugs relate to improved pharmacokinetics (lower dose / sustained release / lower inter-patient variability), targeting of sanctuary sites and improved safety. Clearly, the disease-specific development of nanomedicines needs to consider the pathology of the disease, particularly where perturbation of the immune system occurs as a function of the disease. However, chronicity is important in the context of nanomedicine development since in the absence of eradication, patients require a life-long commitment to therapy. Nanotechnology can be applied to NCEs or existing therapeutic agents and for the latter, the specific toxicological mechanisms for the drugs being employed needs to be considered. Despite the significant advances in antiretroviral therapy, it is clear that many aspects of modern antiretroviral therapy may be improved. The development of NCE can be prohibitively expensive and drugs are often abandoned due to inherent issues in drug exposure, efficacy and/or toxicity. Nanotechnology offers the opportunity to examine existing pharmaceutical agents and address inherent issues in pharmacokinetics (poor absorption, rapid clearance, unfavourable tissue distribution, etc.) whilst maintaining the

favourable properties of the drug (92). Nanoformulation has been applied to address many of the challenges associated with current antiretroviral therapy, including LA formulations, improving dissolution of poorly water soluble drugs, reduction of inter-individual pharmacokinetic variability, paediatric formulations and targeting to HIV-infected cells. This section will outline how nanomedicine has been applied to address some of the challenges associated with existing HIV therapeutics.

1.5.3 Nanotechnology-enabled oral drug delivery

As discussed above, one of the limitations of current antiretroviral therapy is poor bioavailability following oral administration (77), often as a result of low aqueous solubility. Figure 5 shows currently recommended antiretrovirals by the WHO and their aqueous solubility. The Biopharmaceutics Classification System (BCS) categorises drugs on solubility and permeability (class 1 high solubility with high permeability, class 2 low solubility with high permeability, class 3 high solubility with low permeability and class 4 low solubility with low permeability) (93). Many of the first line HIV drugs have inherent solubility or permeability issues. Efavirenz is the preferred antiretroviral agent prescribed. When efavirenz is not tolerated nevirapine is frequently prescribed instead. Both drugs are classified as having solubility issues. Additionally, lopinavir and ritonavir (a frequently prescribed second line therapy) are also classified as having solubility issues (BCS class 2) (93). There are many approaches under investigation for the development of nanomedicines for oral administration and current progress is summarised below.

Figure 5. Antiretrovirals recommended by the WHO and their BCS classification. The following combinations are recommended for first line therapy; zidovudine and lamivudine supported by either efavirenz or nevirapine or tenofovir and emtricitabine supported by either efavirenz. Also shown are the biopharmaceutics classification System (BCS) classifications and log P values (oil/water distribution). Classification is based on the antiretrovirals physiochemical properties and permeability through biological membranes, such as the gut. Data extracted from (77, 94).

Lopinavir is a substrate for both CYP3A4 and P-gp, which both contribute to poor bioavailability of lopinavir when administered alone. Conventional therapy minimises this by boosting the pharmacokinetics (pharmacoenhancement) of lopinavir via co-administration of ritonavir, which potently inhibits both CYP3A4 and P-gp (95, 96). Surfactant-stabilised lopinavir SDN ([solid drug nanoparticle] also known as nanosuspension or nanodispersion) prepared by combination of antisolvent precipitation and high-pressure homogenisation (stabilized by polyvinyl alcohol) followed by a stepwise freeze-drying cycle

(using mannitol as the cryoprotectant) have been studied. Oral administration of lopinavir nanoparticles (12 mg/kg) demonstrated increased plasma exposure when compared to conventional lopinavir (12 mg/kg) co-administered with ritonavir (3 mg/kg), C_{max} (2207 vs 1160 ng/ml), AUC (99806 vs 32002 ng.h/ml) and oral bioavailability was increased 3.1 fold. Additionally, co-administration of ritonavir with the nanoformulated lopinavir yielded a 3.3-fold greater oral bioavailability when compared to the conventional formulation. These data indicate that the nanoformulation provides increased oral bioavailability without reliance on ritonavir (which is not well tolerated due to toxicity), raising the possibility of dose simplification (95).

SDN formulation of efavirenz has also been demonstrated to improve *in vitro* cellular uptake, *in vivo* plasma pharmacokinetics and reduce *in vitro* toxicity indicating the approach may provide a suitable oral treatment for HIV. SDNs of efavirenz were generated using a novel emulsion template freeze-drying technique. The process yielded amorphous SDNs of average size 322 nm (±29), poly dispersity index 0.48 (±0.17) and drug loading of 70% (70% EFV, 20% poly[vinyl alcohol] and 10% α-tocopherol polyethylene glycol succinate) (97). Pharmacological assessment of the efavirenz SDN formulation demonstrated improved Caco-2 uptake (between 1.1 and 1.65 fold) and apparent permeability (up to five-fold), compared to an unformulated efavirenz preparation. Lower cytotoxicity was observed (up to 3.5 fold increase in the IC_{50}) compared to an unformulated efavirenz preparation. *In vitro in vivo* extrapolation predicted that the SDN formulation could achieve similar plasma pharmacokinetics to the standard formulation with 50% less dose (300mg SDN vs 600mg standard

efavirenz). The *in vivo* pharmacokinetics were also investigated via oral administration to rats and higher C_{max} (478.1 vs 125.9 ng/l), minimum plasma concentration ([C_{min}]; 378.9 vs 80.5 ng/l), AUC (1831.0 vs 457.1 ng.l/h) and time to reach maximum plasma concentration (T_{max}; 0.5 vs 0.8h) were observed when compared to a conventional formulation. These data indicate a potentially higher absorption of efavirenz following oral administration, which in turn may reduce dose and cost of efavirenz-containing therapy (97).

1.5.3 Nanotechnology-enabled parenteral drug delivery

Two LA nanoformulations for the treatment of HIV are currently in late stage development and have already transitioned into human studies. LA formulations are of particular interest in the treatment of chronic conditions such as HIV where patient adherence presents a significant issue (98). Poor adherence to therapy can lead to sub-therapeutic concentrations of antiretrovirals, which in turn can lead to viral rebound, and the emergence of viral resistance (81). LA formulations aim to reduce the impact of poor adherence by increasing the dosing interval while maintaining therapeutic concentrations.

The first example is a SDN suspension of the NNRTI, rilpivirine (TMC278). Rilpivirine has been approved for oral administration since 2011. Despite displaying potent antiviral activity, rilpivirine has poor water solubility (<0.1mg/ml) making it compatible with the continuous wet-bead milling process, forming SDN suspended in aqueous vehicle with hydrophilic surfactants.

Following a single SC or intramuscular injection of rilpivirine, plasma concentrations remained detectable for up to 3 weeks in mice and 3 months in dogs (99). Following pre-clinical assessment, phase I trials of rilpivirine LA have commenced. A single injection of 300 mg/ml rilpivirine LA administered as gluteal intramuscular or abdominal SC injections was assessed in 51 healthy volunteers. Rilpivirine concentrations remained >10 ng/ml for up to 26 weeks with no grade 3 or 4 adverse events (100).

The second example of an LA formulation is that of cabotegravir (S/GSK1265744), also produced by wet-bead milling. Cabotegravir is an analogue of the integrase inhibitor dolutegravir under assessment for both oral and LA administration (101). The LA formulation consists of crystalline cabotegravir, milled to a median particle size of 200 nm, along with surfactant, polymer, tonicity agent and water for injection. In a randomized, placebo-controlled phase I study, 56 HIV healthy volunteers received cabotegravir as an intramuscular injection (100, 200, 400 or 800 mg) or a SC injection (100, 200 or 400 mg) or placebo injection. Plasma concentrations of cabotegravir increased rapidly over the first week followed by sustained exposure for >24 weeks following administration of >200 mg. Intramuscular and SC injection were well tolerated with no grade 2 to 4 injection site reactions reported (102).

1.6 The Application of Physiologically Based Pharmacokinetic Modeling to HIV Therapy

There has been much advancement in HIV therapy however as previously discussed, in section 1.5; there are still many clinical issues with current therapeutics. Development of NCE is frequently difficult and expensive. The application of physiologically based pharmacokinetic modeling (PBPK) offers the opportunity to examine clinical issues in silico, testing the properties of NCE or novel formulations aiding in the identification of desired properties (103).

PBPK modelling is a bottom up approach to simulate clinical scenarios using virtual patients. The approach mathematically describes physiological processes by exploiting the relationship between anthropometric measures (such as height, weight and gender) and physiological parameters (such as organ volumes and blood flow) (104). For example whole organ weight may be predicted by allometric scaling to height, age and body surface area (104). In addition to physiological variables, drug specific physicochemical properties (such as logP, Caco-2 apparent permeability and affinity for transporters and metabolic enzymes) are used as input to predict the pharmacokinetics (105).

PBPK modeling has been applied previously to investigate clinical issues applicable to HIV and development of novel nanotherapeutics. As previously discussed in section 1.4.1, the CNS toxicities associated with efavirenz have an element of dose dependency. Siccardi *et al* demonstrated that PBPK modeling

could be applied to investigate the effect of dose reduction on the pharmacokinetics of efavirenz when stratified for *CYP2B6* genotype. The simulations showed that patients homozygous for *CYP2B6 516TT* (slow metabolisers of efavirenz) were at an increased risk of developing CNS toxicity following a standard 600mg once daily oral dose of efavirenz (25% vs. 36% in patients with *CYP2B6 516GG* wild type). Following dose adjustment the simulations predicted a lower risk of CNS toxicity without compromising viral efficacy. A once daily dose of 200mg achieved 20% probability of CNS toxicity with 72% probability of viral suppression (105).

More recently PBPK, has been applied to the development of LA injectable nanoformulated antiretrovirals (106). As discussed in section 1.5, administration of current antiretrovrals is predominantly via the oral route. The inherent disadvantages of oral administration (reduced pharmacokinetics and poor patient adherence) may be overcome by the development of LA nano formulated antiretrovirals, as discussed in section 1.5.3.

1.7 Thesis aims

Efavirenz has been available for the past 17 years and is still one of the most frequently prescribed antiretroviral therapeutics. This can be attributed to its beneficial pharmacological properties (antiviral efficacy, long plasma half-life [$t_{1/2}$] and comparatively favourable toxicity profile versus other antiretrovirals) (66). Despite these favourable attributes efavirenz has several limitations, which may negatively impact therapy, most notably the occurrence of CNS disturbances. Although contributing factors have been identified, the underlying mechanism of efavirenz associated CNS toxicity remains elusive. In addition to CNS toxicity, the poor water solubility of efavirenz potentially reduces bioavailability and limits administration to paediatrics.

Various nanotechnologies have been explored in attempts to mitigate some of the limitations with efavirenz. While there has been progress in increasing the bioavailability of efavirenz there has been no attempt to assess the impact of increased exposure to efavirenz on CNS toxicity.

The body of work presented in this thesis aimed firstly to investigate the underlying mechanism of efavirenz CNS toxicity and secondly to assess uptake and CNS toxicity of efavirenz and a novel SDN formulation of efavirenz.

- Chapter 2 genotyping of patients with early discontinuation of efavirenz containing therapy. This chapter investigated the association of single nucleotide polymorphisms (SNP's) in the gamma aminobutyric acid receptor (GABA) with early treatment discontinuation of efavirenz was investigated.

- Chapter 3 examined the effect of efavirenz and the SDN formulation in a rodent model of anxiogenesis. The EPM has been used previously to demonstrate anxiety (a symptom of efavirenz CNS toxicity).

- Chapter 4 details the development of a liquid chromatography mass spectrometry assay for the detection of efavirenz in plasma, brain tissue homogenate, PBS and cell culture media.

- Chapter 5 the uptake of efavirenz and the SDN formulation was investigated in hCMEC/D3 cell line, immortalised endothelial cells from the BBB. This chapter investigated the effects of inhibitors of transport proteins and multiple mechanisms of endocytosis.

- Chapter 6 discusses the generation of a PBPK model to predict efavirenz penetration in plasma, CSF and brain tissue. Currently CSF concentrations are used as a surrogate for brain penetration of drugs. This chapter investigated if brain concentrations were represented by CSF concentrations in an *in silico* simulation.

Chapter 2

Single nucleotide polymorphisms in the GABAa receptor are not predictors of early treatment discontinuation of efavirenz

Contents

2.1 Introduction

As discussed in chapter 1, efavirenz is one of the key therapeutics currently used in the treatment of HIV. Efavirenz, supported by an NRTI backbone, is currently recommended as first-line therapy by multiple health organisations (26, 64). There is an abundance of reports from clinical trials detailing CNS disturbances such as depression, anxiety, abnormal dreams, suicidal thoughts and hallucinations. CNS adverse effects have been shown to have a high rate of occurrence. Reports of >50% of patients experiencing CNS toxicities are not uncommon. CNS disturbances have been reported to occur transiently in the majority of patients. Symptoms have been reported to develop shortly after taking efavirenz, subsiding within 2 to 4 weeks. Although CNS adverse effects dissipate in the majority of patients, there is a minority (up to 10%) of patients who continue to experience neuropsychiatric adverse effects while receiving efavirenz. The CNS toxicities associated with efavirenz are well documented but the underlying mechanisms have remained elusive.

Although there have been numerous studies to identify predictors of efavirenz CNS toxicity, until recently the majority of studies have investigated polymorphisms in genes determining efavirenz disposition. Given the majority of efavirenz toxicities are mood and sleep disorders (Table 1) there is evidence to indicate an interaction with neurotransmitters. Treatment of naturally occurring depression and anxiety focuses on pharmacological modulation of neurotransmission. There are numerous classes of antidepressants that act to via distinct mechanisms. Serotonin is released at the synaptic cleft to interact with

serotonin receptors. Cessation of signalling is achieved by reuptake of serotonin. Selective serotonin reuptake inhibitors (such as fluoxetine) act via inhibiting reuptake and increasing the duration of serotonin signaling (107). Monoamine oxidase inhibitors (such as moclobemide) also act to increase the duration of not only serotonin signaling but also dopamine by inhibiting the metabolism of monoamine neurotransmitters (107). Anxiety is frequently treated by the administration of benzodiazepines (such as diazepam). Benzodiazepines act via allosteric modulation, binding to the benzodiazepine binding site leads to potentiation of GABAergic signaling. Additionally, benzodiazepines are indicated in the treatment of insomnia (108). There are numerous neurotransmitters implicated in the etiology of abnormal dreams or nightmares. Clinical trials and case reports have demonstrated drugs effecting acetycholine (e.g. donepezil, an acetycholinesterase inhibitor), norepinephrine (e.g atenolol, a β_1 receptor antagonist), serotonin (e.g paroxetine, a selective serotonin reuptake inhibitors) and GABA (e.g nitrazepam, acts via increasing binding affinity of GABA to GABA receptors) (109).

The GABA receptor is the principle mediator of inhibitory neurotransmission in the CNS (110). The receptor is a hetero pentameric ligand gated ion channel, assembled from a combination of 5 subunits leading to the formation of a chloride ion channel (111). Currently there have been 16 different subunits identified ($\alpha_{1\text{-}6}$, $\beta_{1\text{-}3}$ $\gamma_{1\text{-}3}$, δ, ε, π and Θ), with the most common receptor type consisting of 2 α_1 subunits, 2 β_2 subunits and 1 γ_2 subunit (Figure 1) (111, 112). The GABAa receptor has been of significant pharmacological interest, as

dysfunctions of GABAergic signalling have been implicated in neurological disorders including anxiety, insomnia and depression (110, 113, 114). The GABAa receptor has a variety of binding sites; one of the most pharmacologically interesting is the benzodiazepine-binding site. The benzodiazepine binding site is situated at the interface between the α_1 and γ_2 subunits (18). Binding of ligands to this allosteric binding site increases the affinity of the receptor for GABA, thus potentiating GABAergic signalling (115).

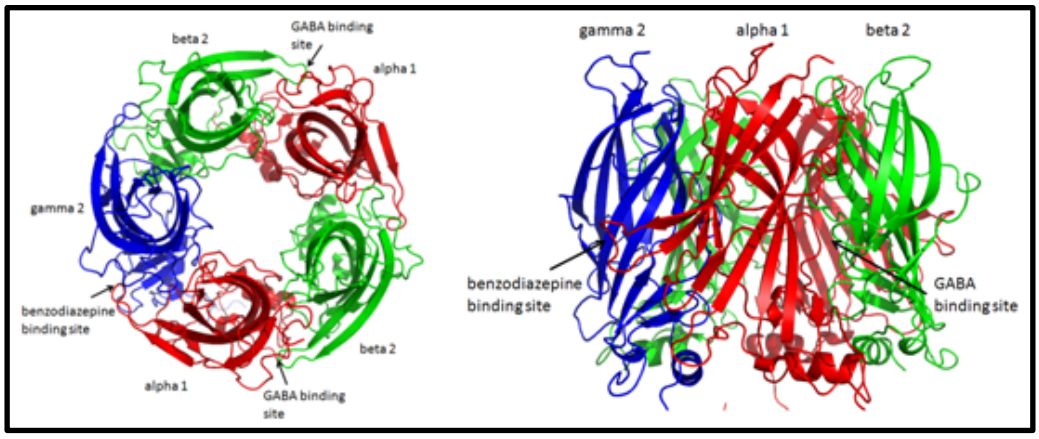

Figure 1 shows the configuration of the extracellular domain of the GABAa receptor. Labelled are the subunit type (α1, β2, and γ2), the 2 GABA binding sites and the benzodiazepine-binding site.

Examination of the adverse effects of drugs acting at the benzodiazepine receptor reveals a similar profile of adverse effects as displayed by efavirenz (see Table 1). Additionally, efavirenz is a 1,4-dihydro-2*H*-3,1-benzoxazin-2-one, which shares a number of structural motifs with the benzodiazepines (116). Previous *in silico* studies (conducted as part of a previous Master by Research degree) performed using homology-modelling techniques have identified that efavirenz and ligands of the benzodiazepine binding site share a common docking location

(Figure 2). The docking results demonstrated that efavirenz and its metabolites did not share any common docking locations with ligands of the GABA binding site. However, models indicated that efavirenz may dock in a similar location to benzodiazepine ligands, showing the potential of efavirenz to interact with key amino acids involved in binding of ligands at this site (117).

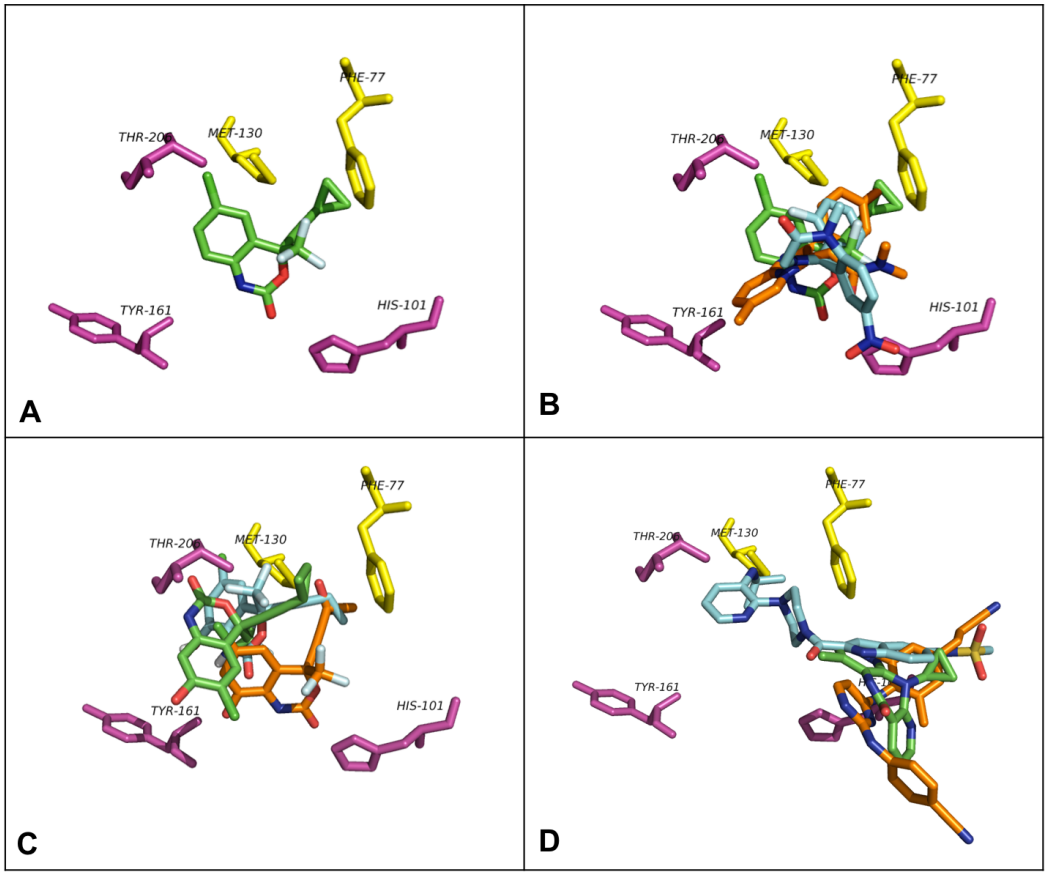

Figure 2 shows the docking results performed using the benzodiazepine-binding site. Each grid shows the most energetically favourable docking position of the following molecules: **A** – efavirenz (green), **B** - efavirenz (green), diazepam (blue) and zolpidem (orange), **C** –7-OHEFV (green), 8-OHEFV (blue), 8,14-OHEFV (orange), **D** – nevirapine (green), delavirdine (blue), rilpivirine (orange). Also shown in each grid are the amino acid residues shown to be important in benzodiazepine binding His 101, Tyr 161, Thr 160 (α_1 purple) Phe77 and Met 130 (γ_2 yellow). Data from this figure was generated during a previous Master by Research degree (unpublished data).

Drug	Side Effects
Efavirenz	Abnormal dreams, anxiety, depression, insomnia, aggression, confusional state, euphoric mood, hallucination, mania, suicide ideation, disturbance in attention, dizziness, headache, somnolence, agitation, amnesia, ataxia, abnormal coordination, convulsions and abnormal thinking.
Zolpidem	Hallucination, agitation, nightmare, somnolence, headache, dizziness, exacerbated insomnia and anterograde amnesia.
Zalepon	Amnesia, paraesthesia, somnolence, ataxia, confusion, decreased concentration, apathy, depersonalisation, depression, dizziness and hallucinations.
Flurazepam	Numbed emotions, reduced alertness, confusion, fatigue, headache, dizziness, muscle weakness, ataxia, and double vision.
Lorazepam	Confusion, depression, Sedation, drowsiness, ataxia and dizziness.
Diazepam	Sedation, drowsiness, unsteadiness, ataxia, headache, vertigo and visual disturbances.

Table 1 shows the chemical structure and side effects associated with efavirenz and drugs acting on the GABA receptor (in particular acting on α_1 GABAa receptor).

When considering the associated side effects and structural similarities to GABAergic drugs, it is reasonable to postulate that the mechanism of efavirenz mediated CNS side effects is via modulation of GABAergic signalling. The aim of this chapter was to investigate the association of single nucleotide polymorphisms (SNP's) in the subunits of the GABA receptor (α_{1+2}, β_2 and γ_2) with early treatment discontinuation of efavirenz containing therapy (Table 2). This genetic association study was performed using patient samples of the German Competence Network for HIV/AIDS (KompNet Cohort). Allele frequencies were compared between patients recorded as early treatment discontinuation (efavirenz treatment for < 3 months) and patients maintaining

efavirenz-containing therapy (≥ 3 months). In this study early treatment discontinuation was employed as a surrogate marker for CNS disturbances.

SNP code	GABA Subunit	Alleles	Population Frequency	Disease Association	References
Rs279858	α_2	A/G (A)	E = A (0.527), G (0.473) SSA = A (0.823), G (0.177)	Alcoholism	(118)
Rs279845	α_2	A/T (T)	E = A (0.492), T (0.508) SSA = A (0.149), T (0.851)	Alcoholism	(119)
Rs279836	α_2	A/T (T)	E = A (0.492), T (0.508) SSA = A (0.149), T (0.851)	Alcoholism	(120)
Rs2229944	β_2	C/T (T)	E = C (0.951), T (0.049) SSA = C (0.810), T (0.190)	Schizophrenia	(121)
Rs6556547	β_2	A/C (C)	E = A (0.059), C (0.941) SSA = A (0.126), C (0.874)	Schizophrenia	(121)
Rs211037	γ_2	C/T (T)	E = C (0.768), T (0.232) SSA = C (0.455), T (0.545)	Epilepsy	(122)
Rs211014	γ_2	A/C (C)	E = A (0.195), C (0.805) SSA = A (0.467), C (0.533)	Heroin Addiction	(123)

Table 2 shows the SNPs examined in the GABAa receptor. Also shown are the subunit affected by the SNP, alleles (bracket indicates common allele) and disease association. Population frequencies were gathered from International Hapmap Project. E = European and SSA = Sub-Saharan African.

2.2 Methods

2.2.1 Materials

QIAamp DNA mini kit genomic DNA isolation kit was purchased from Qiagen (Manchester, UK). Pre validated primers and probes were purchased from Life Technologies (Paisley, UK). Quantitative polymerase chain reaction (QPCR) master mix was purchased from ABgene (Loughborough, UK). All other consumables were purchased from Sigma Aldrich (Dorset, UK).

2.2.2 Patient Information

Blood samples were taken from 439 patients receiving an efavirenz-containing regimen. The 439 patient samples were then assigned to either a training cohort (samples analysed by LGC Genomics [formerly KBioscience], 288 patients) or test cohort (samples analysed in house, 151 patients). Each cohort was subdivided based on duration of efavirenz therapy, the control group and the early discontinuation group. In addition to blood samples the details on the following demographic factors were collected from each patient; gender, ethnicity, age, smoking status and duration of efavirenz therapy. Blood samples were collected from patients of the cohort of the German Competence Network for HIV/AIDS (KompNet). The ethics committee of the Ruhr-Universita ̈t Bochum (Germany) granted ethical approval and patient consent was sought prior to collection of patient samples.

2.2.3 Extraction of Genomic DNA

Genomic DNA was extracted from whole blood using the QIAamp mini kit. Extraction was performed following manufacturer's instructions (spin-column protocol). Patient samples (200µl) were mixed with 20µl of QIAGEN protease and 200µl of buffer AL in microcentrifuge tubes. Samples were thoroughly mixed to ensure sample lysis followed by incubation at 56°C for 10 minutes. Following incubation, 200µl of ethanol was added to each sample and transferred to fresh spin-columns and centrifuged at 6000g for 1 minute at room temperature. 500µl of buffer AW1 was added and samples were then centrifuged at 6000g for 1 minute at room temperature. 500µl of buffer AW2 was added and samples were the centrifuged at 20,000g for 3 minutes at room temperature. 50µl of distilled water was added to each sample and incubated at room temperature. DNA was eluted by centrifugation at 6000g for 1 minute at room temperature. DNA was quantified using PicoGreen dsDNA quantitation reagent and normalised to 20ng/µl. The samples were stored at -40°C until analysis by real-time polymerase chain reaction (PCR) allelic discrimination or until shipping to LGC Genomics for analysis.

2.2.4 Genotyping of GABA Receptor Polymorphisms by qPCR-based allelic discrimination

Genotyping for Rs279858, Rs279845, Rs279836, Rs2229944, Rs6556547, Rs211037 and Rs211014 in the test cohort was conducted LGC genomics. Genotyping was conducted using LGC Genomics proprietary KASP genotyping technology. Primers and Probes were designed using LGC Genomics proprietary software, Kraken™ (124).

The PCR reaction mixture consisted of 10µl master mix, 1µl primer and probe, 1µl of genomic DNA and 8µl of ultra-pure DNase free water for a total reaction volume of 20µl. Primers and probe assays were purchased from Life Technologies Rs211014 (pre-validated assay, ID C_3169569_1_) and Rs6556547 (custom assay, primer and probe sequences are below). Thermal cycling was conducted using a DNA Engine Opticon 2 system (MJ Research Inc., USA) programmed for standard cycling conditions (95˚C for 15 min, followed by 40 cycles of 95˚C for 15 s and 60˚C for 1 min).

Rs6556547 forward sequence 5′TCTGAAACTAGTAATAAATTGCTCACATAAAGACA3′

Rs6556547 reverse sequence 5′GCAAATATCCCATTTTTCCAAAGTTGAAAC3′

Rs6556547 probe sequence 5′TTGTTCCTGTAATCGATAC3′

2.2.5 Statistical analysis

All data are expressed as median (± interquartile range [IQR]). Univariate and multivariate analyses were performed by the χ^2 test and backward logistic regression respectively. Statistical significance was established as $P < 0.05$ with a statistical trend established as < 0.1. All statistical tests were performed using SPSS statistics (v22). All genotypes were assessed for Hardy-Weinberg equilibrium by the χ^2 test using the Hardy-Weinberg equilibrium online calculator (125).

2.3 Results

2.3.1 Cohort Demographics

Patients for this study were recruited between the 1st of January 2006 and the 1st of October 2009. The baseline patient demographics for the training cohort and the test cohort are shown in Table 3 and Table 4 respectively. There were 237 and 100 patients receiving efavirenz containing therapy for over 3 months, constituting the control groups, in the training cohort and the test cohort respectively. There were 51 and 48 patients recorded as discontinuing efavirenz-containing therapy early (less than 3 months) in the training cohort and the test cohort, respectively.

	Sustained therapy (> 3 months)	Early Treatment Discontinuation (< 3 months)	Total
Number of Patients	237 (82.3%)	51 (17.7%)	288 (100%)
Gender (male)	152 (64.1%)	38 (74.5%)	190 (66%)
Ethnicity (White)	155 (65.4%)	42 (82.4%)	197 (68%)
Age	45 (40-53)	43 (39-51)	
Smoking Status (non smoker)	56 (23.6%)	19 (37.3)	75 (26%)

Table 3 shows the demographics collected for the training cohort including gender, ethnicity, age, smoking status and duration of efairenz containing therapy. Data represents frequency with percentage shown in brackets (gender, ethnicity, smoking status) or median with interquartile range shown in brackets (age).

	Sustained therapy (> 3 months)	Early Treatment Discontinuation (< 3 months)	Total
Number of Patients	100 (67.6%)	48 (32.4%)	151 (100%)
Gender (male)	81 (81%)	45 (93.8%)	126 (83%)
Ethnicity (White)	72 (72%)	46 (95.8%)	118 (78%)
Age	46 (41-53)	45.5 (42-50.8)	
Smoking Status (non-smoker)	20 (20%)	12 (25%)	32 (21%)

Table 4 shows the demographics collected for the test cohort including gender, ethnicity, age, smoking status and duration of efairenz containing therapy. Data represents frequency with percentage shown in brackets (gender, ethnicity, smoking status) or median with interquartile range shown in brackets (age).

2.3.2 Association of Demographic Factors with Early Treatment Discontinuation, Univariate Analysis

Patient demographics (gender, ethnicity, smoking status and age) were tested for a univariate association with early treatment discontinuation of efavirenz containing therapy. The training cohort (Figure 3) revealed no association with early treatment discontinuation and age or gender, P = 0.78 and 0.17, respectively. Both ethnicity and smoking status were associated with early treatment discontinuation. Patients of white ethnicity showed a greater degree of early discontinuation (21.3% of patients with white ethnicity discontinued efavirenz vs 10.0% of patients with black ethnicity P = 0.02). There was a higher degree of discontinuation in non-smokers vs smokers (25.3% of patients that were non-smokers discontinued efavirenz vs 21.1% of patients that smoked, P = 0.02).

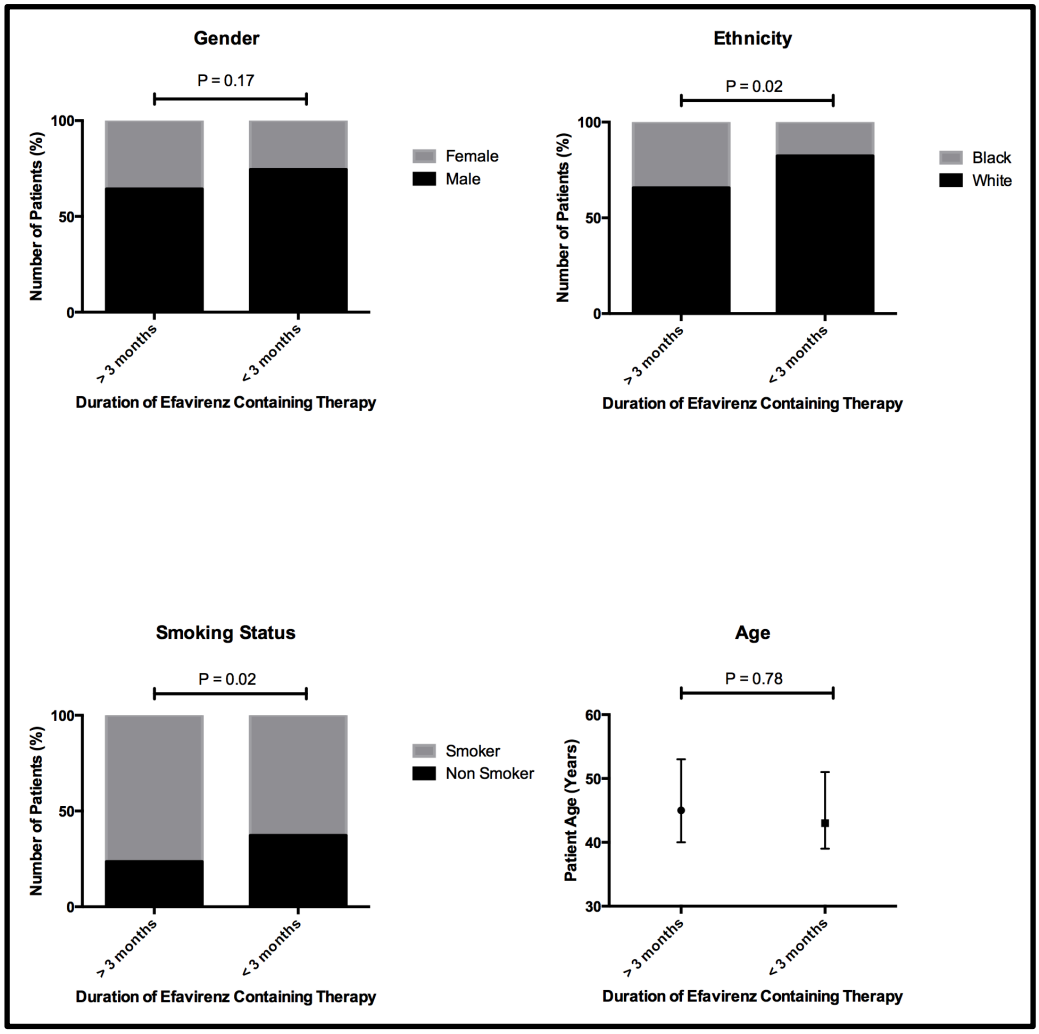

Figure 3 shows the univariate analysis of the training cohort for gender, ethnicity, smoking status and age. Also shown are the P values generated via the χ^2 test.

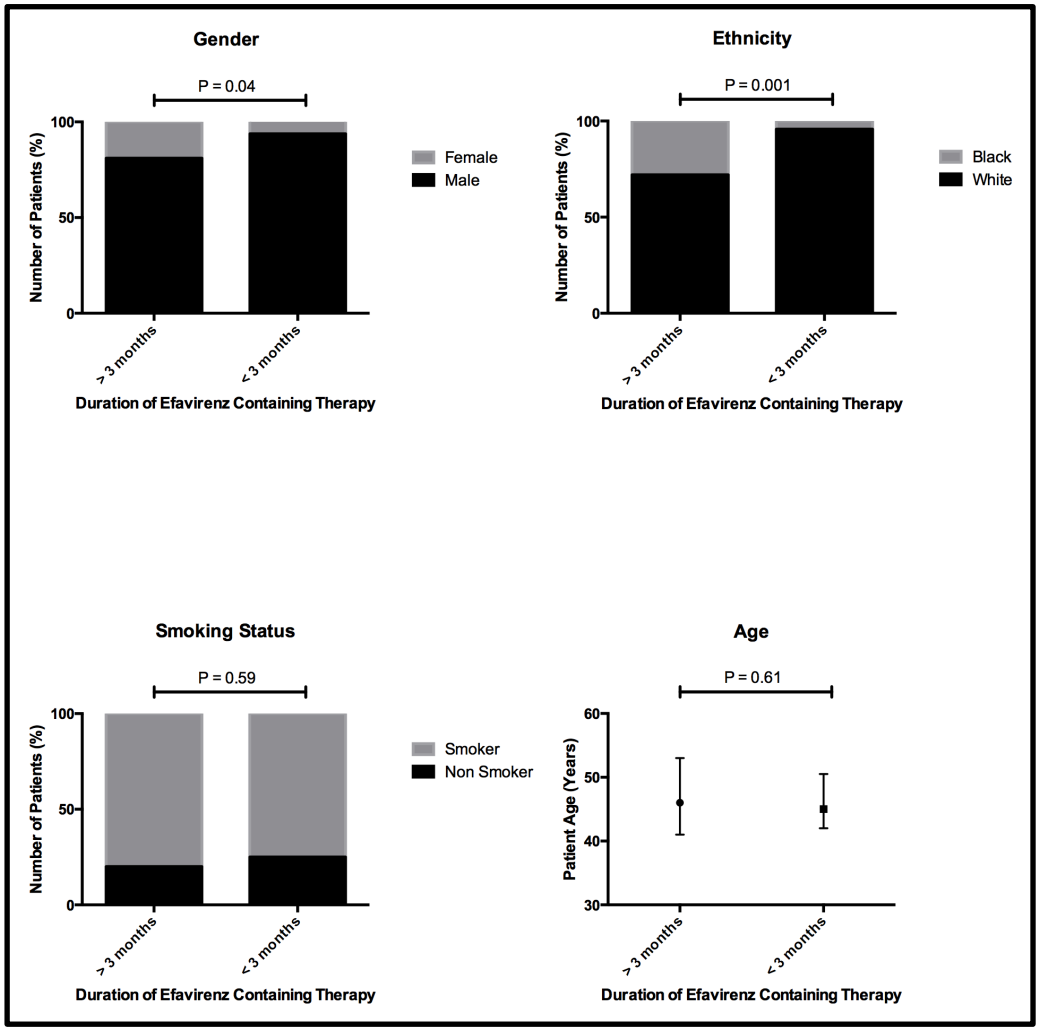

Figure 4 shows the univariate analysis of the test cohort for gender, ethnicity, smoking status and age. Also shown are the P values generated via the χ^2 test.

The test cohort revealed no association with early treatment discontinuation and age or smoking status, P = 0.61 and 0.59, respectively (Figure 4). Both ethnicity and gender were associated with early treatment discontinuation. Patients of white ethnicity showed a greater degree of early discontinuation (39.0% of patients with white ethnicity discontinued efavirenz vs 6.7% of patients with black ethnicity P = 0.02). There was a higher degree of discontinuation in males (35.7% of male patients discontinued efavirenz vs 13.6% of female patients P = 0.02).

2.3.3 Association of GABA SNPs With Early Treatment Discontinuation, Univariate Analysis

Hardy-Weinberg equilibrium was assessed for all genotypes in both the training and test cohorts. Rs211037 was found not to be in Hardy-Weinberg equilibrium ($P > 0.01$), all other genotypes were in Hardy-Weinberg equilibrium ($P < 0.05$).

Patient blood samples were genotyped for SNPs in GABA subunits and tested for a univariate association with early treatment discontinuation of efavirenz containing therapy. The training cohort (Figures 5) revealed no association with early treatment discontinuation.

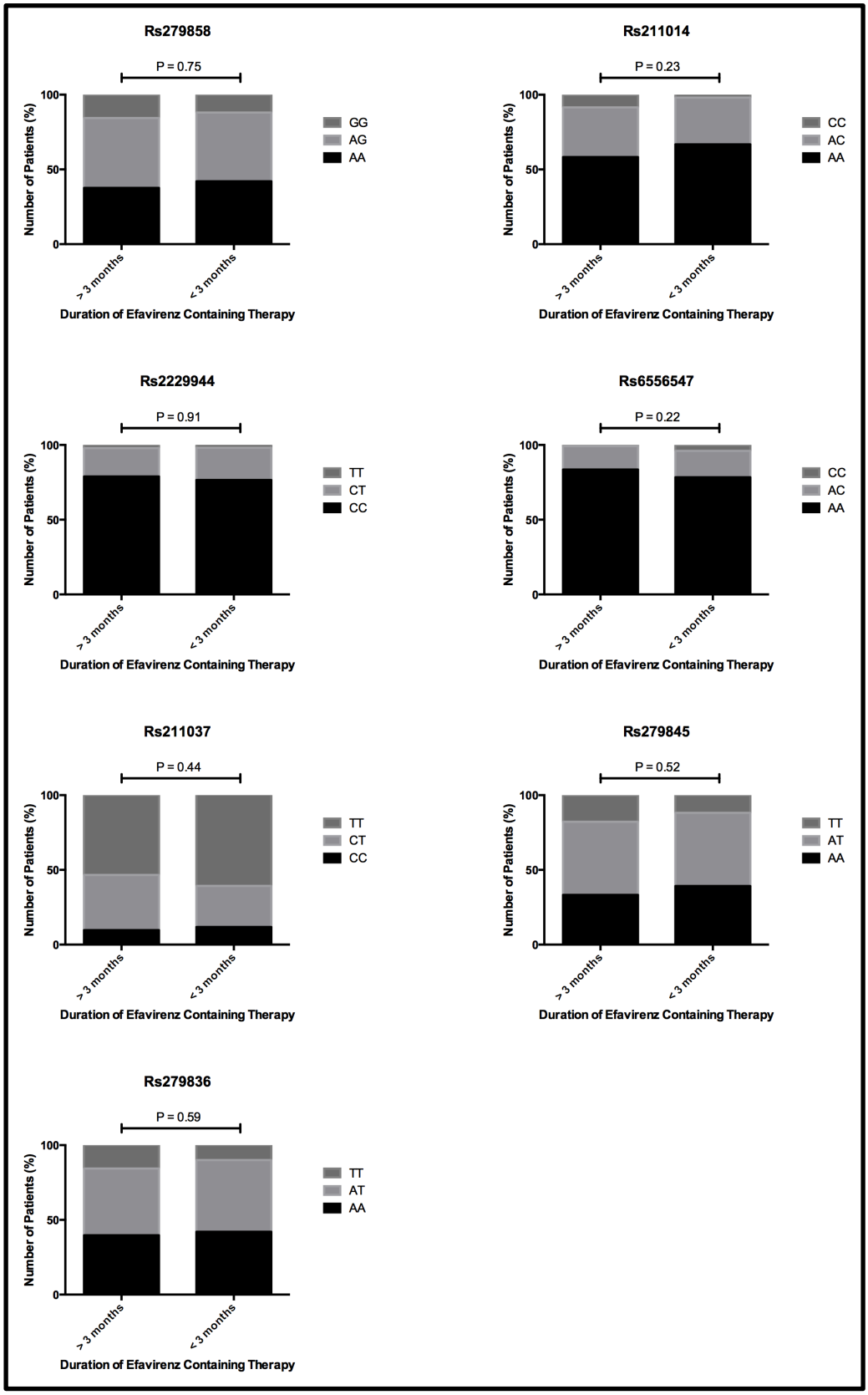

Figure 5 shows the univariate analysis of the training cohort for SNPs in the GABA receptor subunits (Rs279858, Rs211014, Rs2229944, Rs6556547, Rs211037, Rs279845 and Rs279836). Black bars indicate homozygous common allele, light grey indicate heterozygous and dark grey indicate homozygous variant alleles. Also shown are the P values generated via the χ^2 test.

The data was further examined by performing carrier/non-carrier analysis (Table 5). Although no significant associations were determined, 2 SNPs were found to be trending towards significance when analysed for carrier/non-carrier relationship. There was a lower degree of discontinuation in patients with the homozygous variant allele in Rs211014 (2% of patients homozygous for the variant allele vs 8.4% of patients homozygous common allele and heterozygous variant allele, P = 0.1). The converse was observed with Rs6556547. A higher rate of discontinuation was observed in patients with the homozygous polymorphism (3.9% of patients homozygous for the variant allele vs 0.8% of patients homozygous Common allele and heterozygous variant allele, P = 0.09). As a trend towards significance was identified with Rs211014 and Rs6556547, these two SNPs were further investigated in the test cohort.

SNP	Duration of therapy	Homozygous Common allele + Heterozygous variant allele	Homozygous variant allele	P Value	Homozygous Common allele	Heterozygous common allele + Homozygous variant allele	P Value
Rs297858	> 3 months < 3 months	84.4% 15.6%	88.0% 12.0%	0.52	37.6% 62.4%	42% 58%	0.56
Rs211014	> 3 months < 3 months	91.6% 8.4%	98% 2.0%	0.10	58.2% 41.8%	66.7% 33.3%	0.27
Rs2229944	> 3 months < 3 months	97.9% 2.1%	98.0% 2.0%	0.95	78.9% 21.1%	76.5% 23.5%	0.70
Rs6556547	> 3 months < 3 months	99.2% 0.8%	96.1% 3.9%	0.09	83.5% 16.5%	78.4% 21.6%	0.39
Rs211037	> 3 months < 3 months	46.6% 53.4%	39.2% 60.8%	0.34	9.7% 90.3%	11.8% 88.2%	0.66
Rs279845	> 3 months < 3 months	82.3% 17.7%	88.2% 11.8%	0.30	33.3% 66.7%	39.2% 60.8%	0.42
Rs279836	> 3 months < 3 months	84.4% 15.6%	90.0% 10.0%	0.31	39.7% 60.3%	42.0% 58.0%	0.76

Table 5 shows the univariate analysis of the training cohort for SNPs in the GABA receptor subunits when grouped by heterozygotes for the polymorphism of interest with either the homozygous common allele or the homozygous variant allele.

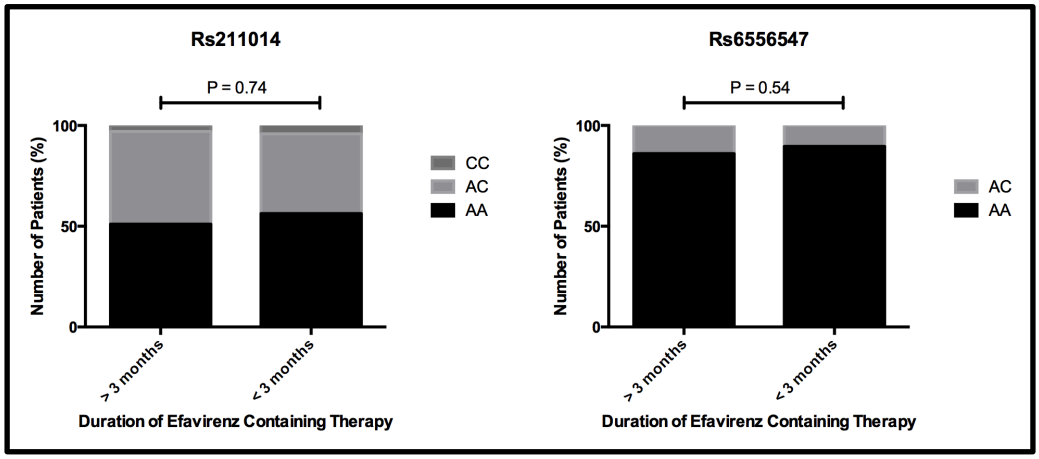

Figure 6 shows the univariate analysis of the test cohort for SNPs in the GABA receptor subunits (Rs211014 and Rs6556547). Black bars indicate homozygous common allele, light grey indicate heterozygous and dark grey indicate homozygous variant alleles. Also shown are the P values generated via the χ^2 test.

Analysis of Rs211014 and Rs6556547 in the test cohort did not show an association with early treatment discontinuation, P = 0.74 and 0.54, respectively (Figure 6). As with the training cohort, the genotypes a carrier/non-carrier analysis was performed. Rs211014 showed no significant difference in the rate of discontinuation when the heterozygotes were grouped with the common allele (40.0% of patients homozygous for the variant allele vs 32.2% of patients homozygous common allele and heterozygous variant allele, P = 0.71) or the variant allele (36.6% of patients homozygous for the variant allele and heterozygous variant allele vs 30.0% of patients homozygous common allele, P = 0.59. There were no homozygous variant alleles for Rs6556547 in the test cohort, precluding further univariate analysis.

2.3.4 Association of GABA SNPs With Early Treatment Discontinuation, Multivariate Analysis

As ethnicity and smoking status were revealed to have a significant association and both Rs211014 and Rs6556547 (when common allele and heterozygotes were compared against homozygous variant alleles) were found to trend towards significance, these 4 variables were considered in the multivariate analysis of the training cohort. The multivariate analysis (Table 6) showed neither Rs211014 and Rs6556547 were associated with early treatment discontinuation. Both Ethnicity and smoking status showed a strong association, P = 0.001 and P < 0.001 respectively.

Covariate	Odds Ratio	P value
Ethnicity	0.25 (0.11-0.54)	0.001
Smoking Status	0.37 (0.23-0.59)	<0.001
Rs211014	NS	0.28
Rs6556547	NS	0.11

Table 6 shows the results of the multivariate analysis of the training cohort for ethnicity, smoking status, Rs211014 and Rs6556547 (when widtype and heterozygotes were compared against homozygous variant alleles). Also shown are the odds ratio (confidence interval) and P value. NS = not significant.

In the test cohort Rs211014 and Rs6556547 were not shown to be significant in the univariate analysis. Only ethnicity and gender were shown to be significant and included in the multivariate analysis (Table 7). Only ethnicity was determined to be significantly associated with early treatment discontinuation.

Covariate	Odds Ratio	P value
Ethnicity	0.13 (0.29-0.62)	0.01
Gender	NS	0.38

Table 7 shows the results of the multivariate analysis of the training cohort for ethnicity and gender. Also shown are the odds ratio (confidence interval) and P value. NS = not significant.

2.4 Discussion

There have been multiple previous studies examining genetic associations with efavirenz-associated CNS toxicity. Polymorphisms in genes such as *CYP2B6*, constitutive androstane receptor (*CAR*), *ABCG2* (BCRP) and *ABCC1* (MRP1) have shown an association with of efavirenz associated CNS toxicity (65, 72, 126). Many of these associations are linked to efavirenz plasma concentrations. However, factors influencing plasma concentrations do not fully explain the development of CNS toxicity. This is demonstrated by examining ethnicity. Despite black patients being at risk of having higher plasma concentrations of efavirenz, studies have demonstrated (including the data presented here) that black patients show decreased rates of CNS toxicity and treatment discontinuation (75). This indicates that confounding factors may be involved in the aetiology of efavirenz CNS toxicity.

This study aimed to investigate the association of SNPs in the GABA receptor and early discontinuation. Despite an initial trend with Rs211014 and Rs6556547 in the univariate analysis of the training cohort, these SNPs were not found to be significant in the multivariate analysis or in either analysis of the test cohort. Although the polymorphisms in the GABAa receptor investigated here did not show an association with efavirenz early discontinuation, there is functional evidence to support the role of the GABA receptor in efavirenz associated CNS toxicity. Gatch *et al* demonstrated that efavirenz was unable to activate the GABA receptor alone. However, efavirenz potentiated signalling in the presence of GABA, indicating a mechanism of action analogous to benzodiazepines (127).

The selected SNPs examined in this study are in the genes coding for the α_2, β_2 and γ_2 subunits. Although the α_{1+2}, β_2 and γ_2 subunits form the most common GABA receptor, there are 15 different subunits that can organise in different ways to form multiple GABA receptors (111). Figure 7 shows the receptors formed from the subunits found in rat brain. Given the wide array of possible receptors it is indeed possible that efavirenz may interact with one or more GABA receptor subtypes. Therefore, future studies may identify genetic associations that implicate GABA receptor subtypes in the development of efavirenz-associated CNS side effects.

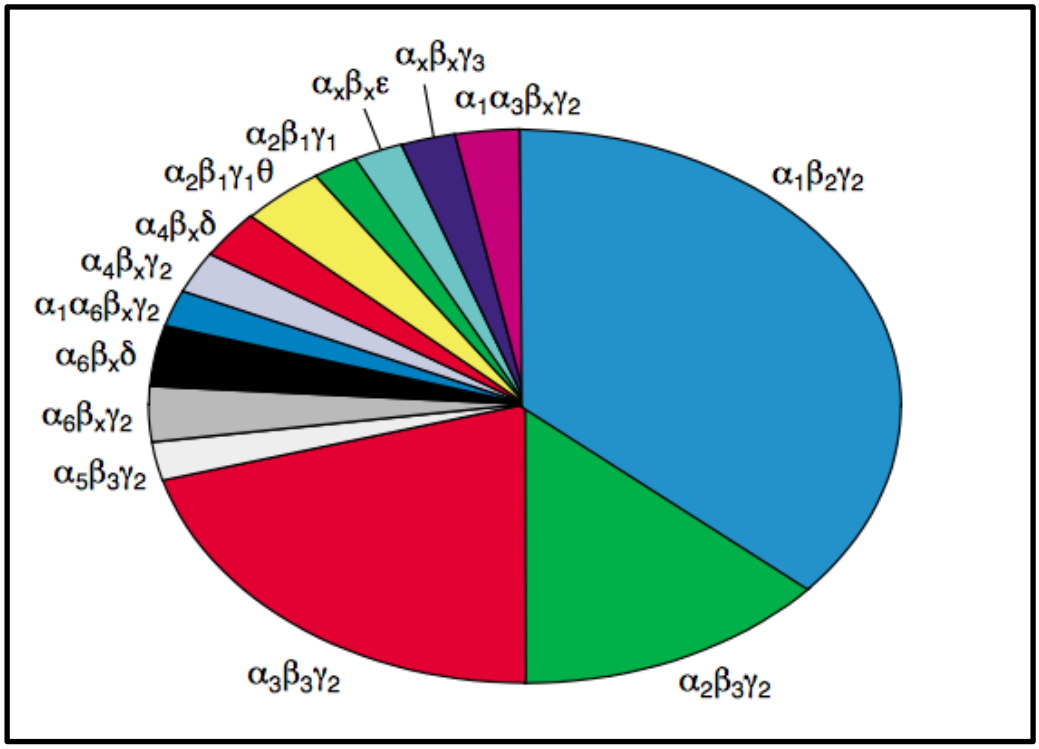

Figure 7 shows the frequency of GABA receptors and the subunits they are composed of. Source (111)

Another reason the SNPs examined here showed no association with early treatment discontinuation is perhaps the GABA receptor does not play a role in CNS toxicity. As previously discussed there are other neurotransmitters implicated in the natural occurrence of symptoms associated with efavirenz CNS toxicity. Indeed, there is data generated from *in vitro* and genetic association studies supporting the role of neurotransmitters. Recent studies have provided evidence to implicate the serotonin receptor 5 hydroxy tryptamine $_{2A}$ (5-HT_{2A}). Efavirenz has been shown to act as a weak partial agonist in cell based assays and induces behavior consistent with activation of the 5-HT_{2A} receptor in rodent behavioral models (127). The *in vitro* evidence is supported by data generated in humans. Following 7 days of exposure to efavirenz, it was found patients suffered several sleep disturbances including reduced time to sleep onset, an increase in non-rapid eye movement sleep and reduced performance on an attention switching task. Treatment with a 5-HT_{2A} antagonist induced some of the effects observed in efavirenz treatment, indicating an interaction with efavirenz and the 5-HT_{2A} receptor (128). Additionally it has been shown that the SNP *5-HT_{2A} 102C>T* has a relationship with reports of sadness in patients receiving efavirenz (P=≤0.01, although this was not reported as significant due to Bonferroni correction) (65). These data suggest further study into the interactions of efavirenz and the serotonin receptors may be warranted. It is worth considering that efavirenz CNS toxicities may not be based on interactions with a single receptor. The wide array of symptoms of CNS toxicity indicates multiple receptors and receptor subtypes may be involved. This may make identifying SNPs difficult as susceptibility to efavirenz CNS toxicity may be due to a combined effect of polymorphisms in multiple genes coding for CNS receptors.

A limitation of this study is treatment discontinuation was used to indicate efavirenz CNS toxicity in place of a detailed patient history of CNS disturbances. In addition to CNS toxicity, patients may discontinue for virological failure, poor adherence. Early treatment discontinuation is assumed to be in response to the development of CNS toxicity. However, this surrogate marker for CNS disturbance may be insufficient to gauge the true frequency of CNS toxicity within the population.

The natural occurrence of conditions such as depression involves a complex interplay of factors influencing neurotransmission. This makes identifying single predictors of efavirenz CNS toxicity more difficult. The GABA receptor may be involved in the aetiology of efavirenz-associated CNS side effect and future studies are required to elucidate this potential interaction.

Chapter 3

The *in vivo* effects of solid drug nanoparticle and conventional efavirenz on anxiogenesis in rodents

Contents

3.1 Introduction

Over the past 30 years there have been remarkable advancements in the therapy of HIV. The approach to treatment has evolved from simple monotherapy to a complex dosing regimen comprised of multiple drugs from numerous classes (129). Despite the significant advances in using this treatment approach, there are many aspects of modern antiretroviral therapy that may be improved. For example, the development of new pharmaceutical agents can be prohibitively expensive and are often abandoned due to inherent issues in drug exposure, efficacy and/or safety. Nano-formulation technologies offer the opportunity to examine existing pharmaceutical agents and address inherent issues in drug pharmacokinetics (poor absorption, rapid clearance, unfavourable tissue distribution, etc) whilst maintaining the favourable properties of the drug (92).

The NNRTI efavirenz has been used in first-line therapy of HIV for over 15 years (130). Efavirenz displays potent activity against wild type HIV-1, IC_{50} (against viral replication) 0.51 ng/mL, K_i (inhibition of the RT enzyme) 2.93 nmol/L and a long $t_{1/2}$ of 40-76 hours, enabling once daily dosing (57, 89). Despite these favourable properties, there are known issues with the pharmacokinetics of efavirenz that have the potential to influence therapy. Specifically, efavirenz has very poor water solubility (<10μg/ml) that may impact negatively on bioavailability by impeding intestinal dissolution and oral drug absorption (97). Additionally, pharmacokinetic exposure to efavirenz shows a high degree of inter-individual variability in patients (97). Our group have previously reported an efavirenz SDN formulation, which attempted to alleviate

the issue of poor drug solubility. Utilising an emulsion-templated freeze-drying process, SDNs were produced that achieved 70% drug loading. *In vitro* studies showed increased cellular accumulation and reduced cytotoxicity of efavirenz in Caco-2 cells while *in vivo* pharmacokinetic studies performed in rats demonstrated an increase in plasma efavirenz concentrations of approximately 4-fold following a single oral dose (97).

Efavirenz is associated with neurocognitive adverse events, which can negatively impact patient treatment (89). Efavirenz CNS toxicity and the negative impact on patient adherence are discussed in section 1.4.1. Although the clinical efficacy of efavirenz is well characterised, there is a paucity of information regarding the underlying mechanisms of efavirenz-associated CNS toxicity, making testing of novel efavirenz formulations problematic.

Behavioural pharmacology has been used previously to assess the CNS toxicity of efavirenz in both rats and mice (131, 132). Romão et al demonstrated efavirenz significantly altered rodent behaviour in multiple behavioural and cognitive performance tests including the elevated plus maze (EPM) (131). Efavirenz significantly reduced exploration in the open arm of the EPM, indicating an anxiogenic effect of efavirenz. The findings of this study demonstrated that efavirenz produced anxiety-like behaviour whereas another NNRTI, nevirapine, did not. This supports clinical data, as it has been observed in humans that CNS side effects are associated with efavirenz treatment discontinuation and not with nevirapine-containing therapy (133).

Here we investigated neurocognitive disturbances in rats using the EPM after administration of a conventional pre-clinical formulation of efavirenz or SDN formulation of efavirenz. In this model, the degree of anxiety was demonstrated by the relative proportions of time spent in the open arms versus the closed arms and central platform, with greater anxiety linked to less time on the open arms (134). In addition to the traditional measures, there are a number of ethological measures that may increase the sensitivity of the EPM test. These measures can be characterised into two groups, risk-assessing behaviour and behaviour-indicating sedation. Risk-assessing behaviour includes head dips, stretch attend posture, rears and closed arm returns. Sedation is described by periods of grooming and other non-exploratory behaviour (135). Recording behaviour associated with risk assessment and sedation allows analysis of behaviour whilst on the EPM that would otherwise be unaccounted.

Since the mechanisms of efavirenz-associated CNS toxicity are currently unknown, there are no *in vitro* tests that can be applied to assess the impact of nanoformulation on the development of efavirenz-associated CNS toxicity. This presents a problem with regards to assessing the safety and impact of novel formulations of efavirenz. Behavioural pharmacology allows for the pre-clinical screening of novel formulations of efavirenz. In this study, the anxiety-like behaviour in rats was assessed using the EPM after administration of a conventional pre-clinical formulation of efavirenz efavirenz, SDN efavirenz formulation or vehicle control. Previously published studies with the SDN formulation have demonstrated the potential to increase the exposure of efavirenz. As efavirenz exposure has been associated with an increased in

occurrence of CNS toxicity (as discussed in section 1.4.1) it was considered prudent to assess the incidence of anxiety (one of the symptoms of efavirenz associated CNS toxicity) in response to conventional pre-clinical formulation of efavirenz and the SDN formulation of efavirenz.

3.2 Methods and Materials

3.2.1 Materials

Male Wistar rats were purchased from Charles River (Oxford, UK) Methylcellulose was purchased from Sigma Aldrich (Dorset, UK). Efavirenz powder (>98% pure) was purchased from LGM Pharma inc (Boca Raton, USA). All other consumables were purchased from Sigma Aldrich (Dorset, UK).

3.2.2 Animals and treatment

Male Wistar rats (Charles River, UK) weighing 180 – 220g on arrival were used in EPM experiments. Animals were singly-housed in the absence of environmental enrichment on a normal light cycle. All experimental testing was conducted during the light phase of the cycle. Food and water were provided *ad libitum*. All experiments were conducted under appropriate personal and project licenses (granted by the Home Office, UK).

3.2.3 Emulsion-Templated Freeze-Drying to Form Efavirenz Nanoparticles

Efavirenz SDNs were prepared as described previously (97). In Brief, a mixture of efavirenz (dissolved in chloroform) and stabilisers (poly[vinyl alcohol] and α-tocopherol polyethylene glycol succinate, dissolved in H_2O) was prepared in the ratio of 70% efavirenz, 20% poly(vinyl alcohol) and 10% α-tocopherol polyethylene glycol succinate. The mixture was emulsified using a Covaris S2x acoustic homogenisation system (Covaris, MA, USA). Samples were immediately freeze-dried leading to the formation of an emulsion template porous monolith. SDNs were dispersed in dH_2O for use in *in vivo* experiments.

3.2.4 Drug Treatment

Wistar rats were assigned to 3 groups (10 rats per group) and dosed with either conventional efavirenz (10 mg/kg, 2ml/kg 0.5% methylcellulose in dH_2O), SDN formulated efavirenz (10mg/kg, 2ml/kg in dH_2O) or vehicle control (2ml/kg 0.5% methylcellulose in dH_2O). Dosage was based on individual weight taken prior to dosing. Dosing was administered once daily via oral gavage over 5 weeks.

3.2.5 Equipment

The EPM was a wooden plus shaped maze with a black Plexiglas floor. The maze consisted of 2 open arms (10x50 cm), 2 closed arms enclosed with clear Plexiglas (10x50x50 cm) and a central platform (10x10 cm). The maze was fixed to a black metal base (50cm) to elevate the maze above ground level. The edges of the maze were raised (0.5cm) to facilitate retention of the rats.

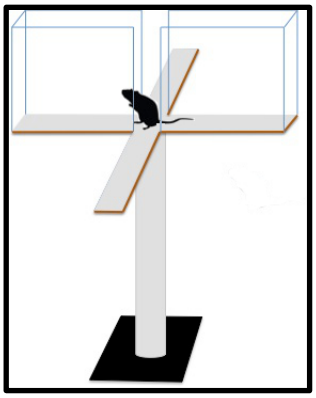

Figure 1 depicts the EPM

3.2.5 Elevated Plus Maze Procedure

Following weighing and oral dosing the rats were taken back to their home cage for 2 hours. The rats were transported individually from the housing room to the testing room. Rats were placed on the central square facing an open arm. The test was administered for 5 minutes. During testing, the experimenter remained in the testing room seated silently in the same position for all tests. At the conclusion of the test the rat was returned to its home cage and the maze was thoroughly cleaned using ethanol (70% ethanol) wipes and allowed to dry. Testing

commenced 7 days after daily dosing was initiated. The EPM was repeated once every 7 days for 5 weeks. All tests were recorded for later analysis using a digital camera (Samsung DV300F) at an angle of approximately 45°. Digital recordings of the EPM were analysed using the Ethowatcher software package (http://ethowatcher.ufsc.br). Data was analysed for spatial distribution and ethological behaviour (Table 1).

Behavioral Measure	Description
Open arm entrance	An entrance to open arm is counted as 4 paws placed on the open arm
Closed arm entrances	An entrance to open arm is counted as 4 paws placed on the closed arm
Time in open arm	The time (expresses as a percentage of total time on the maze) spent on the open arm
Time in closed arm	The time (expresses as a percentage of total time on the maze) spent on the closed arm
Time on central platform	The time (expresses as a percentage of total time on the maze) spent on the central platform
Central platform latency	Time taken to initially move from central square
Risk assessment	The number of occurrences of behaviour indicating assessment of the environment for potential risk factors (stretch attend postures, head dips and rearing)
Sedation	The total time spent stationary (grooming and non-exploratory behaviour)

Table 1 summary of the spatial and ethological measures recorded during exposure to the EPM

3.2.6 Statistics

All data were assessed for normality using the Shapiro Wilk test. Statistical analysis was performed by Mann-Whitney U test and significance was defined as $P < 0.05$. All data are given as median with interquartile range [IQR].

3.3 Results

3.3.1 Spatial distribution

Data for the spatial distribution during the EPM test was collected for the number of open and closed arm entrances, the duration of time (expressed as % of total time on the maze) in the open arms, closed arms and central platform and the central platform latency. The median for each group was plotted against duration of treatment (Figure 2). The AUC was calculated for individual rats in order to examine the effect of each condition over the period of dosing. The median AUC of each group was plotted (Figure 3) and compared for statistically significant differences.

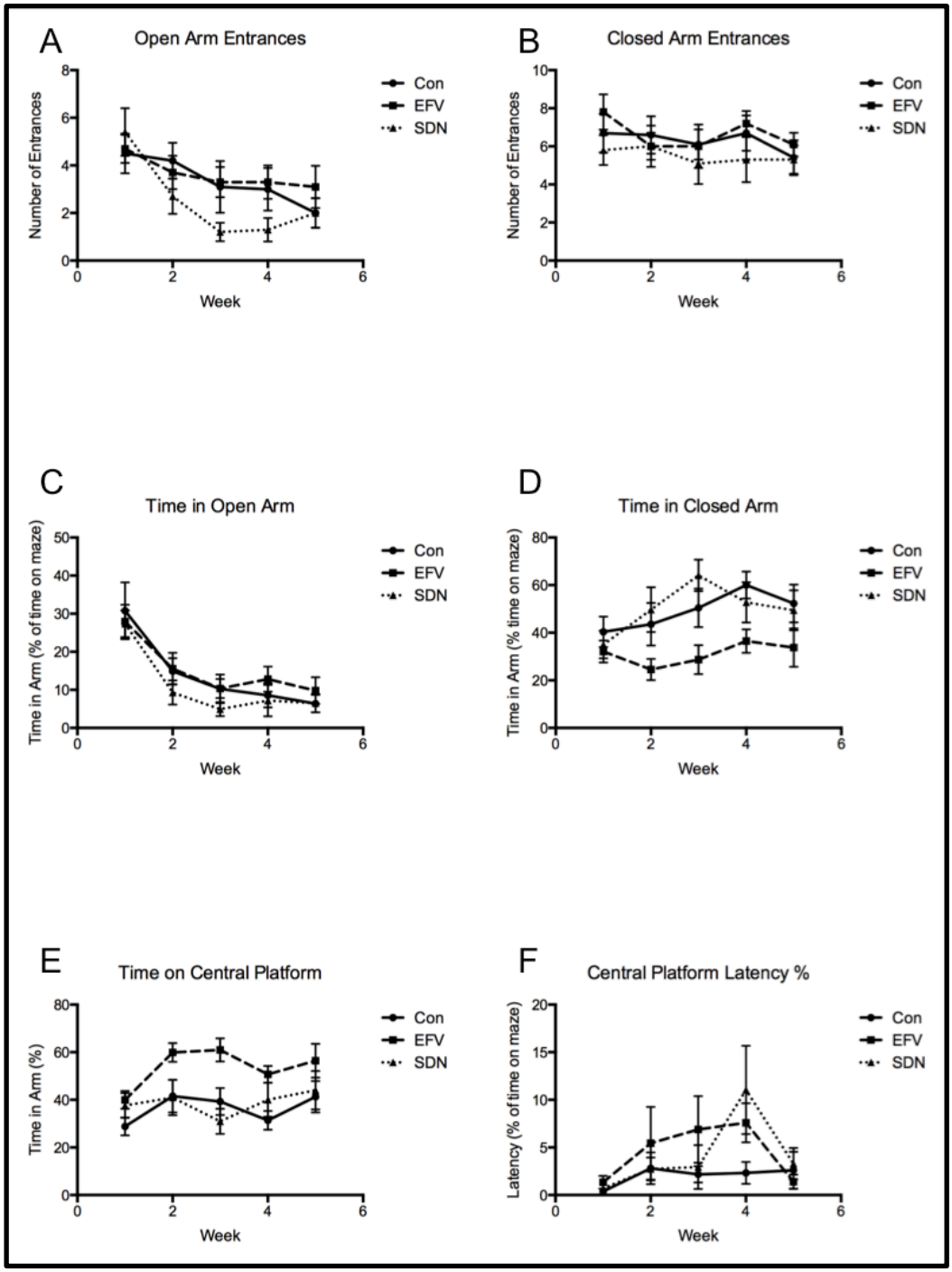

Figure 2 show the behavioral measures plotted against time from the EPM for control (Con), conventional efavirenz (EFV) and solid drug nanoparticle efavirenz (SDN). The graphs display time plotted against spatial measurements open arm entrances (A), closed arm entrances (B), time in open arm (C), time in closed arm (D), time on central platform (E) and central platform latency (F). Data points represent median with interquartile range. N = 10.

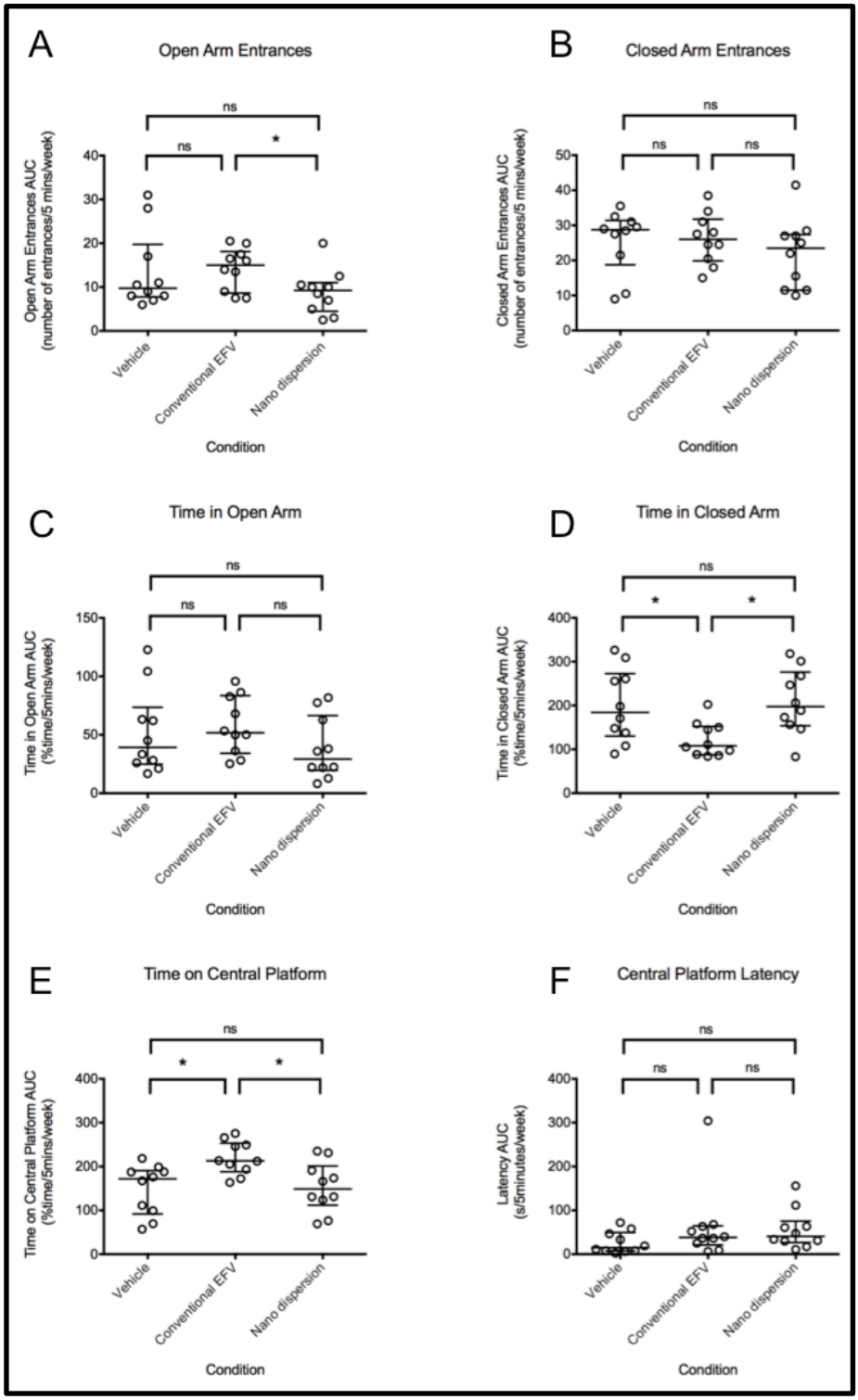

Figure 3 shows the AUC (for each of the measurements displayed in Figure 2) for vehicle control, conventional pre-clincial formulation of efavirenz (EFV) and nano dispersion. The graphs display the AUC of open arm entrances (A), closed arm entrances (B), time in open arm (C), time in closed arm (D), time on central platform (E) and central platform latency (F). Data points represent mean with interquartile range. Also displayed are the results of the Mann-Whitney U test and significance was defined as $P < 0.05$. N= 10.

The number of entrances to the open arm made by the vehicle control group (9.8 events/5mins/week [IQR 7.8-19.8]) was not significantly different from either the pre-clinical formulation of efavirenz (15.0 events/5mins/week [IQR 8.6-18.1], P = 0.44) or SDN (9.3 events/5mins/week [IQR 4.5-11.0], P = 0.32) (Figure 3A). The conventional pre-clinical formulation of efavirenz group made significantly more open arm entrances than the SDN group (P = 0.04). The number of entrances to the closed arm made by the vehicle control group (28.8 events/5mins/week [IQR 18.8-31.4]) was not significantly different from either the conventional pre-clinical formulation of efavirenz (26.0 events/5mins/week, [IQR 19.9-31.8], P = 0.44) or SDN (23.5 events/5mins/week [IQR 11.5-27.4], P = 0.22) (Figure 3B). There was no significant difference in the closed arm entrances between efavirenz and the SDN groups (P = 0.32).

The duration of time spent on the open arm made by the vehicle control group (39.2 % time/5mins/week [IQR 24.8-73.5]) (Figure 3C) showed no significant difference in comparison with either the conventional pre-clinical formulation of efavirenz group (51.8 % time/5mins/week [IQR 34.2-83.6], P = 0.44) or the SDN group (29.2 % time/5mins/week [IQR 19.7-66.5], P = 0.44). The efavirenz group showed no significant difference from the SDN group (P = 0.06). There was no significant change in the time spent on the closed arm (Figure 3D) when comparing the SDN group (197.4 % time/5mins/week [IQR 153.9-276.3]) with the vehicle control group (184.2 % time/5mins/week [IQR 130.3-272.8], P = 0.80. The conventional pre-clinical formulation of efavirenz group spent significantly less time (107.9 % time/5mins/week [IQR 87.7-152.1], on the closed arm than either the vehicle control (P = 0.029) or SDN (P = 0.011)

groups. There was no significant change in the time spent on the central platform (Figure 3E) when comparing the SDN group (111.8 % time/5mins/week [IQR 112.0-201.1]) with the vehicle control group (171.7 % time/5mins/week [IQR 91.9-190.7], P = 0.91. The conventional pre-clinical formulation of efavirenz group showed the inverse of the closed arm, spending increased time (212.9 % time/5mins/week [IQR 188.3-253.3]) on the central platform, when compared to the control group or the SDN group, P = 0.009 and P = 0.011, respectively. The central platform latency (Figure 3F) of the control group (15.0 seconds/5mins/week [IQR 7.5-49.4]) showed no significant difference compared to the efavirenz (38.2 seconds/5mins/week [IQR 21.05-64.6], P=0.17) group or the SDN group (40.6 seconds/5mins/week [IQR 26.7-75.4], P=0.08). The efavirenz group showed no significant difference from the SDN group (P = 1.00).

3.3.2 Ethological measures

In addition to collecting data on the spatial distribution of the rats, a number of ethological measures were recorded. The ethological measures were divided into 2 categories: risk-assessing behaviour (stretch attend postures, head dips and rearing) and behaviour-indicating sedation (instances of grooming and non-exploratory behaviour). From these multiple behaviours 2 composite measures were created: risk assessment (the total number of occurrences of behaviour indicating assessment of the environment for potential risk factors) and sedation (the total duration of time spent stationary). As with the spatial measures the median for each group was plotted against duration of treatment (Figure 4). The

median AUC of each group was plotted (Figure 5) and compared for statistically significant differences.

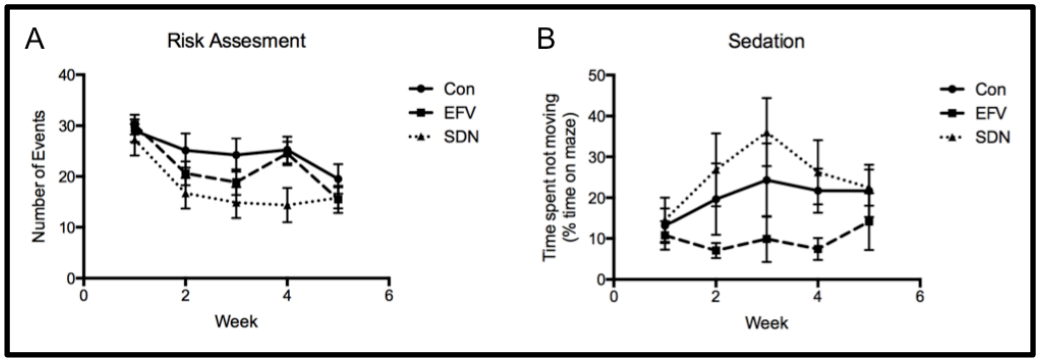

Figure 4 shows the ethological measures plotted against time from the EPM for vehicle control, conventional pre-clincial formulation of efavirenz (EFV) and nano dispersion. The graphs display risk assessment (A) and sedation (B). Data points represent median with interquartile range. N = 10.

The SDN group showed significantly less instances of risk-assessing behaviour (Figure 5A) (66.3 events/5mins/week [IQR 47.3-88.3]) when compared to the vehicle control (99.3 events/5mins/week [IQR 84.0-108.1]), P = 0.02. There was no significant difference in risk assessing behaviour when comparing the conventional pre-clinical formulation of efavirenz group to either the vehicle control or SDN groups, P = 0.35 and P = 0.09, respectively. There was no significant difference in sedation (Figure 5B) in the conventional pre-clinical formulation of efavirenz (111.2 events/5mins/week [IQR 40.3-161.3]), or SDN (309.7 events/5mins/week [IQR 119.5-549.3]), compared to the control (179.6 events/5mins/week [IQR 74.5-443.9]), P = 0.14 and P = 0.44 for conventional pre-clinical formulation of efavirenz and SDN, respectively. There was a

significant increase in the SDN group compared to the conventional pre-clinical formulation of efavirenz group, P = 0.03.

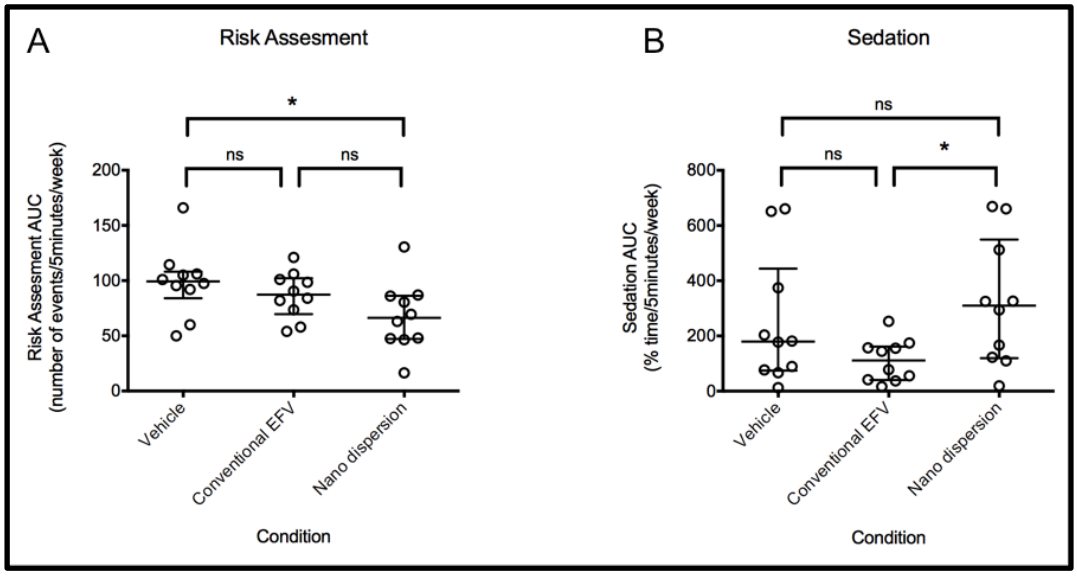

Figure 5 shows the AUC (for each of the measurements displayed in Figure 4) for vehicle control, conventional pre-clinical formulation of efavirenz (EFV) and nanodispersion. The graphs display the AUC of risk assessment (A) and sedation (B). Data points represent mean with interquartile range. Also displayed are the results of the Mann-Whitney U test and significance was defined as $P < 0.05$. N= 10.

3.4 Discussion

The data presented in this chapter show that following multiple doses rats treated with efavirenz, but not SDN efavirenz, exhibited anxiety-like behaviour in the EPM. Our experiment failed to fully replicate the anxiogenic effects of efavirenz that were previously reported in mice using the EPM (131). However, the profile of changes indicated some clear behavioural effects that are likely to be linked to drug-related CNS effects. In particular, a tendency of efavirenz to increase time spent on the central platform may be indicative of anxiogenesis. By contrast, the efavirenz SDN did not consistently affect behaviour in a manner that would indicate anxiogenic activity.

The EPM has been used for over 20 years to investigate anxiety in rodents (136). Typically the EPM has been used to focus on the spatial distribution of the rodent over time, measuring the ratio of time spent on the open and closed arms. These measures assess the rodent's natural tendency towards enclosed spaces and aversion towards open spaces and heights against their natural instinct to investigate novel environments (134). Using traditional measures anxiolytics (such as benzodiazepines) and anxiogenics (such as N-methyl-B-carboline-3-carboxamine, FG 7142) will increase and decrease time spent in the open and closed arms respectively (137). However, over the years of usage a number of groups have identified additional measures of anxiety, which can be used for the EPM system. Time spent on the central platform is a factor that is not frequently reported, although there have been previous publications that associated increased time spent here with anxiety-like behaviour (138, 139). Additionally,

benzodiazepines such as nitrazepam have been shown to decrease time spent on the central square (137).

The data presented here show no significant differences in exploration of the open arm in either the efavirenz or SDN groups when compared to the control group. Using only traditional measures these data would indicate no anxiogenesis in response to either treatment. However, by employing additional measures, subtle differences in behaviour were observed. The time spent in the closed arm and central platform was significantly different when comparing efavirenz to the control or SDN groups for the majority of the testing period. In week 2, the percentage of time spent on the central platform was increased in the efavirenz group, with an associated decrease in time spent on the closed arm, compared to either the SDN or control. The pattern of increased time on the central square in response to conventional efavirenz was also observed in weeks 3 and 4. There was no difference in the distribution of time spent in open arm, closed arm or central square in weeks 1 and 5, possibly due to efavirenz having not accumulated enough in the rodents to induce anxiety at week 1, and in week 5 the rodents may have fully habituated to the EPM.

A previous study used the EPM to investigate the anxiety-related behaviour and cognitive performance in mice following dosing with efavirenz or nevirapine. This study showed a clear distribution of open arm vs closed arm exploration (131). The behaviour was recorded following 28 days of treatment with a single administration of the EPM. One potential explanation why our study did not

show the same open:closed arm distribution may be repeat exposure to the EPM in our study. The data presented here were collected from 5 weekly tests. Efavirenz may not have accumulated enough in the rodents to induce anxiety at week 1 and the behaviour in each of the 4 remaining tests was likely to have been affected by habituation. There is evidence demonstrating that initial exposure to the EPM will affect the behaviour in subsequent testing. File *et al* demonstrated that benzodiazepines reduced anxiety in initial exposure to the EPM but on a subsequent test the same anxiolytic effect was no longer observed (140). The anxiety observed in our study may be more pronounced if only a single EPM test was applied. However, this initial study aimed to investigate the progression of anxiety after multiple doses.

Currently, it is unknown how long the SDN efavirenz remains *in vivo* as nanoparticles or even whether intact nanoparticles enter the systemic circulation. However, utilising fluorescence resonance energy transfer (FRET), intact nanoparticles were shown to pass through Caco-2 cell monolayers in transcellular permeation experiments (141). These *in vitro* data indicate that paracellular transport may be possible and that intact nanoparticles may traverse the gut barrier *in vivo*. The SDNs used in this study have an average diameter of 200nm (141). If SDNs do indeed enter the circulation, they may be too large to interact with the body in the same manner as solubilised efavirenz.

Although the mechanisms of efavirenz CNS side effects are currently unknown, there is evidence implicating the hydroxylated metabolites of efavirenz (OH

efavirenz). In a previous study, isolated rodent hippocampal neurons were exposed to efavirenz, 7OH efavirenz and 8OH efavirenz. Although all 3 produced neuronal damage, 8OH efavirenz was shown to be more toxic (142). 8OH efavirenz has also been shown to stimulate glycolytic flux resulting in altered glucose metabolism, which may contribute to the CNS side effects (143). Efavirenz contained within the nanoparticles may be protected from metabolism and subsequently lead to a decrease in the formation of 8OH efavirenz in comparison to conventional formulation. Indeed, this hypothesis would may also explain the higher pharmacokinetic exposure observed previously when dosed orally to rats (97)

Other potential mechanisms of CNS toxicity involve interactions of efavirenz with neurotransmitters and the associated receptors (discussed in sections 2.1 and 2.4). Behavioural analysis of rats treated with efavirenz revealed behaviour associated with modulation of the 5-HT_{2A} (127). If intact SDNs are present within the circulation and pass the BBB, the size of the SDNs may preclude interaction with the receptor where free efavirenz may be able to interact and modulate neuronal signalling via 5-HT_{2A} receptor.

We interpret these results as indicating that the nanoformulation of efavirenz may have reduced potential to induce neurocognitive disturbance, either acutely or following chronic administration.

Enhanced single dose pharmacokinetics of this formulation has previously been shown, but the limitation of the current project was that steady state pharmacokinetics was not assessed during the behavioural analysis. Previous studies have demonstrated an association with increased plasma exposure in humans and the occurrence of CNS toxicity (74). Pharmacokinetics data in plasma and brain tissue paired with the behavioural data presented here will provide a better indication of the effects of nanoformulation on the efavirenz associated CNS toxicities.

Chapter 4

Liquid Chromatography Tandem Mass Spectrometry Method for Quantification of Efavirenz in Plasma, Brain and Cell Culture Medium

Contents

4.1 Introduction

The work presented in the remainder of this thesis required the development of a liquid chromatography tandem mass spectrometer (LC-MS/MS) bio-analytical method. This chapter discusses the optimisation of the detection and quantification of efavirenz using lopinavir as internal standard (IS). The assay presented here was developed and validated in accordance with FDA guidelines (144). Criteria such as linearity, accuracy (the degree of variation from known value, assessed by controls [QCs]), precision (the degree of variation within repeated measurements), selectivity (ensuring detection of the analyte and not an endogenous compound within the sample matrix) and recovery (determining the percentage of recovery and more importantly the reproducibility of the extraction process) were all assessed.

Efavirenz was first licensed for the treatment of HIV in 1998, since then multiple methods for detection in plasma have been developed for LC-MS/MS. Many of the methods developed have been utilised to assess association with efavirenz plasma concentrations and CNS toxicity or polymorphisms in key proteins influencing efavirenz disposition (72, 74). Some recently published methods show linearity with lower limit of quantification ranging from 20ng/ml to 300pg/ml (145, 146).

Despite the major focus being on the concentrations of efavirenz in plasma, other matrices have also been investigated such as recent work on breast milk.

Currently, the WHO recommends “on demand” breast-feeding for new born (147). This presents a unique difficulty as mothers receiving antiretroviral therapy are at risk of introducing antiretroviral agents to their children via breast milk. To assess this Olagunju *et al* have recently developed a novel LC-MS/MS method for detection of efavirenz in dried breast milk spots (147). The assay was linear from 50ng/ml to 7500ng/ml. Accuracy and precision ranged between 95.2% and 102.5%, 1.05% and 9.53%, respectively. Extraction from dried breast milk spots showed excellent recovery, methanol extraction yielded an average recovery of 106.4%.

As discussed previously in section 1.4.1, efavirenz CNS toxicity has been associated with high plasma concentrations. One of the limitations with such analyses is plasma concentrations of efavirenz do not necessarily correlate with concentrations in CSF and brain tissue. To investigate CNS concentrations of efavirenz, multiple LC-MS/MS methods have been developed to analyse efavirenz concentrations in CSF (50, 57, 148). An example of these methods achieved linearity over the range of 1.1ng/ml to 51ng/ml (50). Accuracy and precision were reported to exhibit <10% variability with >80% recovery. Although assessing CSF is a step towards understanding efavirenz concentrations in the CNS, CSF and brain tissue concentrations of drugs may vary wildly and may not represent the disposition of efavirenz in the CNS *per se* (as discussed in section 1.4).

Recently, an LC-MS/MS method was developed to analyse efavirenz concentrations in homogenised tissue from macaques, following orally administered efavirenz. The assay demonstrated linearity over the range of 200pg/ml to 20ng/ml. The authors assessed efavirenz concentrations in HIV sanctuary sites (discussed in section 1.5), in particular the brain, lymph nodes and GI tract. The data presented showed efavirenz accumulated in tissue when compared to plasma (~3 fold higher than plasma in the GI tract and ~2 fold higher than plasma in lymph nodes) or CSF (>6 fold greater than CSF) (149).

The work presented in this thesis required the detection of efavirenz in multiple matrices. Therefore, an assay was optimised for efavirenz from plasma and then the performance of the assay was assessed in cell culture medium, phosphate buffered saline (PBS), and brain tissue homogenate. A major concern was the interference from endogenous analytes within the non-plasma matrices that may have been present at a lower concentration or absent from plasma. The aim of this chapter was the development of a rapid, sensitive and replicable assay for the detection of efavirenz in multiple matrices.

4.2 Methods and Materials

4.2.1 Materials

Efavirenz powder (>98% pure) was purchased from LGM Pharma inc (Boca Raton, USA). Lopinavir powder (>98% pure) was purchased from LGC Pharma (London, UK). All other consumables were purchased from Sigma Aldrich (Dorset, UK).

4.2.2 Tuning for Efavirenz and Internal Standard

Detection of efavirenz and lopinavir was conducted using a TSQ endura LC-MS/MS (Thermo scientific). Tuning was performed using direct infusion (20µl/min) of a 500ng/ml stock of efavirenz with 50% mobile phase A (100% H_2O [LC-MS/MS grade] 5mm ammonium formate), 50% mobile phase B (100% acetonitrile [ACN] 5mm ammonium formate) at a flow rate of 300µl/min. Ionisation was achieved via heated electron spray ionization in negative mode. The following parameters were optimised to achieve the highest signal intensity for efavirenz spray voltage, sheath gas and auxiliary gas. The IS was then directly injected (500ng/ml) to ensure detection using the optimised efavirenz settings. Following optimization for the parent mass of efavirenz (315) and IS (628), selected reaction monitoring (SRM) scan was utilised for detection of the break down products.

4.2.3 Chromatographic Separation

The chromatographic separation was achieved using a multi-step gradient with a Hypersil gold C-18 column (Thermo scientific; Table 1). The assay was conducted over 8 minutes at a flow rate of 300µl/min.

Time (mins)	Mobile Phase A (%)	Mobile Phase B (%)
0.0	90	10
0.1	90	10
0.5	14	86
5.0	8	92
5.1	3	97
6.0	3	97
6.0	90	10
8.0	90	10

Table 1 shows the chromatographic conditions for the detection of efavirenz and IS.

4.2.4 Extraction from Plasma and Cell Culture Medium and PBS

One hundred µl of sample (20% ACN was added to both cell culture medium and PBS to aid efavirenz dissolution in these matrices) were diluted with ACN (sample: ACN ratio 1:4) and thoroughly vortexed. Samples were then centrifuged at 4000g for 10 minutes at 4°C. The supernatant fraction was transferred to a fresh glass vial and evaporated, samples were placed in a rotary vacuum centrifuge at 30°C and then reconstituted in 140µl of H_2O:ACN (60:40). 100µl of the sample was then transferred into 200µl chromatography vials. 5µl of each sample was injected for analysis.

4.2.5 Extraction from Brain Tissue

Male Wistar rats (Charles River, UK) weighing 180 – 220g on arrival were sacrificed using an appropriate schedule 1 method. Following termination brain was extracted and stored at -80˚C. (150). Rat brain tissue was then homogenised in 3 volumes (W:V) of plasma. Extraction was performed using protein precipitation detailed in the previous section.

4.2.6 Assay Validation

The assay was validated according to the most recent FDA guidelines (144). The following criteria were assessed: linearity, recovery, specificity, accuracy, precision, inter-assay and intra-assay variability.

Linearity

A calibration curve of efavirenz was prepared in plasma via serial dilution, ranging from 1.9ng/ml to 500ng/ml. Extraction was performed using protein precipitation. Linearity was assessed by 3 independent preparations of the standard curve. Maximum allowed deviation of standards was set at 15% of the stated value, excluding the lower limit of quantification where deviation was set at no more than 20%.

Recovery

Recovery experiments were performed by comparing the results for extracted samples of efavirenz at three concentrations (20ng/ml, 100ng/ml and 400ng/ml) with non-extracted standards that were taken to represent 100% recovery.

Specificity

The degree of interference from the matrix (due to potential interfering substances including endogenous matrix components, metabolites and decomposition products) was assessed via comparison of extracted blank samples with the lowest point of the standard curve (lower limit of quantification). The lower limit of quantification was a minimum of 5 times greater than the background signal.

Accuracy and Precision

The accuracy of an analytical method describes the closeness of mean test results obtained by the method to the actual value (concentration) of the analyte. Accuracy was assessed by preparation of three concentrations (in the range of the standard curve 20ng/ml, 100ng/ml and 400ng/ml) with each preparation in triplicate. The mean value of each concentration should be within 15% of the stated concentration (except the lower concentration, where deviation should be less than 20%**)**. Accuracy was calculated using the following formula:

$$\%\ variability\ of accuracy = \frac{error}{stated\ value}\ x\ 100$$

The precision of an analytical method describes the closeness of individual measures of an analyte when the procedure is applied repeatedly to multiple aliquots of a single volume of biological matrix. Precision of the assay was determined by preparation of three concentrations (in the range of the standard curve 20ng/ml, 100ng/ml and 400ng/ml) with each preparation in triplicate. The mean value of each concentration should be within 15% of the stated concentration (except the lower concentration, where deviation should be less than 20%**)**. Precision was calculated using the following formula:

$$\%\ variation\ of\ precision = \frac{standard\ deviation}{mean\ assay\ value}\ x\ 100$$

Accuracy and precision were assessed for intra and inter assay variability. The standard curve and QCs were prepared in triplicate and analysed 3 times. Variance in accuracy and precision should not vary within 15% of the stated

concentration (except the lower concentration, where deviation should be less than 20%) within a single assay or between repetitions of the assay (144).

4.2.7 Statistics

Data were assessed for normality using the Shapiro Wilk test. Statistical analysis was performed by unpaired T test and significance was defined as $P < 0.05$. All data are given as mean with standard deviation.

4.3 Results

4.3.1 Tuning Settings

The aim of optimising the tuning settings was firstly to maximise the detection of efavirenz and secondly to ensure detection of the IS. Table 2 shows the finalised settings.

Parameter	Optimised Setting
Negative Ion (V)	2700
Sheath Gas	35
Aux Gas	15
Sweep Gas	0

Table 2 shows the optimised tuning settings for the detection of the parent compounds of efavirenz and IS.

In addition to detecting the parent molecule, the detection of the product ions of each compound was also optimised. By searching for both the parent and product ions, sensitivity and specificity are increased. This is particularly advantageous when analytes are contained in complex matrices such as plasma (151). Table 3 shows the product ions produced during the selected reaction monitoring scan for efavirenz and IS.

Compound	Precursor (m/z)	Product (m/z)	Collision Energy (V)
Efavirenz	315	242.1	16.5
		244.0	17.0
		250.0	17.0
Lopinavir	627	121.2	33.5
		178.1	26.5
		198.1	22.5

Table 3 shows the parent mass, product ion and the collision energy for efavirenz and IS.

4.3.2 Extraction Efficiency from Plasma, Brain Tissue and Cell Culture Medium

The recovery was measured at three QC concentrations (Figure 1). The mean recovery (across all 3 QCs) from plasma, brain tissue, EBM-2 medium and PBS were 95% (standard deviation 8.9), 91% (standard deviation 7.8), 59% (standard deviation 6.1) and 84% (standard deviation 11.6), respectively. When compared to plasma, there were no statistically significant differences in recovery from brain tissue, or PBS at the low and medium QCs. The high QC was significantly lower for both brain tissue (90.72%, P = 0.01) and PBS (77.84%, P = 0.001) Recovery from the EBM-2 medium was significantly lower at all the QCs (low QC 60.06% P = 0.001, medium QC 53.24% P = 0.004 and high QC 64.98% P = 0.002).

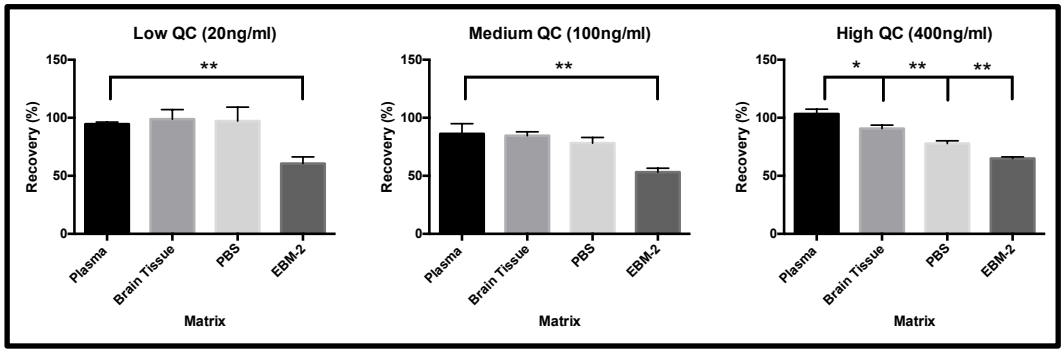

Figure 1 shows the percentage recovery for the low (a), medium (b) and high (c) QCs in extracted plasma, extracted brain tissue, EBM-2 medium (complete media is described in section 5.2.2) and PBS. Data is show percentage of unextracted standards.

4.3.3 Assay Validation

Linearity

Standards extracted from plasma showed good linearity (R^2 = 0.992). The peak area ratio (analyte to IS; variation of IS was less than 15% in each run) was proportional to the stated concentrations over the range of 500ng/ml to 1.9ng/ml. Figure 2 shows a representative calibration curve. Calibration curve was generated using a quadratic equation with a weighting of 1/X.

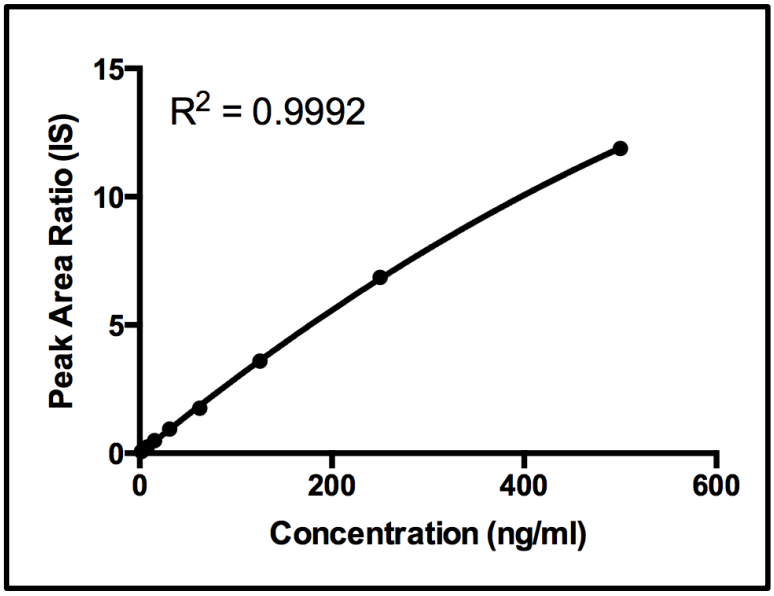

Figure 2 shows the standard curve generated from extracted plasma standards of efavirenz over the range of 500ng/ml to 1.9ng/ml.

Specificity

The matrix effect of plasma was examined by comparing extracted blank plasma to extracted plasma spiked with 1.9ng/ml of efavirenz. Figure 3a shows the chromatogram produced by the extracted blank. There is a visible peak (area of 134) at the retention time of efavirenz (3.7 minutes). FDA guidelines require the lower limit of quantification produce a peak area of at least five-fold greater than that observed in the blank matrix. Figure 3b shows the peak produced from the lower limit of quantification (1.9ng/ml). The peak area is 1491, which complies with FDA guidelines. Figure 3c shows the peak produced by the upper limit of quantification (500ng/ml).

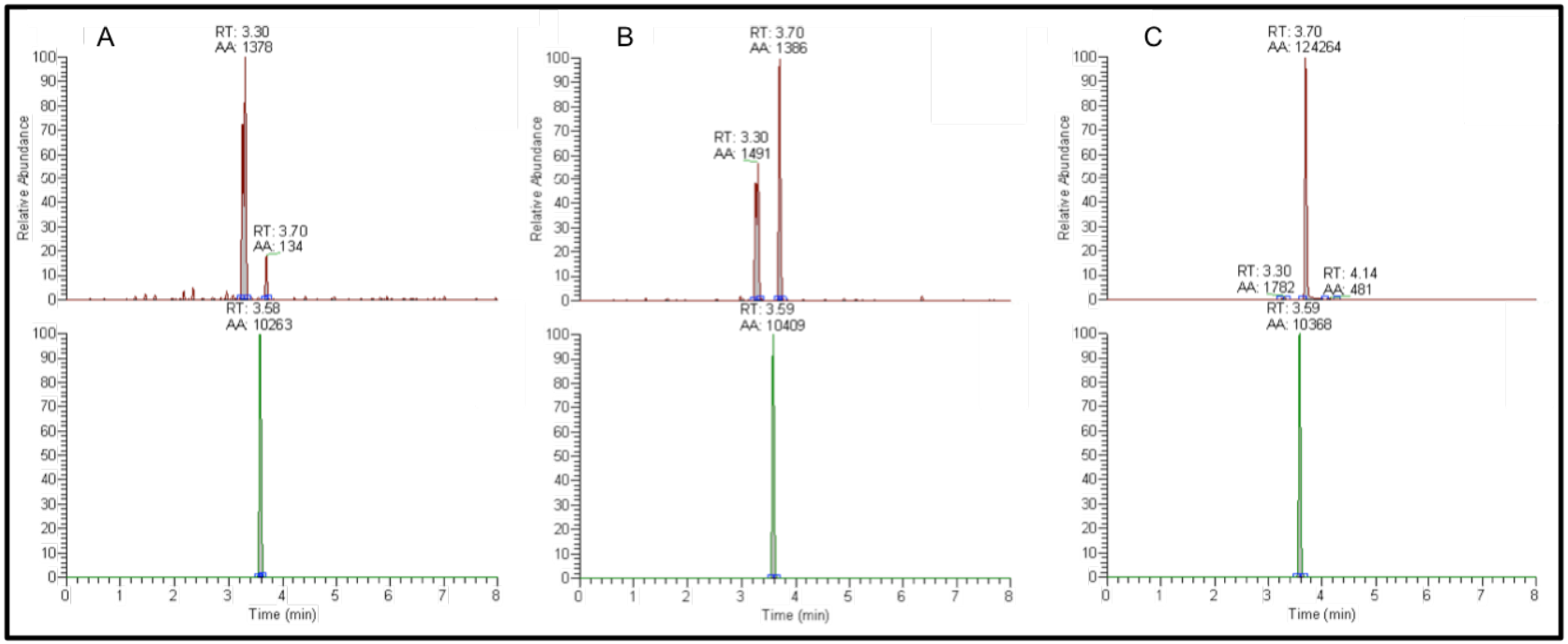

Figure 3 shows a representative chromatogram from blank plasma (A), lower limit of quantification (B) and the upper limit of quantification (C). The upper panel and lower panel of each figure shows the peak produced by efavirenz (retention time 3.7) and IS respectively (retention time 3.58).

Accuracy and Precision

The accuracy and precision for each individual run at 3 QC levels (low (20ng/ml), medium (100ng/ml) and high (400ng/ml) is shown in table 4. The percentage error of accuracy fell below 15% for each of the 3 repeats (1 varied between -0.25% and -11.45%, 2 varied between 0.01% and -6.32%, 3 varied between 0.78% and -4.66%). The percentage error of precision also fell below 15% for each of the 3 repeats (1 varied between -5.52% and 11.05%, 2 varied between 2.93% and 5.66%, 3 varied between 1.25% and 3.78%).

Inter-assay Variability

The variability between assays was calculated to demonstrate that the assay maintained accuracy and precision across repetitions of the assay. Table 5 shows the variance of accuracy and precision calculated from the mean values of the 3 repetitions of the assay. The percentage error in accuracy fell below 15% across all 3 repeats (range between -0.52% and -6.34). Percentage variance of precision also fell below 15% across all 3 repeats (range between 1.48% and 5.61%).

	Assay 1	Variance of accuracy (%)	Variance of precision (%)	Assay 2	Variance of accuracy (%)	Variance of precision (%)	Assay 3	Variance of accuracy (%)	Variance of precision (%)
Low (20ng/ml)	19.95	-0.25	11.05	19.58	-0.42	5.66	20.16	0.78	2.74
Medium (100ng/ml)	89.38	-10.62	5.52	100.01	0.01	3.88	95.34	-4.66	3.78
High (400ng/ml)	354.21	-11.45	6.63	374.70	-6.32	2.93	394.97	-1.26	1.25

Table 4 shows the accuracy and precision of 3 repetitions of the assay. Accuracy and precision were assessed in triplicate at 3 levels (low (20ng/ml), medium (100ng/ml) and high (400ng/ml).

	Average (ng/ml)	Standard Deviation	Variance of Accuracy (%)	Variance of Precision (%)
Low (20ng/ml)	19.90	0.29	-0.52	1.48
Medium (100ng/ml)	94.91	5.33	-5.09	5.61
High (400ng/ml)	374.63	20.38	-6.34	5.44

Table 5 shows the accuracy and precision of 3 repetitions of the assay. Accuracy and precision were assessed in triplicate of 3 QCs (low [20ng/ml], medium [100ng/ml] and high [400ng/ml]).

4.4 Discussion

The assay presented here represents a simple, robust and sensitive LC-MS/MS assay. In addition to accurate and precise quantification in plasma this assay has been shown to be versatile allowing quantification in brain tissue homogenate, EBM-2 culture medium and PBS. The assay was fully validated in plasma. As the change in matrix represents a minor change to the assay only partial validation for the change of matrices was required, in accordance with FDA guidelines (144).

Primary validation was conducted in plasma satisfying FDA bioanalytical method development guidelines, demonstrating good accuracy, precision and linearity. Although full validation for different matrices is not required, matrix effects must be assessed for each matrix. The change in matrix may potentially affect the behaviour of the assay significantly. Brain tissue homogenate and cell culture medium both contain different quantities of protein compared to plasma. As efavirenz is highly protein bound (99% in plasma) and poorly water soluble (<10μg/ml), the change in matrix has the potential to alter efavirenz recovery (97, 105). As the change in matrix is considered a minor change, partial validation was acceptable. Partial validation required the determination of intra assay variability in accuracy and precision (152). These data demonstrate the versatility and reliability of the assay presented here.

The sensitivity of the assay developed here is of a comparable standard to recent publications. Some of the newer assays surpass the sensitivity here, 200pg/ml in brain tissue and 300pg/ml in plasma (145, 149). The greatest advantage of the assay developed in this chapter is the ability to assess efavirenz in multiple matrices. It should also be noted that the assay was developed to assess a range of concentrations not predicted to be lower than 10ng/ml. Given the low signal produced by blanks, the lower limit of detection had not been established. The true limit of the assay is potentially much lower than the range validated here.

One significant improvement would be to include the major metabolites of efavirenz, 8OH efavirenz and 7OH efavirenz. Recent publications have demonstrated, *in vitro*, a higher cytotoxicity of 8OH efavirenz compared to the parent compound (as discussed in section 3.4). LC-MS/MS methods have been developed to examine efavirenz and its metabolites in CSF (153). The authors investigated dose reduction of efavirenz (600mg once daily to 400mg once daily) and demonstrated 8OH efavirenz concentrations in CSF did not appear to be dependant on plasma concentrations of efavirenz. The assay presented in this chapter could potentially be modified to include 8OH efavirenz and 7OH efavirenz and also optimised for use in CSF. The added advantage would be to analyse concentrations in brain tissue allowing a more complete description of the distribution of efavirenz and its metabolites in the CNS. However, these additional features were not a prerequisite for progression of the research in this thesis so further optimisation was unnecessary.

This chapter details the optimization of a robust, simple and sensitive LC-MS/MS assay. The final assay conformed to FDA bioanalytical development guidelines and was capable of assessing efavirenz in multiple matrices. Although the assay satisfied the requirements for its application in subsequent chapters, the assay could be modified to suit additional requirements as discussed.

Chapter 5

In vitro Characterisation of solid drug nanoparticle compositions of efavirenz in the hCMEC/D3 cell line

Contents

5.1 Introduction

The data generated in chapter 3 indicated reduction in anxiety in response to the SDN formulation, in comparison to a conventional pre-clinical formulation of efavirenz. Currently, it is unknown if and how long intact particles survive in the circulation. However, some published *in vitro* data indicate the possibility of SDNs entering the circulation. Using SDNs composed of FRET dyes, co-localisation of both dyes demonstrated that intact particles were able to traverse a Caco-2 monolayer in a transwell system (141). If intact particles enter the systemic circulation, differential passage across the BBB may contribute to the observations in chapter 3.

The BBB is highly effective at preventing the entry of antiretrovirals to the brain, as discussed in section 1.4. One of the major obstacles presented by the BBB, is the presence of multiple transport proteins covering a wide array of substrates. Many xenobiotics are substrates for one or more drug transporters, limiting or even completely preventing entry to the brain.

The interactions of efavirenz with transporters are not thoroughly characterised. One of the most clinically important transporters is P-gp (154). P-gp has been demonstrated to significantly impact the pharmacokinetics of numerous drugs (154). P-gp performs adenosine triphosphate (ATP)-dependent efflux from cells and it is expressed in many excretory and barrier tissues (155). In humans, P-gp is encoded by *ABCB1* and is expressed in liver, kidney, adrenal gland, intestine,

BBB, placenta, blood–testis and blood–ovarian barriers (155). Although there have been genetic associations with efavirenz concentrations, *in vitro* evidence demonstrates efavirenz is not a substrate for P-gp (156, 157). However, there is some evidence that efavirenz may be a substrate for BCRP (ABCG2). Inhibition of BCRP in an *ex vivo* model showed increased mucosal to serosal permeation of efavirenz in everted gut sacs (158). Efavirenz may also be a substrate for one or more of solute carrier organic anion transporters (SLCO) transporters. The cellular accumulation of efavirenz was reduced by montelukast and estrone-3-sulphate, suggesting inhibition of a SLCO transporter (157). The effects of montelukast may be via inhibition of other transporters, as efavirenz has previously been shown not to be a substrate of the major SLCO transporters (SLCO1A2, SLCO1B1 or SLCO1B3) (159, 160). The interactions of efavirenz and drug transporters have not been fully described, as determination of the substrate kinetics have not been conducted.

One of the potential benefits of nanoformulation is that due to their size, nanoparticles are unlikely to interact with drug transporters. This has been demonstrated *in vitro* with doxorubicin nanoparticles and BCRP (161). Although the size of a nanoparticle may preclude interactions with transport proteins, other methods of cellular uptake may begin to affect the disposition of nanoscale formulations. Endocytosis is an umbrella term to describe the multiple mechanisms (including clatharin-mediated endocytosis, calveolae-mediated endocytosis and macropinocytosis) mammalian cells have developed for the uptake of molecules from the extracellular environment (162). Nanoparticle characteristics have been demonstrated to influence the mechanisms of

endocytotic uptake (such as surface chemistry, shape and size). For example, size has been demonstrated to play an important role in which mechanism is activated. Macropinocytosis is typically used in larger particle sizes (<2μM), whereas clatharin-mediated (<300nm) and caveolae-mediated (<80nm) endocytosis are activated by smaller particles (163). Therefore, the mechanism of uptake may play an influential role in determining the intracellular fate of nanoparticles (164).

Differential uptake of efavirenz and SDN formulated efavirenz may affect the *in vivo* CNS distribution and toxicity. In order to investigate the *in vitro* mechanisms of uptake, the hCMEC/D3 cell line was used in uptake and inhibition studies. The hCMEC/D3 is an immortalised cell line derived from human microvascular brain endothelial cells. The aim of this chapter was to investigate the mechanisms of uptake of conventional pre-clinical and SDN formulations of efavirenz *in vitro* utilising the hCMEC/D3 cell line. As reduced anxiety was observed in chapter 3 and increased *in vivo* pharmacokinetics have been previously reported, we aimed to determine if different mechanisms of uptake may contribute to the observations (97).

5.2 Methods

5.2.1 Materials

EBM-2 medium was purchased from Lonza (Slough, UK), Penicillin-Streptomycin, Chemically Defined Lipid Concentrate and HEPES were purchased from Invitrogen (Paisley, UK). Fetal Bovine Serum (FBS) gold were purchased from PAA, the Cell Culture Company (Cambridge, UK). The hCMEC/D3 cell line was a kind gift from Pierre-Olivier Couraud, (INSERM, Paris, France). All other consumables were purchased from Sigma Aldrich (Dorset, UK).

5.2.2 hCMEC/D3 culture

hCMEC/D3 were cultured in EBM-2 medium supplemented with FBS gold 5%, penicillin-streptomycin 1%, hydrocortisone 1.4μM, ascorbic acid 5μg/ml, Chemically Defined Lipid Concentrate 1/100, HEPES 10mM and bFGF 1ng/mL. All culture flasks and plates were coated with rat collagen type 1 for 1 hour prior to use. Cells were cultured at 37°C in 5% CO_2. Cells ere passaged every 3-4 days when confluent.

5.2.3 MTT Assay

Cells were seeded on a pre-collagenated 96-well plate at 100µl of $1x10^5$ cells/ml. The plates were then incubated for 24 hours at 37°C in 5% CO_2 to allow cell adherence. Following incubation, the medium was replaced with 100 µl of fresh medium containing the drug at desired concentrations. Positive and negative controls were represented by no cells (representing 100% cell death) and by cells cultured in the presence of a vehicle control (representing 100% cell viability), respectively. Following 1 hour incubation with the drug, the medium was removed and replaced by 20 µl of MTT reagent (5 mg/ml solution 3-(4,5-Dimethylthiazol-2-yl)-2,5-diphenyltetrazolium bromide in Hanks balanced salt solution [HBSS]). The cells were incubated for 2 hours in the MTT reagent. Following incubation, 100 uL of lysis buffer (50% N-N-dimethylformamide in water containing 20% sodium dodecyl sulfate, 2.5% glacial acetic acid and 2.5% HCl, pH 4.7) was added to each well. Cells were then incubated overnight at 37°C in 5% CO_2 to allow complete cell lysis. Following incubation, the absorbance of each well was monitored using a TECAN GENios plate reader, with filters set to 560 nm.

5.2.4 The Effects of Inhibitors of Drug Transporters on Efavirenz Accumulation

Cells were seeded on pre-collagenated 6 well plates at a density of $2x10^6$/ml and allowed to adhere overnight. Medium was aspirated and replaced with 1ml fresh medium containing 10µM (0.014µCi) of conventional pre-clinical formulation of

efavirenz or efavirenz SDNs (in the presence or absence of transporter inhibitors, Table 1). Cells were incubated at 37°C in 5% CO_2 in the presence of the drugs for 1 hour. Following incubation, 100µl of medium was aspirated and added to scint vials with 4ml goldstar scintillation fluid (extra cellular drug content). Cells were then washed 3 times with ice-cold HBSS. Following washes, 1ml of trypsin was added to the cells and then incubated at 37°C in 5% CO_2 for 15 minutes. The trypsin was then aspirated and added to scint vials with 4ml goldstar scintillation fluid (intracellular content).

Cellular accumulation ratios were calculated using the following formula (where DPM = disintegrations per minute):

$$CAR = \frac{(intracellular\ DPM/total\ cell\ colume)}{(extracellular\ DPM/extracellular\ volume)}$$

Cellular volumes were determined using the Scepter™ cell counter 2.0 (Merck Millipore, Billerica USA). Cell volumes were taken from a mean of 3 replicates, hCMEC/D3 volume 2.27pl.

Inhibitor	Known to inhibit	Concentration used (μM)	Reference
Verapamil	ABCB1, organic cation transporter (OCT) 1	50	(165)
Probenecid	ABCC1, BCRP, multidrug resistance proteins (MRPs), organic anion transporter (OATs)	50	(166)
Prazosin	OCT1 and OCT3	50	(165, 167)
Montelukast	ABCC2, organic anion-transporting polypeptide (OATP) 1B3 OATP2B1	50	(157)
Amantadine	OCT1 and OCT2	100	(165)
Cyclosporine A	SLCO1B1, BCRP	10	(168)
Naringin	OATP1A2	50	(169)
Corticosterone	OCT3, SLCO1B1	10	(165)

Table 1 shows transport protein inhibitors used. Also shown are the transporters known to be inhibited and references.

5.2.5 The Effects of Inhibitors of Endocytosis on Efavirenz Accumulation

Cells were seeded on pre-collagenated 6 well plates at a density of $2x10^6$/ml and allowed to adhere overnight. Medium was aspirated and replaced with 1ml fresh medium containing dynasore (100μM), indomethacin (100μM) or cytochalasin B (5μM) and incubated for 30 minutes at 37°C, 5% CO_2. The mechanisms of action of these inhibitors are detailed in table 2. Following incubation, the medium was aspirated and replaced with fresh medium containing 10μM of conventional pre-clinical formulation or efavirenz SDNs. Cells were incubated at

37°C in 5% CO_2 in the presence of the drugs for 1 hour. Following 1 hour incubation, 1ml of medium was aspirated and added to 1.5ml Eppendorf tubes (extra cellular content). Cells were then washed 3 times with ice-cold HBSS. Following washes, 1ml of trypsin was added to the cells then incubated at 37°C in 5% CO_2 for 15 minutes. The trypsin was then aspirated and added to 1.5ml Eppendorf tubes (intracellular content). Samples were stored at -80°C until analysis via LC-MS/MS (detailed in chapter 4).

Cellular accumulation ratios were calculated using the following formula:

$$CAR = \frac{(intracellular\ concentration)}{(extracellular\ concentration)}$$

Cellular volumes were determined using the Scepter™ cell counter 2.0 (Merck Millipore, Billerica USA). Cell volumes were taken from a mean of 3 replicates, hCMEC/D3 volume 2.27pl.

Inhibitor	Known to inhibit	Concentration used (μM)	Reference
Dynasore	Clatharin-dependent endocytosis	100	(170)
Indomethacin	Calveoli-dependent endocytosis	100	(171)
Cytochalasin B	Actin-dependent mechanisms (including macropinocytosis and phagocytosis)	5	(172, 173)

Table 2 shows endocytosis inhibitors used. Also shown are the mechanisms known to be inhibited and references.

5.2.6 The Effects of Inhibitors of Endocytosis on Nanoparticle Uptake

In addition to investigating the effect of endocytosis inhibitors on intra-cellular efavirenz concentrations, we also aimed to investigate the uptake of SDN particles. Recently, Liptrott *et al* developed a flow cytometric method to investigate the protein binding characteristics of SDNs. In order facilitate detection, 1,1'-dioctadecyl-3,3,3',3'-tetramethylindodi-carbocyanine perchlorate (DiD) was incorporated into the SDNs. This method was adapted to investigate the uptake of DiD labeled SDNs.

Cells were seeded on pre-collagenated 6 well plates at a density of $2x10^6$/ml and allowed to adhere overnight. Medium was aspirated and replaced with 1ml fresh

medium containing dynasore (100μM), indomethacin (100μM) or cytochalasin B (5μM) and incubated for 30 minutes. Following incubation, medium was aspirated and replaced with fresh medium containing 10μM of SDN formulated efavirenz containing 1% DiD or dissolved SDN DiD particles (dissolved in 50% H_2O and 50% MeOH). The DiD labeled SDNs were made as described in section 3.2.3 with the exception of 69% efavirenz and 1% DiD replacing 70% efavirenz (174). Cells were incubated at 37°C in 5% CO_2 in the presence of the drugs for 1 hour. Following 1 hour incubation, medium was aspirated and cells were then washed 3 times with ice-cold HBSS. Following washes, 1ml of trypsin was added to the cells, then incubated at 37°C in 5% CO_2 for 15 minutes. The cells were then aspirated and transferred to 1.5ml Eppendorf tubes. Samples were then centrifuged at 2000rpm for 5 minutes at 10°C. The trypsin was aspirated and the cell pellet was re-suspended in 500μl of Macs buffer for analysis by flow cytometer.

5.2.7 Statistics

All data were assessed for normality using the Shapiro-Wilk test. Statistical analysis was performed by unpaired t test or Mann-Whitney U test and significance was defined as $P < 0.05$ (calculated in SPSS v21). All data are given as mean with standard deviation. IC_{50} values were calculated in Prism v6.0.

5.3 Results

5.3.1 MTT

Prior to accumulation studies, it was necessary to determine the concentrations of efavirenz, SDN efavirenz and the various inhibitors that did not affect cell viability. To assess the cellular toxicity of the compounds used in accumulation studies, a concentration range of each drug was assessed using the MTT assay. The MTT assay is a colorimetric assay measuring the conversion of tetrazolium dye (3-[4,5-Dimethylthiazol-2-yl]-2,5-diphenyltetrazolium bromide) to formazan (measured by increased absorbance at a wavelength of 560nm). The assay is frequently used as a marker of cellular toxicity, as the more cells present, the more metabolic activity is observed (97, 175).

Figure 1 shows the MTT results for the conventional pre-clinical formulation (1A) (1B) and the SDN formulation of efavirenz over the range of 0.19μM to 100μM. The IC_{50} values were 66.8μM (SD 21.3μM) and 57.6μM (SD 6.0μM) for the conventional pre-clinical formulation and SDN formulation of efavirenz, respectively. There was no statistically significant difference observed in IC_{50}, P = 0.49.

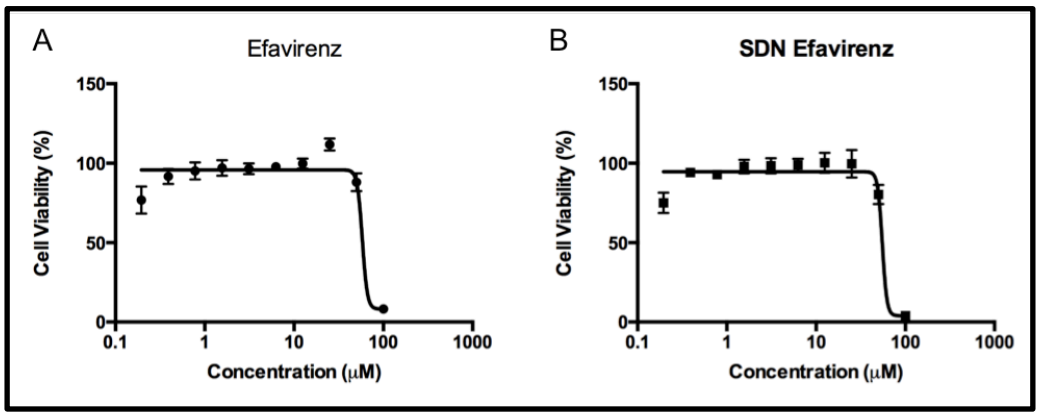

Figure 1 shows the toxicity data produced by MTT for efavirenz (A) and SDN efavirenz (B). Data points represent mean (± SD), N = 4. Also shown is the sigmoidal dose response curve fitted to calculate IC_{50}.

Figure 2 shows the MTT data for the inhibitors of transport proteins (amantadine [A], probenecid [B], verapamil [C], naringin [D], corticosterone [E], montelukast [F], prazosin [G] and cyclosporine A [H]) over the range of 0.98μM to 500μM. The IC_{50} could not be fitted for amantadine, probenecid, verapamil, naringin, corticosterone, montelukast and cyclosporine A as toxicity was not observed at this time point. The IC_{50} of prazosin was shown to be 142.5μM (SD 7.1μM).

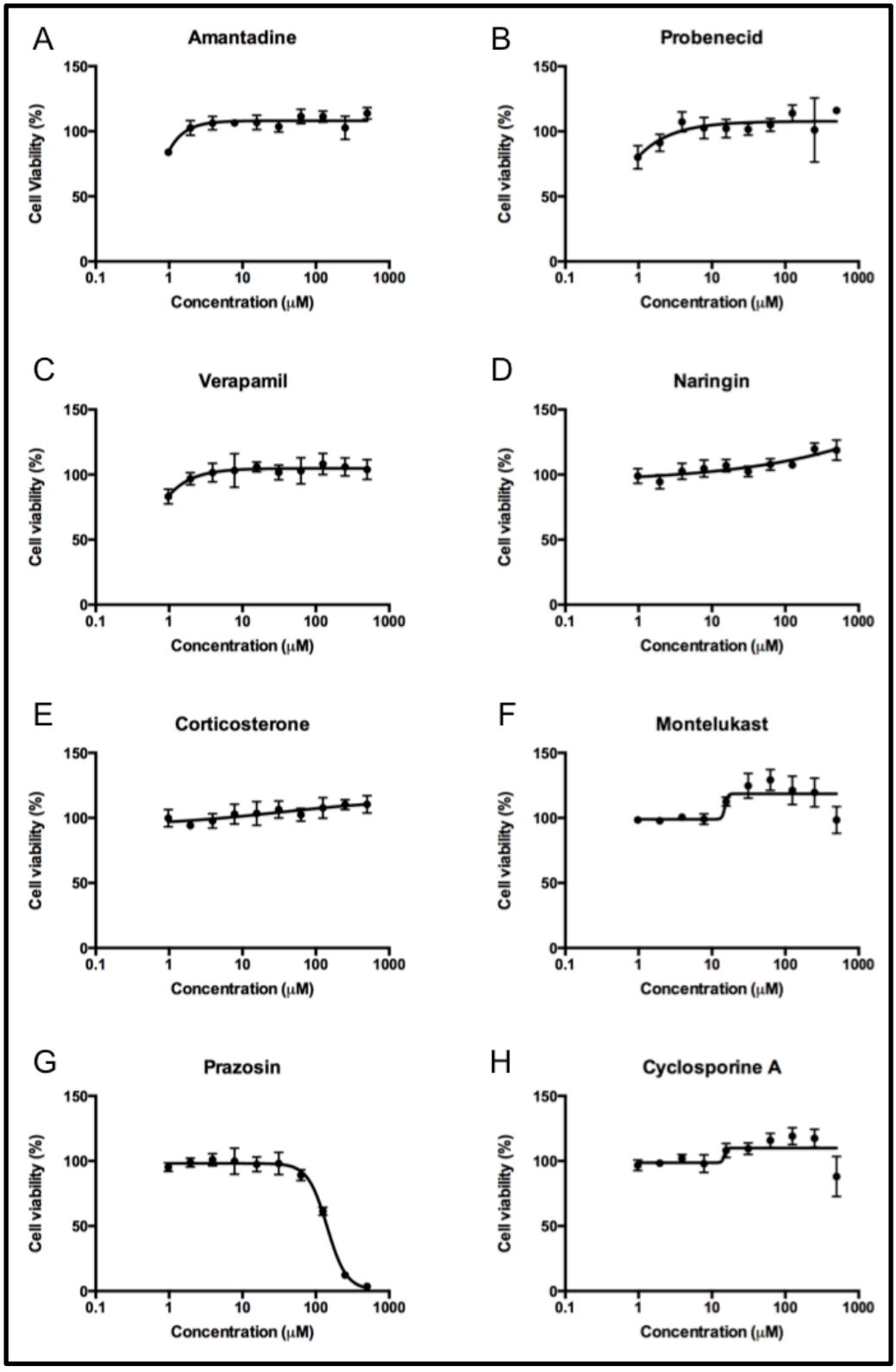

Figure 2 shows the toxicity data produced by MTT for amantadine (A), probenecid (B), verapamil (C), naringin (D), corticosterone (E), montelukast (F), prazosin (G) and cyclosporine A (H). Data points represent mean (± SD), N = 4. Also shown is the sigmoidal dose response curve fitted to calculate IC_{50}.

Figure 3 shows the MTT data for the inhibitors of endocytosis (dynasore [A], indomethacin [B] and cytochalasin B [C]) over the range of 0.39µM to 200µM. The IC_{50} could not be fitted for dynasore and indomethacin, as toxicity was not observed at this time point. The IC_{50} of cytochalasin B was shown to be 12.1µM (SD 5.1µM).

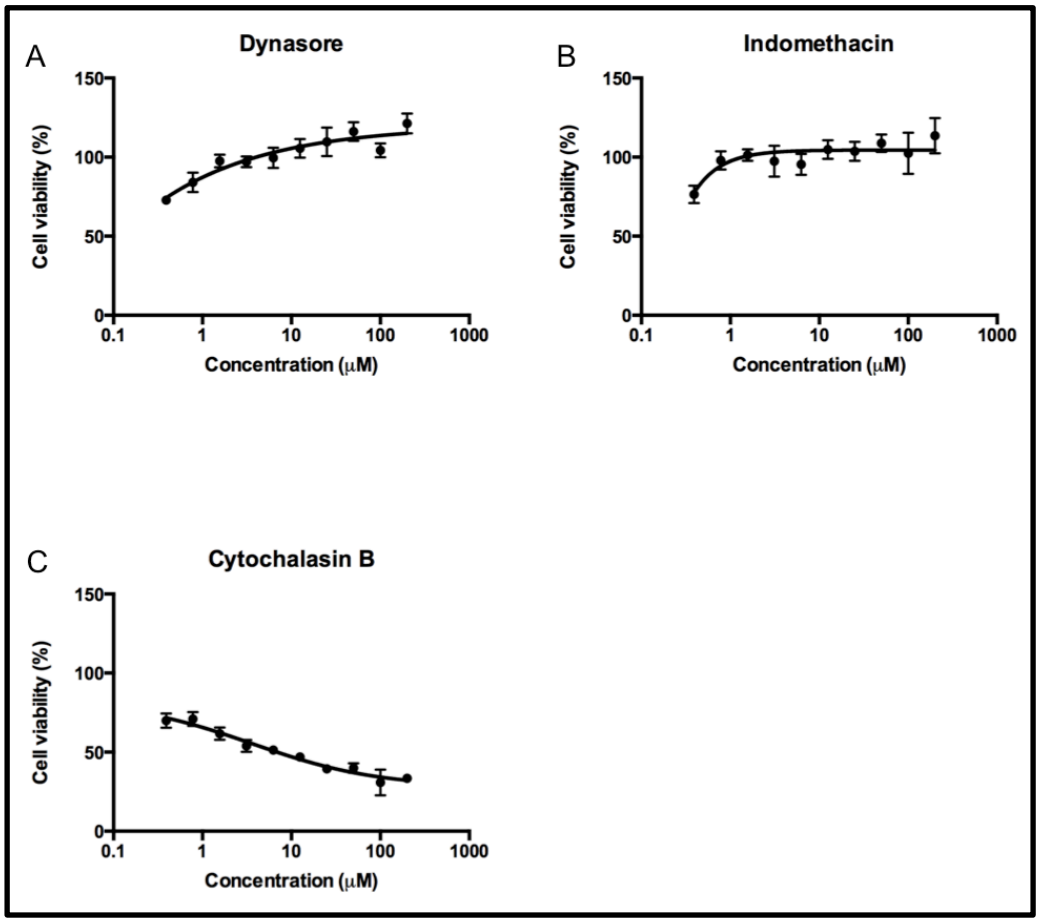

Figure 3 shows the toxicity data produced by MTT for dynasore (A), indomethacin (B) and cytochalasin B (C). Data points represent mean (± SD), N = 4. Also shown is the sigmoidal dose response curve fitted to calculate IC_{50}.

5.3.2 The Effects of Inhibitors of Drug Transporters on Efavirenz Accumulation

Cellular accumulation studies were performed in the hCMEC/D3 cell line, in order to probe the interactions of conventional pre-clinical and SDN formulated efavirenz at the BBB. A panel of transporter inhibitors (Table 1) was employed to probe potential interactions of conventional pre-clinical or SDN formulated efavirenz (Figure 4).

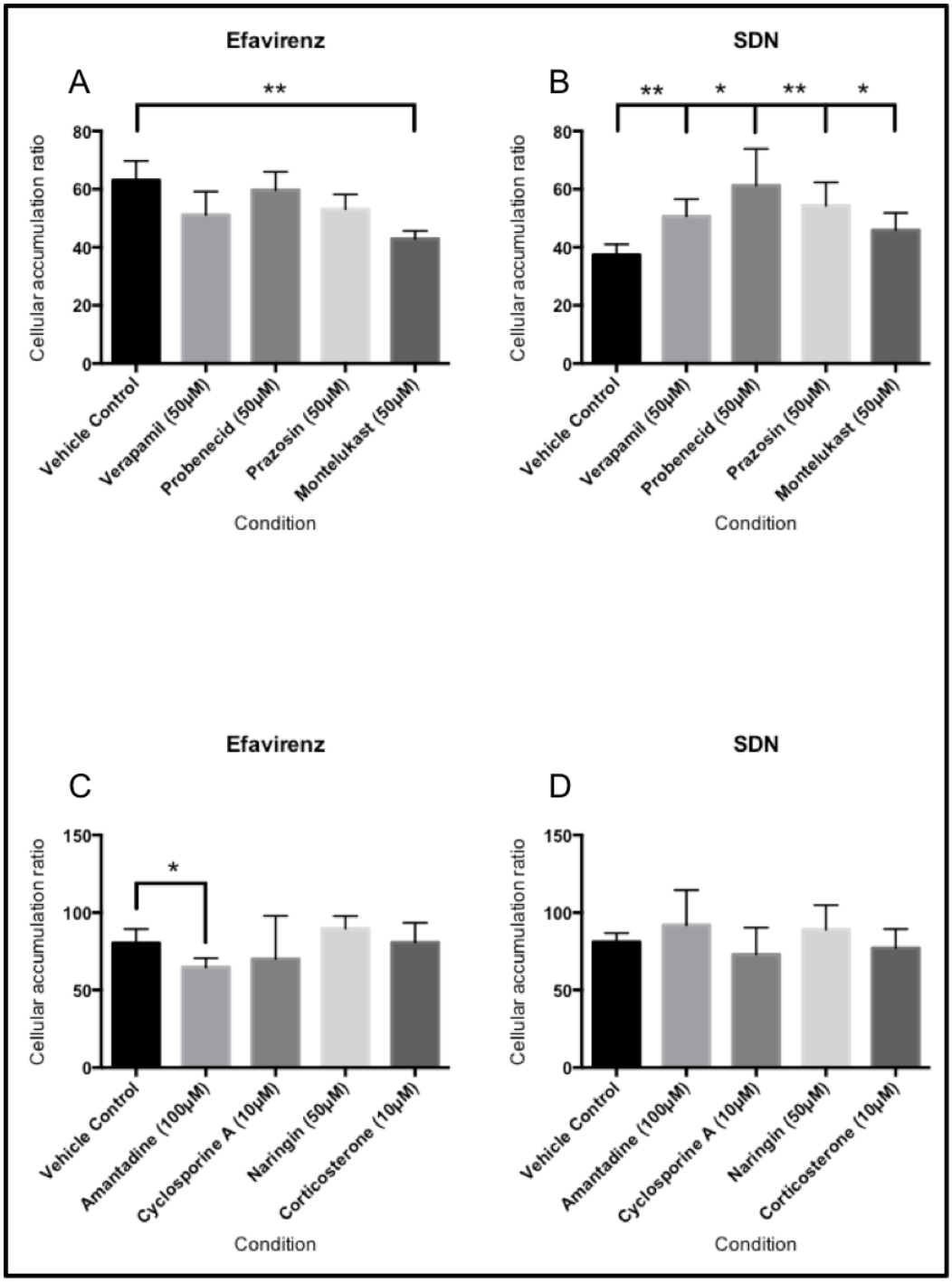

Figure 4 shows the cellular accumulation ratios generated for efavirenz (A and C) and SDN efavirenz (B and D). Also shown are the cellular accumulation ratios in the presence of verapamil, probenecid, prazosin, montelukast (A and B), amantadine, cyclosporine A, naringin and corticosterone (C and D). Data points indicate mean (± SD), N = 4.

The screen of transporter inhibitors demonstrated no effect on the accumulation ratio of the conventional pre-clinical formulation of efavirenz (Table 3) when in the presence of verapamil (CAR 51.08 ±8.1, P = 0.062), probenecid (CAR 59.68 ±6.26, P = 0.485), cyclosporine A (CAR 70.25 ±27.7, P = 0.512) naringin (CAR 89.63 ±8.13, P = 0.179) and corticosterone (CAR 80.84 ±12.54, P = 0.957). The accumulation ratio was significantly reduced in the presence of montelukast (CAR 42.91 ±2.70, P = 0.001) and amantadine (CAR 64.69 ±5.95, P = 0.027). The accumulation ratio of efavirenz was also reduced in the presence of prazosin, trending towards statistical significance (CAR 53.09 ±5.06, P = 0.054).

The accumulation ratio of the SDN formulation of efavirenz was not affected by the presence of amantadine (CAR 91.89 ±22.70, P = 0.396), cyclosporine A (CAR 73.10 ±17.2, P = 0.404), naringin (CAR 89.05 ±15.74, P = 0.384) or corticosterone (CAR 77.23 ±12.16, P = 0.574). The accumulation ratio (Table 4) was significantly increased in the presence of verapamil (CAR 50.65 ±5.89, P = 0.009), probenecid (CAR 61.22 ±12.62, P = 0.011), prazosin (CAR 54.29 ±8.08, P = 0.009) and montelukast (CAR 45.89 ±5.95, P = 0.050).

Condition	Efavirenz	SDN Efavirenz
Vehicle Control	63.1 (6.61)	37.4 (3.71)
Verapamil	51.1 (8.10)	50.7 (5.91)
Probenecid	59.7 (6.31)	61.2 (12.62)
Prazosin	53.1 (5.12)	54.3 (8.10)
Montelukast	42.9 (2.31)	45.9 (6.10)

Table 3 shows the cellular accumulation ratios generated for efavirenz and SDN efavirenz. Also shown are the cellular accumulation ratios in the presence of verapamil, probenecid, prazosin, montelukast. Data points indicate mean (± SD), N = 4.

Condition	Efavirenz CAR	SDN Efavirenz CAR
Vehicle Control	80.4 (9.02)	81.2 (6.10)
Amantadine	64.69 (6.10)	91.9 (22.70)
Cyclosporine A	70.3 (27.70)	73.1 (17.20)
Naringin	89.6 (8.13)	89.1 (15.74)
Corticosterone	80.8 (12.54)	77.2 (12.16)

Table 4 shows the cellular accumulation ratios generated for efavirenz and SDN efavirenz. Also shown are the cellular accumulation ratios in the presence of amantadine, cyclosporine A, naringin and corticosterone. Data points indicate mean (± SD), N = 4.

5.3.3 The Effects of Inhibitors of Endocytosis on Efavirenz Accumulation

In addition to transport proteins, endocytosis is a potential mechanism for cellular uptake. In order to probe the impact of endocytosis on the uptake of conventional pre-clinical and SDN formulations of efavirenz, a panel of endocytosis inhibitors was screened (Table 2).

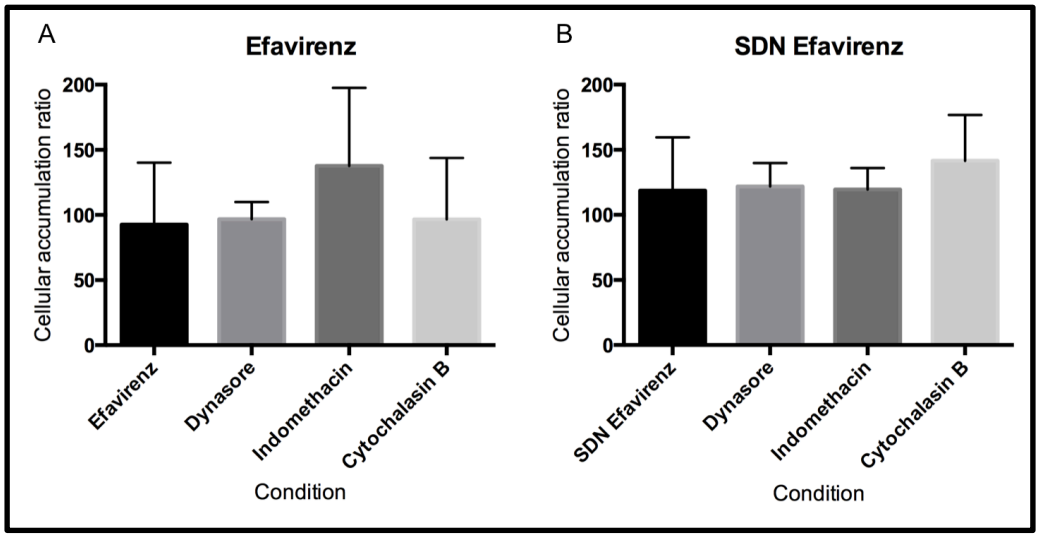

Figure 5 shows the cellular accumulation ratios generated for efavirenz (A) and SDN efavirenz (B). Also shown are the cellular accumulation ratio in the presence of dynasore, indomethacin and cytochalasin B. Data points indicate mean (± SD).

The screen of endocytosis inhibitors demonstrated no effect on the accumulation ratio of either the pre-clinical formulation (CAR 92.65 ±47.41) or SDN formulation (CAR 118.7 ±40.98) of efavirenz when in the presence of dynasore (efavirenz CAR 96.74 ±13.14, P = 0.874, SDN CAR 121.8 ±17.99, P = 0.895), indomethacin (efavirenz CAR 137.6 ±60.04, P = 0.285, SDN CAR 119.4 ±16.5,

P = 0.975) or cytochalasin B (efavirenz CAR 96.53 ±47.18, P = 0.911, SDN CAR 141.4 ±35.44, P = 0.434).

5.3.4 The Effects of Inhibitors of Endocytosis on Nanoparticle Uptake

The addition of the DiD fluorescent dye was used as a marker for SDN uptake in order to determine the effects of endocytosis inhibitors on not only efavirenz uptake but also SDN uptake. The uptake of DiD labeled SDN efavirenz particles (4.02 ±0.86 relative fluorescence units [RFU]) were significantly reduced (Figure 6) by dynasore (0.918 ±0.45 RFU, P = 0.001). Indomethacin had no effect on uptake of DiD labeled SDN efavirenz particles (3.44 ±0.58 RFU, P = 0.307), whereas cytochalasin B significantly increased uptake (5.40 ±0.70 RFU, P = 0.048) (Figure 7).

The uptake of dissolved DiD labeled SDN efavirenz particles (8.75 ±1.14 RFU) was significantly reduced by dynasore (0.43 ±0.13 RFU, P = <0.0001) and indomethacin (4.45 ±0.54 RFU, P = <0.000). Cytochalasin B significantly increased the uptake of dissolved DiD labeled SDN efavirenz particles (12.12 ±0.20 RFU, P = <0.001) (Figure 7).

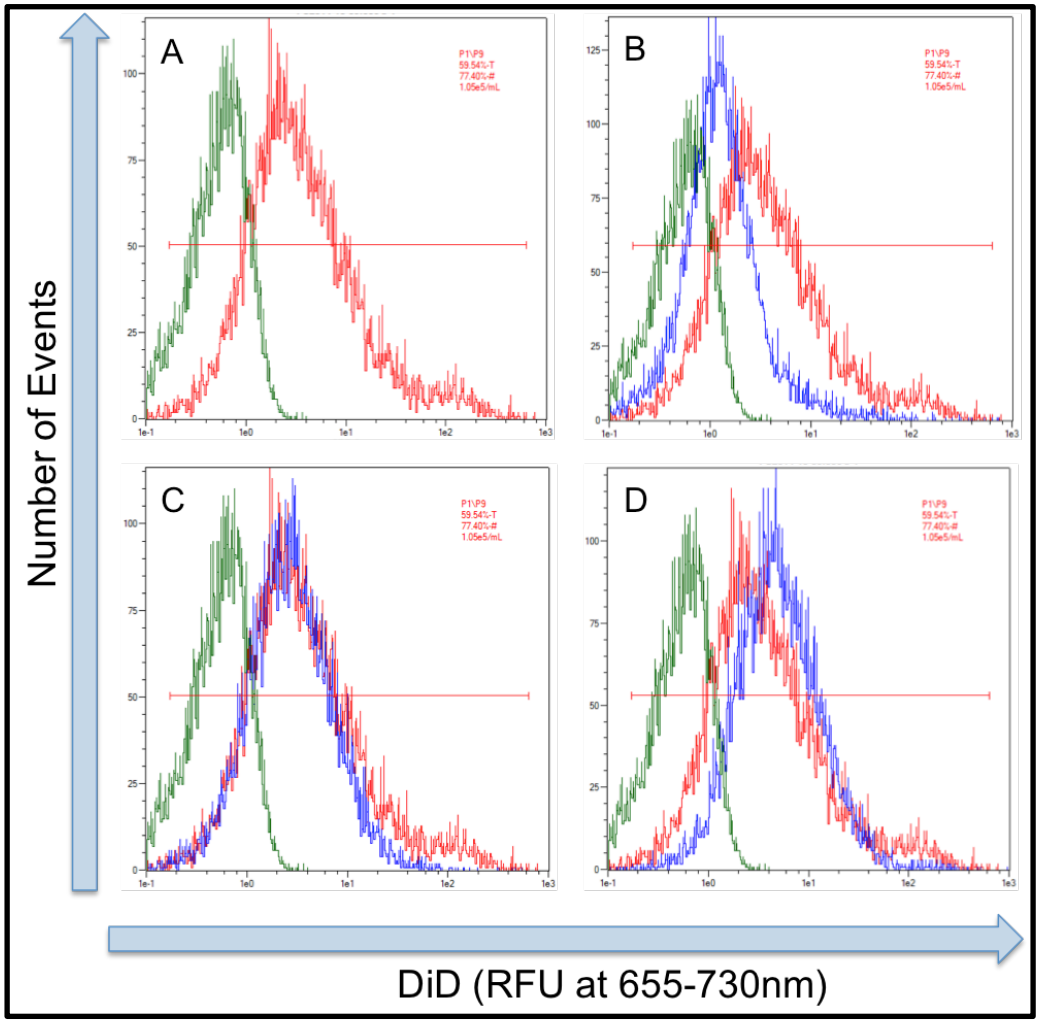

Figure 6 shows a scatter plot of the fluorescence detected at 655-730 nm. The green plot represents untreated cells (A-D). The red plot represents cells treated with SDN DiD (A-D). The blue plot represents the fluorescence in the presence of dynasore (B), indomethacin (C) and cytochalasin B (D).

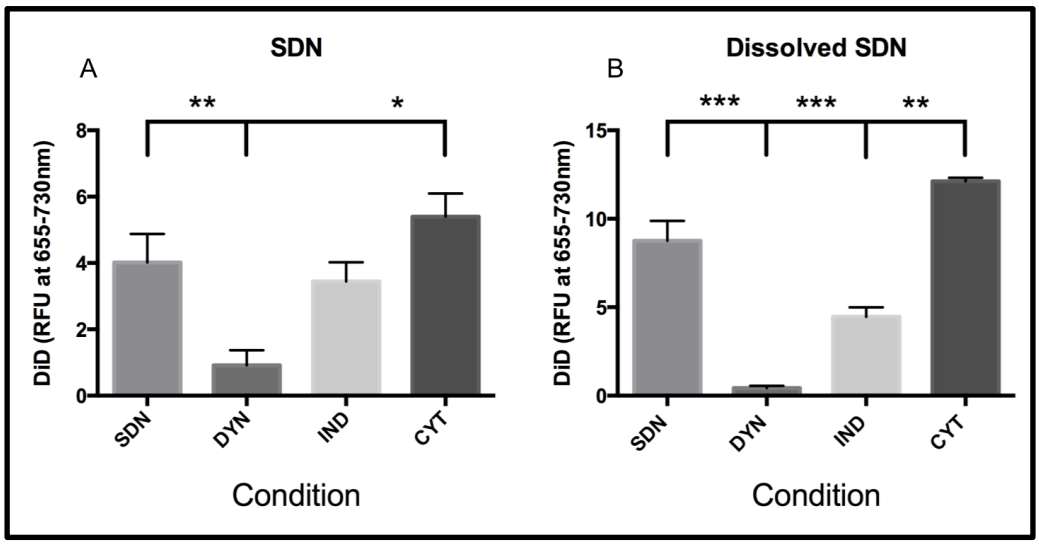

Figure 7 shows the fluorescence produced by cells treated with SDN DiD efavirenz (A) and dissolved SDN DiD efavirenz (B) in the presence of dynasore, indomethacin and cytochalasin B. Data points indicate mean (± SD).

5.4 Discussion

The data presented here demonstrated cellular accumulation of efavirenz was reduced significantly by montelukast and amantadine, with the reduction in accumulation by prazosin bordering on significance. Montelukast and prazosin have been previously shown to inhibit efavirenz accumulation *in vitro*; indicating one of the SLCO transporters may also be involved in the accumulation of efavirenz (157, 176). However, previous data demonstrated no interaction between efavirenz and SLCO1A2, SLCO1B1 or SLCO1B3 indicating a role of other transporters inhibited by montelukast (159, 160). The data also indicated the SDN formulation may interact with verapamil, probenecid, prazosin and montelukast. However, these data may be compromised due to low accumulation of the control in this experiment. The SDN formulation procedure generates particles in the size range of 322 ± 29nm. As described in section 5.1, particles of this size activate endocytosis and nanoformulation has been used previously to reduce the impact of the transporter, BCRP on drug uptake (161, 163). Further studies are required to fully elucidate the interactions of both the conventional pre-clinical and SDN formulations of efavirenz.

The experiments utilising the endocytosis inhibitors provided some conflicting data. When the drug accumulation ratio was examined, the endocytosis inhibitors had no effect on either the pre-clinical conventional formulation or the SDN formulation of efavirenz. Interestingly, uptake of the DiD labelled SDNs was reduced by dynasore, indicating a role for dynamin-mediated uptake. However, the uptake of the dissolved DiD labelled SDNs was also reduced by both

dynasore and indomethacin. This may indicate the incomplete dissolution of the SDN particles, or that the dissolution process altered the structure of the SDN particles, enabling uptake via calveoli-dependent endocytosis. The data also demonstrated higher uptake for the dissolved DiD SDN particles. This is not entirely unexpected, as DiD is a lypophilic dye and would be expected to readily pass through the lipid cell wall. This limitation could be resolved by use of a cell impermeable dye, such as propidium iodide (fluorescence only observed when associated with intracellular nucleic acids). Propidium iodide has previously been incorporated into rhodamine B isothiocyanate–labeled silica nanoparticles to indicate cellular uptake (177). These data indicate the importance of measuring both nanoparticle uptake and drug uptake. Although the drug concentrations may be equal in both formulations, the mechanism of cell entry and consequently intracellular fate may be significantly different.

The hCMEC/D3 cell line has been demonstrated to express many of the proteins found in the enterocytes of the BBB, making this cell line a suitable model for probing interactions at the BBB (178). One of the limitations of the hCMEC/D3 cell line, is the incomplete formation of tight junctions (179). The BBB is characterised by the presence of tight junctions, limiting paracellular transport. In order to fully replicate the presence of tight junctions, the hCMEC/D3 cell line require technically demanding and prohibitively expensive culture conditions. It has been demonstrated to reproduce the tight junctions observed *in vivo*, sheer stress induced by a pulsatile flow was required (180). Therefore, although accumulation experiments are useful for identifying potential mechanisms of uptake at the BBB, they do not demonstrate permeability across the BBB.

One of the limitations of investigating transporter interactions in cell lines, is the lack of specificity in pharmacological transport inhibitors. For example Ko143 was thought to be a specific inhibitor for BCRP. However, recently it has been demonstrated that Ko143 also inhibits ABCB1 and ABCC1 (181). Lack of specificity is also a consideration when examining inhibitors of endocytosis (182). In addition to other mechanisms of endocytosis, endocytosis inhibitors have also been shown to influence transport proteins, such as inhibition of ABCC1 by indomethacin (166). Furthermore, cytochalasin B was shown to disrupt actin filaments and increase the intracellular accumulation of doxorubicin via this mechanism. The authors concluded that organisation of actin filaments may play a role in the function of P-gp (183). The conclusions that are drawn here are based on the known interactions of the inhibitors used. It is possible that the transport inhibitors may inhibit other as yet unidentified transporters. Further studies utilising more specific methods (such as knock-down models, small interfering RNA and oocyte uptake experiments) may be utilised in future studies to further elucidate the interactions of efavirenz and transporters.

Another limitation of the experimental design was that all experiments were conducted at 1 hour. This snapshot may not fully represent the mechanisms of uptake. Liptrott *et al* demonstrated that the cellular accumulation ratio of SDN efavirenz varied over 24 hours in THP-1 cells, with highest accumulation achieved within the first hour (184). Repetition of the experiments conducted in this chapter over multiple time points may provide further insight into the

mechanisms of uptake of the conventional pre-clinical and SDN formulations of efavirenz.

The data presented in this chapter indicate that SDN formulated efavirenz may not traverse the BBB via the same mechanisms as the conventional formulation. Amantadine significantly reduced efavirenz uptake, while there was no effect observed with the SDN formulation. Additionally, dynasore reduced the uptake of SDN DiD labelled particles indicating a role of dynamin-mediated endocytosis. Differential mechanisms of uptake by the BBB may impact on the occurrence of CNS toxicity associated with efavirenz.

Chapter 6

Efavirenz is predicted to accumulate in brain tissue: an *in silico, in vitro and in vivo* investigation

Contents

6.1 Introduction

Despite its widespread use, patients receiving efavirenz-containing therapy frequently report CNS disturbances. Symptoms of efavirenz-associated adverse drug reactions (ADRs) occur with a high frequency and can include depression, anxiety, abnormal dreams and hallucinations (65). The majority of patients report development of CNS disorders shortly after commencing efavirenz therapy with symptoms dissipating during the initial months of therapy. A minority of patients continue to experience symptoms for the duration of efavirenz use (66). More recently, efavirenz CNS ADRs have been shown to have more long-term effects (67).

In addition to the negative impact on the quality of the patient's life, CNS ADRs may also lead to a decrease in patient adherence. Poor patient adherence to antiretroviral medication is a major concern with regards to HIV therapy, in particular drugs displaying a low genetic barrier to resistance such as efavirenz (185). The impact of CNS side effects on patient adherence is not clearly defined. Some previous studies indicate that patients demonstrate tolerance to CNS side effects with minimal impact on patient adherence (69, 70). However, a recent study demonstrated 60% of patients reported CNS side effects as the primary reason for discontinuation vs. 3% of patients receiving alternative antiretroviral therapies (67).

There is a paucity of information regarding penetration of efavirenz into brain tissue. Due to impracticalities in obtaining brain tissue from patients, some groups have used concentrations in cerebrospinal fluid CSF as a surrogate for brain concentrations. The majority of pharmacokinetic studies have focused on describing efavirenz plasma concentrations and elucidating genetic factors that contribute to the variability in efavirenz pharmacokinetics or genetic associations to predict patients at risk of developing CNS toxicity (65, 72, 74). However there are a few small studies that investigated efavirenz pharmacokinetics in both plasma and CSF. CSF concentrations have been shown to be much lower (around 0.5%) than plasma. However, even at 0.5% of the plasma concentration efavirenz concentrations in the CSF exceed the IC_{50} of efavirenz for wild type HIV (57).

The appropriateness of CSF concentrations as a surrogate for brain concentrations is currently the subject of debate (54-56). It has been demonstrated in guinea pigs that brain tissue concentrations of nevirapine not only differ from those in the CSF but also vary between brain regions (54). nevirapine uptake was shown to be 0.32 ml/g in the CSF whereas nevirapine uptake was lower in the choroid plexus (0.25 ml/g) and higher in the pituitary (1.61 ml/g) when compared to the CSF (54). Indeed, concentrations within CSF have been shown to vary depending on where the sample was taken for other antiretroviral drugs. Lamivudine has been shown to be 5-fold higher in CSF sampled from the lumbar region compared to ventricular CSF in rhesus monkeys (55). Although there are no comparable data for efavirenz in the literature, these data exemplify the challenges associated with predicting brain tissue concentrations in CSF.

PBPK modelling is a bottom up approach to simulate drug distribution in virtual patients. The approach mathematically describes physiological and molecular processes defining pharmacokinetics, integrating drug-specific properties (such as logP, Caco-2 apparent permeability and affinity for transporters and metabolic enzymes) and patient-specific factors (such as height, weight, gender, organ volumes and blood flow) (104). The model presented here is based on a full body PBPK model, supplemented with a 6-compartment model of the CNS and CSF as previously described (186).

The aim of this investigation was to evaluate efavirenz penetration into the CSF and brain using PBPK modelling. Simulated efavirenz pharmacokinetic data were then compared to available experimental data from rodents and clinical data from humans.

6.2 Materials & Methods

6.2.1 Materials

Male Wistar rats were purchased from Charles River (Oxford, UK). Efavirenz powder (>98% pure) was purchased from LGM Pharma Inc (Boca Raton, USA). All other consumables were purchased from Sigma Aldrich (Dorset, UK).

6.2.2 Animals and treatment

Male Wistar rats (Charles River UK) weighing 180 – 220 g on arrival were used for pharmacokinetic analysis of efavirenz. Food and water were provided *ad libitum*. All animal work was conducted in accordance with the Animals (Scientific Procedures) Act 1986 (ASPA), implemented by the United Kingdom Home Office.

6.2.3 Drug Treatment

Eight male Wistar rats were dosed with efavirenz (10 mg/kg, 2 ml/kg 0.5% methylcellulose in dH_2O) based on individual weight taken prior to dosing. Dosing was administered once daily *via* oral gavage over 5 weeks. The animals were terminated 2 hours after the final dose and blood was collected *via* cardiac puncture. Blood samples were centrifuged at 2000g for 10 minutes at 4°C to separate plasma. Plasma was immediately frozen at -80°C and stored for later

analysis. Brain tissue was also collected and immediately stored at -30°C for analysis.

6.2.4 Rapid Equilibrium Dialysis

The protein binding of efavirenz in brain tissue was performed using rapid equilibrium dialysis (RED) as described by Liu *et al.* (150). Rat brain tissue was homogenised in 2 volumes (W:V) of 1% saline solution. Since efavirenz is highly protein bound, a dilution of brain tissue (10% and 20% brain tissue were prepared with 1% PBS) was used. 200 µl of brain homogenate was spiked with 5000 ng/ml efavirenz and added to the donor chamber. The receiver chamber contained 350 µl of Sorensons buffer. The RED plate (Thermo, UK) was then placed in a shaking incubator for 4 hours at 37°C at 100 rpm. 250 µl were removed from the receiver chamber and frozen at -80°C for analysis. The fraction of drug unbound (fu) in brain tissue was then calculated from the diluted brain tissue using the following formula (187):

$$Undiluted\ fu = \frac{\left(\frac{1}{D}\right)}{\left[\frac{1}{fu(apparent)} - 1\right] + \left(\frac{1}{D}\right)}$$

Where fu = fraction unbound and D = dilution factor.

6.2.5 Sample preparation for bioanalysis

Efavirenz was extracted by protein precipitation. 20µl of IS (lopinavir 1000ng/ml) was added to 100µl of sample, standard or QC which was then treated with 400µl of ACN. Samples were then centrifuged at 4000g for 10 minutes at 4°C. The supernatant fraction was transferred to a fresh glass vial and evaporated, samples were placed in a rotary vacuum centrifuge at 30°C and then reconstituted in 140 µl of H_2O:ACN (60:40). 100µl of the sample was then transferred into 200µl chromatography vials. 5µl of each sample was injected for analysis by LC-MS/MS.

Rat brain tissue was homogenised in 3 volumes (W:V) of plasma for 1 minute at maximum power using a Minilys® homogeniser (Bertin technologies, FR). Extraction was performed using protein precipitation detailed in the previous section. Recovery was tested at 3 levels (400 ng/ml 100 ng/ml and 20 ng/ml). Mean recovery was 95% (SD 8.9) and 91% (SD 7.8) for plasma and brain, respectively. Samples generated from the RED experiment were pre-treated with 20% ACN (PBS and Sorensons buffer were spiked with 20% ACN in order to aid efavirenz solubility in these matrices) and mean recovery was 84% (SD 11.6).

6.2.6 Quantification of Efavirenz

Quantification of efavirenz was achieved utilising the validated LC-MS/MS method described in chapter 4.

6.2.7 PBPK Parameters

The full body PBPK model used here has been previously published using equations from the physB model (Figure 1) (104, 106). The model generates virtual patients based on a statistical description of human anatomy. The model simulates flow rates, organ volumes and other tissue volumes based on anthropometric measures and allometric scaling.

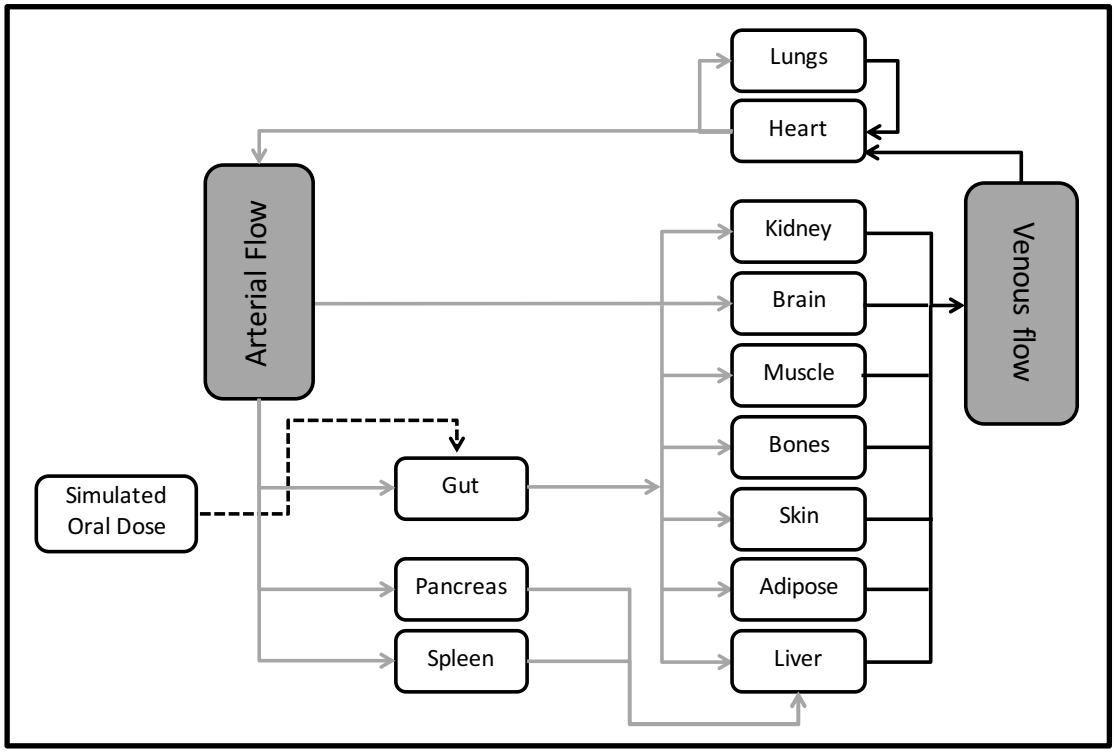

Figure 1 shows a diagram of the full body PBPK model generated from the physB equations.

Briefly, the equations required to simulate factors such as volume of distribution were previously published. Volume of distribution was simulated using the Poulin and Theil equation (188). This method describes the tissue to plasma ratio based on the individual organ volumes generated from the physB equations. Clearance was calculated using allometric scaling of metabolism of efavirenz in microsomes and accounting for activity and abundance of CYP2B6, CYP2A6, CYP1A2, CYP3A4 and CYP3A5, and UGT2B7. Physicochemical properties of efavirenz data (including log P, molecular weight, pKa) and *in vitro* data (permeation across Caco-2 cells and protein binding) were gathered from the literature and incorporated into the full body model (105).

The CNS portion of the model was based on validated parameters describing CNS and CSF physiology and anatomy (186). A schematic of this model is shown in Figure 2. Physiological and physicochemical properties used are displayed in Table 1.

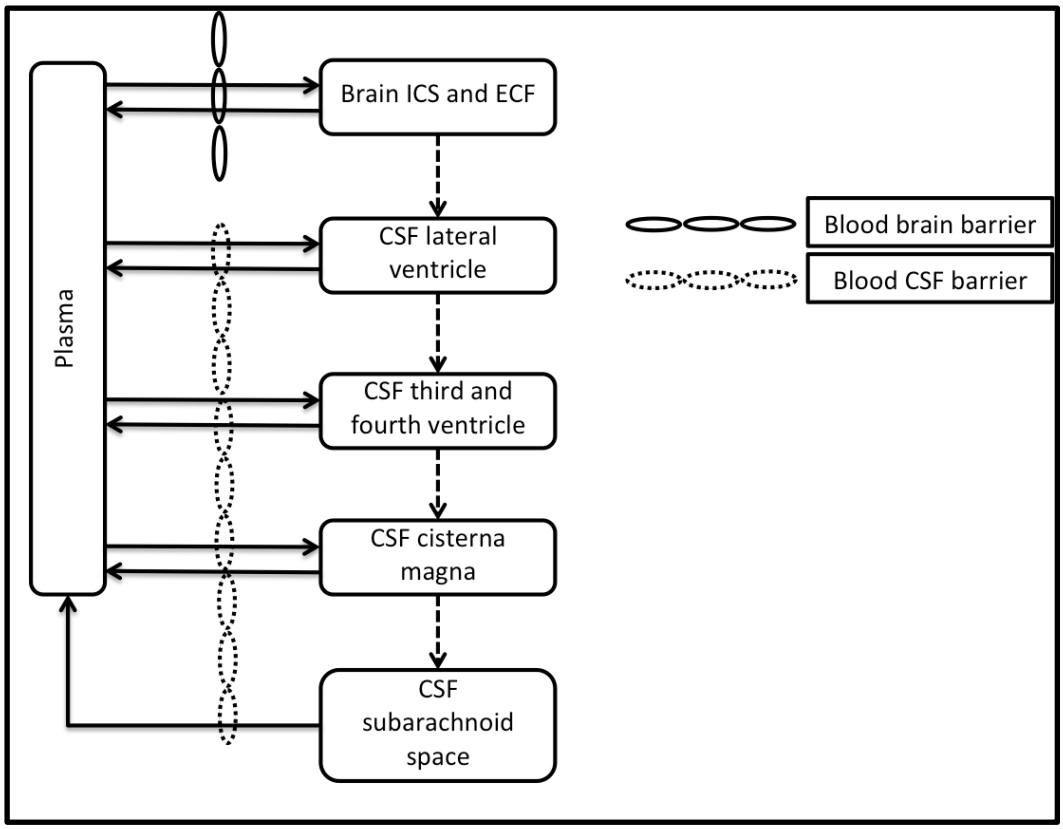

Figure 2 shows a diagram of the CNS component of the PBPK model to describe efavirenz movement within the CNS.

Model Parameter	Value	Reference
Molecular Weight	315.7	Siccardi *et al*, (105)
LogP	4.6	Siccardi *et al*, (105)
pKa	10.2	Siccardi *et al*, (105)
Caco-2 permiability (10^{-6} cm/s)	2.5	Siccardi *et al*, (105)
Fraction unbound		
Plasma	0.01	Almond *et al*, (189)
CSF	0.238	Avery *et al*, (190)
Brain tissue	0.00197	
Qcsf (ml/min)	0.175	Westerhout *et al*, (186)
Qecf (ml/min)	0.4	Westerhout *et al*, (186)
Brain ICS (ml)	960	Westerhout *et al*, (186)
Brain ECF (ml)	240	Westerhout *et al*, (186)
CSF LV (ml)	22.5	Westerhout *et al*, (186)
CSF TFV (ml)	22.5	Westerhout *et al*, (186)
CSF CM (ml)	7.5	Westerhout *et al*, (186)
CSF SAS (ml)	90	Westerhout *et al*, (186)

Table 1 shows the physiological and physicochemical variables used to generate the PBPK model.

The equations used in the model presented here are as follows:

1. $logPS = -2.19 + 0.262\ logD + 0.0583\ vas_{base} - 0.00897\ TPSA$

Equation 1 shows a 3-descriptor QSAR (quantitative structure–activity relationship) model of permeability surface area product (log PS) of the developed by Liu *et al.* (191). The three descriptors are log D (octanol/water partition coefficient at pH 7.4), vas_{base} (van der Waals surface area of the basic atoms) and TPSA (van der Waals polar surface area). Permeability surface area product of the blood CSF barrier (pse) was calculated by dividing the permeability surface area product of the BBB (psb) by 1000, to reflect the smaller surface area of the blood CSF barrier (192).

2. $\frac{\Delta EFV_{Br}}{\Delta t} = psb * \left(\frac{EFV_{Ar} * fu}{R}\right) - EFV_{Br} * fu_{Br} - Q_{ecf} * EFV_{Br} * fu_{Br}$

Equation 2 describes the movement of efavirenz from arterial plasma to the brain where concentration of arterial efavirenz ($efavirenz_{Ar}$), fraction unbound in plasma (fu), blood to plasma ratio (R), concentration of efavirenz in the brain ($efavirenz_{Br}$), flow of brain extracellular fluid (Q_{ecf}), and fraction unbound in brain and (fu_{Br}).

3. $\frac{\Delta EFV_{CSF\,LV}}{\Delta t} = pse * \left(\frac{EFV_{Ve} * fu}{R}\right) - pse * EFV_{LV} * fu_{CSF} - Q_{ecf} * EFV_{Br} * fu_{Br} - Q_{csf} * EFV_{LV}$

4. $\frac{\Delta EFV_{CSF\,TFV}}{\Delta t} = pse * \left(\frac{EFV_{Ve} * fu}{R}\right) - pse * EFV_{TFV} * fu_{CSF} - Q_{csf} * EFV_{LV} - Q_{csf} * EFV_{TFV}$

5. $\frac{\Delta EFV_{CSF\,CM}}{\Delta t} = pse * \left(\frac{EFV_{Ve} * fu}{R}\right) - pse * EFV_{CM} * fu_{CSF} - Q_{CSF} * EFV_{TFV} - Q_{csf} * EFV_{CM}$

6. $\frac{\Delta EFV_{CSF\,SAS}}{\Delta t} = Q_{csf} * EFV_{CM} - Q_{csf} * EFV_{SAS}$

Equations 3 to 6 describe the movement of efavirenz from the brain to CSF, including movement across the blood CSF barrier. The CSF is subdivided into 4 compartments left ventricle (LV), third and fourth ventricle (TFV), cisterna magna (CM) and the subarachnoid space (SAS) where concentration of efavirenz in veins ($efavirenz_{Ve}$), fraction unbound in plasma (fu), blood to plasma ratio (R), concentration of efavirenz in the brain ($efavirenz_{Br}$), concentration of efavirenz in the CSF compartments ($efavirenz_{CSF}$), flow of brain extracellular fluid (Q_{ecf}), flow of CSF (Q_{csf}) fraction unbound in CSF (fu_{CSF}) and fraction unbound in brain and (fu_{Br}).

6.2.8 Simulation Design

A virtual cohort of 100 patients of ages 18 to 60 were generated and a once-daily dose of efavirenz (600 mg) was simulated over 5 weeks. Physiological parameters (such as weight, height and body mass index) were described be Bosgra *et al* (104). The physiological values were the used to generate organ volumes via allometric scaling. Simulations were conducted using SimBiology v4.3.1 (a module of Matlab v8.2). The pharmacokinetics in plasma, CSF and brain tissue were recorded during the final 24 hours at steady state. Plasma and CSF pharmacokinetic simulations were compared with previous data generated from clinical trials. Brain tissue to plasma ratios were also calculated and compared to data generated in rodents.

6.3 Results

The protein binding of efavirenz in brain tissue was determined using rapid equilibrium dialysis. The mean (± SD) concentration of efavirenz detected in the receiver chamber was 209.7 ± 33.4 ng/ml, and 165 ± 22.0 ng/ml 10% and 20% brain homogenate respectively. The fraction unbound in brain tissue (fu_{Br}) was calculated to be 0.00181 and 0.00212 in 10% and 20% brain homogenate, respectively. The average fu_{Br} was 0.00197.

Following 5 weeks of oral dosing of efavirenz (10 mg/kg), the median plasma concentration of efavirenz in rats was 69.7 ng/ml (IQR 44.9 – 130.6). Median efavirenz concentrations in brain tissue were 702.9 ng/ml (IQR 475.5 – 1018.0). The median tissue to plasma ratio was 9.5 (IQR 7.0 – 10.9).

6.3.1 Simulation

A standard dosing schedule of efavirenz (600 mg once daily) was simulated in 100 patients for the duration of 5 weeks. The results for efavirenz concentrations in plasma (Figure 3A), CSF (Figure 3B) and brain tissue (Figure 3C) were all taken from the final 24 hours of the simulation.

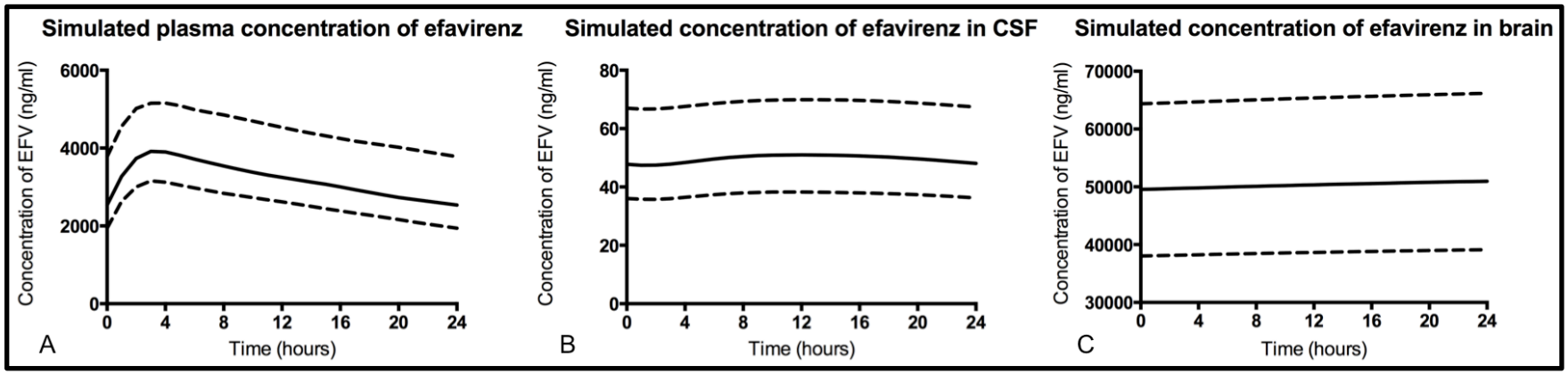

Figure 3 shows the median (solid line) simulated plasma (A), CSF (B) and brain tissue (C) concentrations of efavirenz during the final 24 hours following 5 weeks of once daily efavirenz (600mg). Also shown is the interquartile range (dotted line).

The maximum concentration (C_{max}), minimum concentration (C_{min}) and area under the curve (AUC_{24}) of efavirenz in plasma were 3184 ng/ml (IQR 2219-4851), 2537 ng/ml (IQR 1942-3779) and 76,991 ng.h/ml (IQR 62,170-107,560). The CSF was predicted to have lower concentrations of efavirenz C_{max} 51.0 ng/ml (IQR 38.3-70.0), C_{min} 47.8 ng/ml (IQR 36.1-66.7) and AUC_{24} 1193 ng.h/ml (IQR 898-1649). At 24 hours efavirenz in the CSF was 1.6% of plasma concentrations. The simulation predicted efavirenz concentrations in the brain to exceed CSF and plasma, C_{max} 50,343 ng/ml (IQR 38351-65799) C_{min} 49,566 ng/ml (IQR 38044-64374) and AUC_{24} 1,207,542 ng.h/ml (IQR 926,900-1,567,974). The brain tissue to plasma partition ratio at 24 hours was 15.8.

The absorption constant (K_a) was predicted to be 0.19 h^{-1} (IQR, 0.18-0.21). Volume of distribution (V_{SS}) and clearance (Cl) were predicted to be 2.15 l/kg (IQR 2.06-2.31) 4.56 l/h (IQR 3.52-5.33) respectively. The fraction absorbed (fa) of efavirenz was predicted to be median 0.46 (IQR, 0.44-0.49) and was used to calculate apparent V_{SS} and apparent Cl, 323.31 l (IQR 308.31-346.28) and 9.79 l/h (7.54-11.41) respectively.

6.3.2 Comparison with clinical data

The simulated pharmacokinetic parameters in plasma produced by the model were in agreement with data published from human trials and population pharmacokinetic studies (popPK). Table 2 shows the results from the simulation and a number of clinical studies and popPK studies. The mean/median observed plasma concentrations of efavirenz ranged from 1973 ng/ml to 3180 ng/ml (57,

148, 193-195). Simulated Cl, V_{SS} and K_a were 1.04 fold, 1.28 fold and 0.6 fold different compared to observed data (195). The average simulated CSF concentrations were 49.9 ng/ml (IQR 36.6-69.7) compared to a range of 11.1 ng/ml to 16.3 ng/ml observed in previously published clinical studies (57, 193). It is worth considering that the CSF concentrations were gathered from relatively small cohorts (Best N=80, Yilmaz N=1 and Tashima N=10) and may not fully represent CSF concentrations larger populations. Currently there are no clinical data describing the concentrations of efavirenz in human brain tissue.

	Simulated data		Yilmaz *et al* 2012* (193)	Best *et al* 2011 (57)	Tashima *et al* 1999 (148)	Sánchez *et al* 2011 (194)	Csajka *et al* 2003 (195)
	Mean	Median	Median	Median	Mean	Mean	Mean
Plasma concentration (ng/ml)	3183 (SD ±447)	3184 (IQR 2219-4851)	3718 (range 2439-4952)	2145 (IQR 1384-4423)	1973.8 (range 792.2-2950.9)	3180 (SE ±1610)	
Plasma AUC (ng.h/ml)	91924 (SD ±51619)	76991 (IQR 62170-107560)	86,280				
Apparent Cl ($l\ h^{-1}$)	9.29 (SE ±0.26)	9.79 (IQR 7.54-11.44)				9.61 (SE ±0.38)	9.4 (SE ±0.36)
Apparent V_{SS} ($l\ kg^{-1}$)	329.43 (SE ±2.38)	323.31 (IQR 308.31-346.28)				291 (SE ±44.81)	252 (SE ±35.28)
K_a (h^{-1})	0.20 (SD ±0.02)	0.19 (IQR 0.18-0.21)					0.3 (SE ±0.09)
CSF concentration (ng/ml)	49.9 (SD ±1.2)	49.9 (IQR 36.6-69.7)	16.3 (range 7.3-22.3)	13.9 (IQR 4.1-21.2)	11.1 (range 2.1-18.6)		
CSF AUC (ng.h/ml)	1401 (SD ±809)	1193 (IQR 898-1649)	380				
Brain tissue concentration (ng/ml)	50312.5 (SD ±438)	50343 (IQR 38351-65799)					
Brain tissue AUC (ng.h/ml)	1397820 (SD ±815657)	1207542 (IQR 926900-1567974)					

Table 2 shows the results from the simulation and a number of human trials and popPK studies. * all samples in this study were obtained from a single patient over 24 hours.

6.4 Discussion

The data presented here show that the PBPK model predicts efavirenz to accumulate in the brain. This is to a higher degree than concentrations in the CSF, indeed concentrations of efavirenz in the brain were predicted to exceed even plasma concentrations, with a brain to plasma ratio of 15.8. The rodent data presented here supports the model prediction of a higher concentration of efavirenz in brain tissue, with a median tissue to plasma ratio of 9.5. Recently, efavirenz has been demonstrated to accumulate in the brain tissue of macaques. Following 8 days of orally administered efavirenz (60 mg/kg) the concentrations in plasma and CSF were 541 and 3.30 ng/ml respectively. Concentrations of efavirenz in the cerebellum and basal ganglion were 6.86 μg/g (tissue to plasma ratio 12.7) and 2.01 μg/g (tissue to plasma ratio 3.7), respectively (149).

Accumulation of efavirenz in brain tissue may be driven by physicochemical properties of efavirenz, in particular lipophilicity. Since efavirenz is a highly lipophilic compound (logP 4.6) and has high accumulation in multiple cell types, it shows high cellular permeation (105). The brain has been shown to have a high fat content, with approximately 60% of the brain consisting of fat, providing a lipophilic environment for efavirenz (196). An additional factor that favours penetration is the high degree of protein binding of efavirenz. In plasma, efavirenz is highly protein bound (fu 0.01) (189). Protein binding in the CSF is much lower leading to more free efavirenz, fu 0.238 (190). The data presented here from rapid equilibrium dialysis shows efavirenz fu in rodent brain tissue to be 0.00197. Further experimentation is required to define the factors determining

efavirenz accumulation in the CNS however, further *in silico* experiments may also identify important factors. By performing sensitivity analyses on each of the model parameters (e.g. fu_{Br}, blood brain barrier permeability and blood CSF barrier permeability), simulations can be designed to identify the impact of each factors identifying which variables have the greatest influence on efavirenz CNS accumulation. Taken collectively, it is tempting to speculate that a combination of low fu and affinity for the lipophilic environment of the brain result in accumulation of efavirenz in the CNS. Lypophilicity has been shown to be a significant factor in uptake of drugs into the brain (51) as has been demonstrated with benzodiazepines. Lypophilicity, but not plasma protein binding, was shown to correlate with uptake of benzodiazepines into the brain. However, this study did not consider fu in the brain and plasma fu may not be a good indicator of brain fu. Kalvass *et al* examined the fu in plasma and brain tissue of 34 drugs covering multiple drug classes. The data presented showed that plasma fu both under and overestimated brain fu depending on the drug (197).

Although this is the first study to employ PBPK modelling to investigate efavirenz penetration into the CNS, PBPK has been used previously to investigate efavirenz dose optimisation, drug-drug interactions and pharmacokinetics in special populations (105, 198).

Limitations of this work include that the presented model does not take into account genetic variability (i.e. *CYP2B6* variants), the brain fu values were generated in rodent brain rather than human brain, the current model is not able

to estimate local concentrations in individual brain regions, and permeability of efavirenz was calculated using a QSAR model of passive permeability which often rely on extrapolated data from animals with important differences to humans (191, 199). However, these aspects could be expanded in future modelling strategies as the necessary input data emerges.

The BBB is highly effective at preventing xenobiotics penetrating the CNS. Tight cellular junctions prevent paracellular transport of drugs and the metabolising enzymes and transport proteins remove drugs from the CNS. As such, another potential limitation of the model that warrants further elaboration is that penetration of efavirenz across the BBB may not be governed purely by passive permeability. The potential influence of influx and efflux transporters was not considered because efavirenz is not classified as substrate of any transporters and effects of transporters on efavirenz pharmacokinetics have not been described. The model presented here potentially may be improved upon in the future if efavirenz is demonstrated to be a substrate for such transporters.

There are numerous studies demonstrating that efavirenz plasma concentrations are associated with the development of CNS toxicity. Additionally, there are a number of studies showing efavirenz readily passes the BBB and is present in CSF. However, both plasma and CSF concentrations indicate that efavirenz is present in brain tissue, the site of CNS ADRs. The simulations presented here indicate both plasma and CSF may underestimate efavirenz exposure within the brain. Limitations associated with obtaining tissue biopsies and paired plasma

and CSF samples from patients make PBPK modelling an attractive tool for estimating such drug distribution.

Chapter 7

General Discussion

Currently, the WHO recommends global treatment of HIV should consist of 1 NNRTI supported by an NRTI backbone (64). The most frequent combination administered is efavirenz, co-administered with tenofovir and emtricitabine. This combination is co-formulated into a single tablet (Atripla), which is administered once daily (26).

Patients receiving efavirenz-containing therapy frequently report CNS disturbances. Symptoms occur with a high frequency and can include depression, anxiety, abnormal dreams and hallucinations (65). The majority of patients report development of CNS disorders shortly after commencing efavirenz, with symptoms dissipating during the initial months of therapy. A minority of patients continue to experience symptoms for the duration of efavirenz-containing therapy (66). More recently however, efavirenz CNS toxicities have been shown to have more long-term (as discussed in section 1.4.1) (67). The mechanisms of efavirenz-associated CNS toxicity are complex and multifactorial. The difficulties in determining the underlying mechanisms of CNS toxicity are further compounded by the paucity of information detailing the distribution of efavirenz in the CNS.

The aims of this thesis were firstly to investigate the underlying mechanism of efavirenz CNS toxicity, and secondly to assess uptake and CNS toxicity of efavirenz and a novel SDN formulation of efavirenz. To investigate the mechanisms of efavirenz-associated CNS toxicity, a cohort of patients were assessed for the association of efavirenz discontinuation and polymorphisms in

the GABAa receptor (chapter 2). Currently, it is not understood how efavirenz enters or is restricted from the CNS. To investigate the mechanisms, a panel of transport inhibitors were screened using the hCMEC/D3 cell line (chapter 5). While plasma and CSF concentrations are published, there is no data on human brain tissue concentrations. Given the importance of the CNS in efavirenz therapy (both as a site of continued HIV replication and CNS side effects), its penetration into the CNS has not been fully characterised. Given the obvious difficulties of obtaining brain tissue samples, PBPK modelling coupled with *in vitro* and *in vivo* techniques were utilised to simulate efavirenz distribution in the CNS (chapter 6).

The interactions of a novel SDN formulation with the CNS were also investigated. As the underlying mechanisms of efavirenz-associated CNS toxicity are currently unknown, the effect of SDN formulation on the occurrence of neurocognitive disturbances was assessed in a rodent model of anxiogenesis (chapter 3). As with efavirenz, the mechanisms of uptake of SDNs into the CNS are currently unknown. To investigate the mechanisms of uptake, a panel of transport and endocytosis inhibitors were screened using the hCMEC/D3 cell line (chapter 5). In order to quantify efavirenz in multiple matrices examined in this thesis, a robust bioanalytical method was required (chapter 4).

Despite being available for prescription for almost 20 years, the underlying mechanisms of CNS toxicities associated with efavirenz are still poorly characterised (26). One of the aims of this thesis was to investigate the role of the

GABAa receptor in the occurrence of efavirenz CNS toxicity. Despite *in silico* evidence (produced during a previous masters course) and *in vitro* data (published by Gatch *et al*), the genotyping of patients failed to support a role of the GABAa receptor (127). As discussed in chapter 2, this may be due to limitations of the study design, or indeed the GABAa receptor playing no part in the aetiology of efavirenz-associated CNS toxicities. The approach used in chapter 2 may not have been optimal in identifying genetic associations with the complex phenotype of efavirenz CNS toxicity. The symptoms observed in efavirenz associated CNS disturbances are potentially due to interactions with multiple receptors. SNPs in a single receptor would need to be very strongly associated with the occurrence of CNS toxicity to be detected by the selection of SNPs. An alternate approach that may be employed in future studies is haplotype tagged SNPs. This approach allows detection of variation in not only candidate genes but also entire gene regions. This allows the examination of larger regions, increasing the potential to identify genetic associations (200). The data presented in this thesis could be built upon with further *in vitro* mechanistic and genetic studies examining the many isoforms of the GABAa receptor but this was beyond the scope of the current analysis (111).

Another source of inter-patient variability may be due to the mechanisms of efavirenz entry into the CNS. The data presented in chapter 5 indicates efavirenz may be a substrate for OCT1 and possibly one of the SLCO transporters. If these interactions are confirmed via further *in vitro* experimentation, genotyping for polymorphisms may contribute to explaining the variation in occurrence of efavirenz CNS toxicity. Additionally, if these interactions are confirmed and

fully characterised (determination of maximum velocity [V_{max}] and Michaelis constant [Km]), they could be used to improve the PBPK model in chapter 6. The current model is forced to assume passive permeation, due to incomplete characterisation of efavirenz interactions with transporters. PBPK modeling would offer the opportunity to assess the clinical relevance of any transporter interaction.

Current human studies indicate that efavirenz shows moderate penetration into the CNS, determined by concentrations in CSF. Plasma concentrations of efavirenz have been shown to vary between 154- and 228-fold greater than those found in CSF (50, 57, 148). The data presented in this thesis demonstrates that CSF concentrations may underestimate the concentrations present in brain tissue, estimated to have a brain to plasma ratio of 15.8. The simulated data was supported by *in vivo* data indicating higher accumulation of efavirenz in the brain tissue (149). These data demonstrate the importance of considering the concentrations of efavirenz in brain tissue, particularly in the scope of CNS toxicity.

The second aim of this thesis was to assess uptake and CNS toxicity of a novel SDN formulation of efavirenz. The data presented indicate the SDN formulation may induce anxiety to a lesser extent than the conventional pre-clinical formulation, whilst displaying superior *in vivo* pharmacokinetics (97). A significant disadvantage of this study was comparing pharmacokinetic data determined following a single dose to behavioural data generated at steady state.

In order to fully interpret these data, the pharmacokinetics must be assessed at steady state. These data, in conjunction with the data presented in chapter 5, indicate the SDN formulation of efavirenz may interact with the CNS via different mechanisms to the conventional pre-clinical formulation of efavirenz.

Chapter 5 investigated the mechanisms of uptake of SDN formulated efavirenz in the hCMEC/D3 cell line. The screen of transport inhibitors indicated the cellular accumulation of the SDN formulation was reduced by verapamil, probenecid, prazosin and montelukast. These data indicate a potential interaction with multiple transporters. However, (as discussed in section 5.4) these data require repetition before any definitive conclusions may be drawn. The transport inhibitors also demonstrated no significant reduction in the CAR of SDN efavirenz in the presence of amantadine, which significantly reduced the CAR of the conventional pre-clinical formulation of efavirenz. These data indicate efavirenz may be a substrate of OCT 1 or 2 and SDN efavirenz may reduce the influence of this interaction. The screen of endocytosis inhibitors indicated that dynamin-mediated uptake may be important for particle uptake but the effect on intracellular drug concentrations is uncertain. Although the data indicated no significant difference in efavirenz intracellular concentrations, the mechanism of uptake may influence the intracellular fate of efavirenz. Further investigations could be planned to investigate the mechanisms of efavirenz uptake and determine the potential impact on systemic distribution and intracellular concentrations.

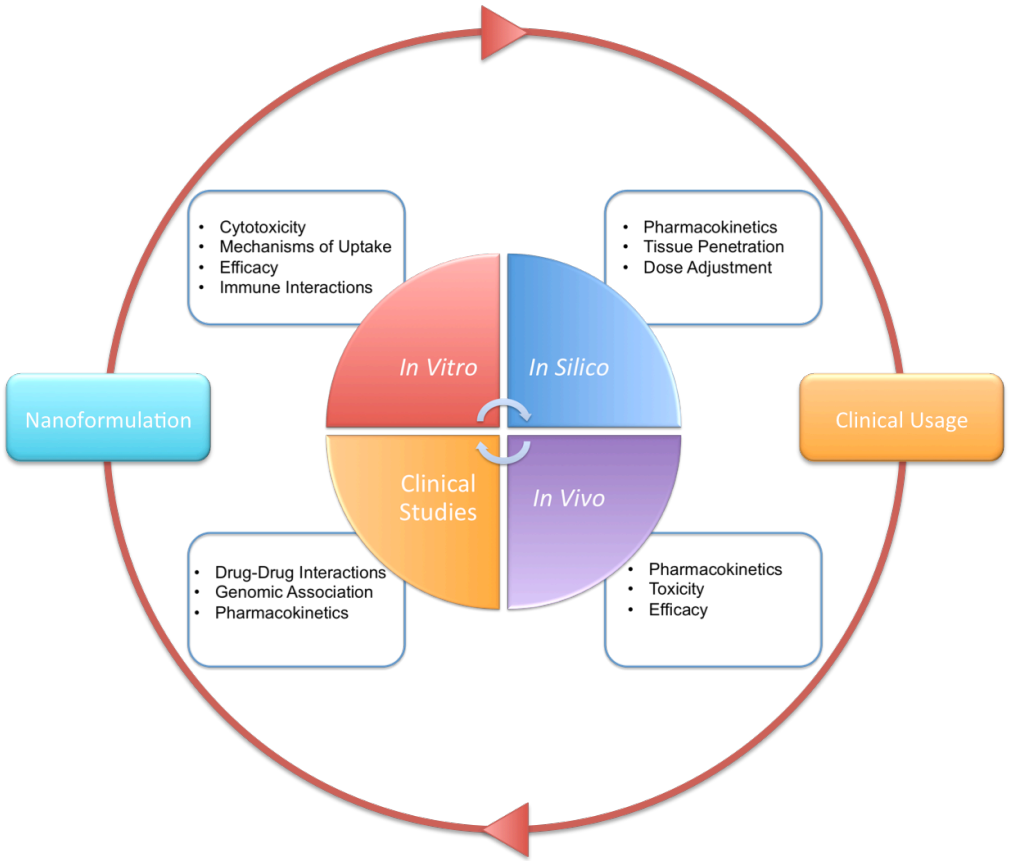

Figure 1 shows a schematic demonstrating how the different approaches used in this thesis may be applied to the generation of novel nanoformulations. Observations from the clinical usage of existing therapeutics can identify opportunities to improve therapy via nanoformulation. The pharmacological assessment of nanoformulations may be broadly divided into 4 areas *in vitro*, *in silico*, *in vivo* and clinical studies (examples of applications are displayed in the associated text boxes). Information gained from each stage may be used to inform subsequent stages. This iterative process can be used to refine a screen of numerous potential formulations to the generation of lead candidates for clinical application.

Although presented in isolation, the work conducted in this thesis forms part of an iterative process that connects drugs available for clinical usage and the generation on novel nanoformulations with bespoke behaviours (Figure 1). Once a need has been identified (in this case to overcome poor water solubility of efavirenz), a screen of potential nanoformulations can be generated to address this issue. The initial formulation process, described by McDonald *et al,* included a screen of 49 polymers and surfactants and characterisation of the properties of the resulting SDN formulations (97).

Following generation of candidates, initial pharmacological assessment (including Caco-2 accumulation, cytotoxicity, transwell permeability, *in vivo* pharmacokinetics and PBPK simulation) lead to the generation of the SDN formulation used in this thesis (97). The work presented in this thesis examined the SDN efavirenz formulation in detail, examining potential interactions with the CNS (chapter 3 and 5). However, all the techniques in this thesis may be applied to the investigation of SDNs of other xenobiotics, or indeed other formulation techniques.

Although the *in vivo* data generated in chapter 3 was specific for examining the CNS toxicity of efavirenz, other appropriate animal models may be used. For example, if nevirapine were to be formulated to produce SDNs, an animal model of hypersensitivity or hepatotoxicity may be more appropriate (201). The screening process detailed in chapter 5 could be adapted to focus on known transporter interactions (e.g. the interactions of lopinavir and transporters such as

P-gp and OATP1B1 are well characterised), or to examine other key anatomical areas of interest (e.g. testis, gut-associated lymphoid tissue and lymph nodes) (83, 202). The PBPK model presented in chapter 6 may be further refined to examine the distribution of SDN formulated efavirenz or indeed other novel formulations, offering the opportunity to predict the impact of various formulation strategies. The data generated at each of these steps may be used to further inform each of the other steps to lead to the further refinement and eventual clinical application of nanoformulated drugs.

To summarise, the data presented in this thesis failed to identify an association with efavirenz treatment discontinuation and polymorphism in the GABAa receptor. However, the evidence presented here is not strong enough to discount interactions with the GABAa receptor completely. Further investigation is required to identify potential interactions. This could be accomplished via *in vitro* assessment of activation or inhibition of the GABAa receptor by efavirenz (using expression of various isoforms of the GABAa receptor in cell lines or *xenopus laevis* oocytes followed by receptor electrophysiology experimentation). Chapter 3 demonstrated the potential of SDN formulation to reduce the impact of anxiogenesis in a rodent model. The key limitation that must be addressed in future studies is that the steady state pharmacokinetics were not assessed. Chapter 5 demonstrated efavirenz might be a substrate for OCT1 and one of the SLCO transporters. Further experimentation is required to confirm and characterise these potential interactions. Additionally, genetic studies may be employed to assess the clinical relevance of the interactions of efavirenz with transporters. Finally, chapter 6 demonstrated *in vivo* and *in silico* accumulation of efavirenz in brain tissue. The model presented in chapter 6 could be further modified (following the relevant *in vitro*, *ex vivo* and *in vivo* experimentation) to investigate the penetration of other drugs, not only into CSF, but also brain tissue. The data presented in this thesis may be built upon to understand the mechanisms governing efavirenz disposition in the CNS and factors influencing the occurrence of CNS toxicity.

References

1. WHO WHO. HIV/AIDS 2015 [updated November 2014; cited 2015 25th March]. Available from: http://www.who.int/features/qa/71/en/.

2. UNAIDS UNPoHA. AIDS by the numbers. 2013.

3. Laskey SB, Siliciano RF. A mechanistic theory to explain the efficacy of antiretroviral therapy. Nature reviews Microbiology. 2014 Sep 29. PubMed PMID: 25263222.

4. Lifson JD, Engleman EG. Role of CD4 in normal immunity and HIV infection. Immunological reviews. 1989 Jun;109:93-117. PubMed PMID: 2475427.

5. Luckheeram RV, Zhou R, Verma AD, Xia B. CD4(+)T cells: differentiation and functions. Clinical & developmental immunology. 2012;2012:925135. PubMed PMID: 22474485. Pubmed Central PMCID: 3312336.

6. Guerro AC, Andretta IB, Bello SL, Trevisol DJ, Schuelter-Trevisol F. Causes of hospital admission of AIDS patients in southern Brazil, 2007 to 2012. Revista da Sociedade Brasileira de Medicina Tropical. 2014 Sep 26;0:0. PubMed PMID: 25271786.

7. Mao Y, Wang L, Gu C, Herschhorn A, Desormeaux A, Finzi A, et al. Molecular architecture of the uncleaved HIV-1 envelope glycoprotein trimer. Proceedings of the National Academy of Sciences of the United States of America. 2013 Jul 23;110(30):12438-43. PubMed PMID: 23757493. Pubmed Central PMCID: 3725050.

8. Turville SG, Arthos J, Donald KM, Lynch G, Naif H, Clark G, et al. HIV gp120 receptors on human dendritic cells. Blood. 2001 Oct 15;98(8):2482-8. PubMed PMID: 11588046.

9. Engelman A, Cherepanov P. The structural biology of HIV-1: mechanistic and therapeutic insights. Nature reviews Microbiology. 2012 Apr;10(4):279-90. PubMed PMID: 22421880. Pubmed Central PMCID: 3588166.

10. Melikyan GB, Markosyan RM, Hemmati H, Delmedico MK, Lambert DM, Cohen FS. Evidence that the transition of HIV-1 gp41 into a six-helix bundle, not the bundle configuration, induces membrane fusion. The Journal of cell biology. 2000 Oct 16;151(2):413-23. PubMed PMID: 11038187. Pubmed Central PMCID: 2192659.

11. Gomez C, Hope TJ. The ins and outs of HIV replication. Cellular microbiology. 2005 May;7(5):621-6. PubMed PMID: 15839891.

12. Ambrose Z, Aiken C. HIV-1 uncoating: connection to nuclear entry and regulation by host proteins. Virology. 2014 Apr;454-455:371-9. PubMed PMID: 24559861. Pubmed Central PMCID: 3988234.

13. Frankel AD, Young JA. HIV-1: fifteen proteins and an RNA. Annual review of biochemistry. 1998;67:1-25. PubMed PMID: 9759480.

14. Schauer GD, Huber KD, Leuba SH, Sluis-Cremer N. Mechanism of allosteric inhibition of HIV-1 reverse transcriptase revealed by single-molecule and ensemble fluorescence. Nucleic acids research. 2015;42(18):11687-96. PubMed PMID: 25232099.

15. Gotte M, Li X, Wainberg MA. HIV-1 reverse transcription: a brief overview focused on structure-function relationships among molecules

involved in initiation of the reaction. Archives of biochemistry and biophysics. 1999 May 15;365(2):199-210. PubMed PMID: 10328813.

16. Roberts JD, Bebenek K, Kunkel TA. The accuracy of reverse transcriptase from HIV-1. Science. 1988 Nov 25;242(4882):1171-3. PubMed PMID: 2460925.

17. Abram ME, Ferris AL, Das K, Quinones O, Shao W, Tuske S, et al. Mutations in HIV-1 reverse transcriptase affect the errors made in a single cycle of viral replication. Journal of virology. 2014 Jul;88(13):7589-601. PubMed PMID: 24760888. Pubmed Central PMCID: 4054409.

18. Craigie R, Bushman FD. HIV DNA integration. Cold Spring Harbor perspectives in medicine. 2012 Jul;2(7):a006890. PubMed PMID: 22762018. Pubmed Central PMCID: 3385939.

19. Ott M, Geyer M, Zhou Q. The control of HIV transcription: keeping RNA polymerase II on track. Cell host & microbe. 2011 Nov 17;10(5):426-35. PubMed PMID: 22100159. Pubmed Central PMCID: 3478145.

20. Kao SY, Calman AF, Luciw PA, Peterlin BM. Anti-termination of transcription within the long terminal repeat of HIV-1 by tat gene product. Nature. 1987 Dec 3-9;330(6147):489-93. PubMed PMID: 2825027.

21. Frankel AD. Activation of HIV transcription by Tat. Current opinion in genetics & development. 1992 Apr;2(2):293-8. PubMed PMID: 1638124.

22. Karn J, Stoltzfus CM. Transcriptional and posttranscriptional regulation of HIV-1 gene expression. Cold Spring Harbor perspectives in medicine. 2012 Feb;2(2):a006916. PubMed PMID: 22355797. Pubmed Central PMCID: 3281586.

23. Yedavalli VS, Jeang KT. Rev-ing up post-transcriptional HIV-1 RNA expression. RNA biology. 2011 Mar-Apr;8(2):195-9. PubMed PMID: 21358275. Pubmed Central PMCID: 3127099.

24. Ono A. HIV-1 Assembly at the Plasma Membrane: Gag Trafficking and Localization. Future virology. 2009;4(3):241-57. PubMed PMID: 19802344. Pubmed Central PMCID: 2676728.

25. Sundquist WI, Krausslich HG. HIV-1 assembly, budding, and maturation. Cold Spring Harbor perspectives in medicine. 2012 Jul;2(7):a006924. PubMed PMID: 22762019. Pubmed Central PMCID: 3385941.

26. FDA. Antiretroviral drugs used in the treatment of HIV infection [cited 2014 13/12/2014]. Available from: http://www.fda.gov/ForPatients/Illness/HIVAIDS/Treatment/ucm118915.htm.

27. WHO WHO. Consolidated Guidelines On The Use Of Antiretroviral Drugs For Treating And Preventing HIV Infection Recommendations For A Public Health Approach 2013 [cited 2015 9th June]. Available from: http://apps.who.int/iris/bitstream/10665/85321/1/9789241505727_eng.pdf.

28. Fryer HR, Frater J, Duda A, Roberts MG, Investigators ST, Phillips RE, et al. Modelling the evolution and spread of HIV immune escape mutants. PLoS pathogens. 2010;6(11):e1001196. PubMed PMID: 21124991. Pubmed Central PMCID: 2987822.

29. Zolopa AR. The evolution of HIV treatment guidelines: current state-of-the-art of ART. Antiviral research. 2010 Jan;85(1):241-4. PubMed PMID: 19883695.

30. Mitsuya H, Weinhold KJ, Furman PA, St Clair MH, Lehrman SN, Gallo RC, et al. 3'-Azido-3'-deoxythymidine (BW A509U): an antiviral agent that inhibits the infectivity and cytopathic effect of human T-lymphotropic virus type III/lymphadenopathy-associated virus in vitro. Proceedings of the National Academy of Sciences of the United States of America. 1985 Oct;82(20):7096-100. PubMed PMID: 2413459. Pubmed Central PMCID: 391317.

31. Cherry CL, Wesselingh SL. Nucleoside analogues and HIV: the combined cost to mitochondria. The Journal of antimicrobial chemotherapy. 2003 May;51(5):1091-3. PubMed PMID: 12668570.

32. Merry C, Barry MG, Mulcahy F, Ryan M, Heavey J, Tjia JF, et al. Saquinavir pharmacokinetics alone and in combination with ritonavir in HIV-infected patients. Aids. 1997 Mar 15;11(4):F29-33. PubMed PMID: 9084785.

33. Flexner C. HIV-protease inhibitors. The New England journal of medicine. 1998 Apr 30;338(18):1281-92. PubMed PMID: 9562584.

34. Imamichi T. Action of anti-HIV drugs and resistance: reverse transcriptase inhibitors and protease inhibitors. Current pharmaceutical design. 2004;10(32):4039-53. PubMed PMID: 15579086.

35. McColl DJ, Chen X. Strand transfer inhibitors of HIV-1 integrase: bringing IN a new era of antiretroviral therapy. Antiviral research. 2010 Jan;85(1):101-18. PubMed PMID: 19925830.

36. Hicks C, Gulick RM. Raltegravir: the first HIV type 1 integrase inhibitor. Clinical infectious diseases : an official publication of the

Infectious Diseases Society of America. 2009 Apr 1;48(7):931-9. PubMed PMID: 19231980.

37. INFO A. FDA-Approved HIV Medicines 2015 [cited 2015 9th February]. Available from: http://aidsinfo.nih.gov/education-materials/fact-sheets/21/58/fda-approved-hiv-medicines.

38. Flexner C, Saag M. The antiretroviral drug pipeline: prospects and implications for future treatment research. Current opinion in HIV and AIDS. 2013 Nov;8(6):572-8. PubMed PMID: 24100879.

39. Henrich TJ, Kuritzkes DR. HIV-1 entry inhibitors: recent development and clinical use. Current opinion in virology. 2013 Feb;3(1):51-7. PubMed PMID: 23290628. Pubmed Central PMCID: 4213740.

40. Lieberman-Blum SS, Fung HB, Bandres JC. Maraviroc: a CCR5-receptor antagonist for the treatment of HIV-1 infection. Clinical therapeutics. 2008 Jul;30(7):1228-50. PubMed PMID: 18691983.

41. Dorr P, Westby M, Dobbs S, Griffin P, Irvine B, Macartney M, et al. Maraviroc (UK-427,857), a potent, orally bioavailable, and selective small-molecule inhibitor of chemokine receptor CCR5 with broad-spectrum anti-human immunodeficiency virus type 1 activity. Antimicrobial agents and chemotherapy. 2005 Nov;49(11):4721-32. PubMed PMID: 16251317. Pubmed Central PMCID: 1280117.

42. Clapham PR, McKnight A. HIV-1 receptors and cell tropism. British medical bulletin. 2001;58:43-59. PubMed PMID: 11714623.

43. Kilby JM, Lalezari JP, Eron JJ, Carlson M, Cohen C, Arduino RC, et al. The safety, plasma pharmacokinetics, and antiviral activity of

subcutaneous enfuvirtide (T-20), a peptide inhibitor of gp41-mediated virus fusion, in HIV-infected adults. AIDS research and human retroviruses. 2002 Jul 1;18(10):685-93. PubMed PMID: 12167274.

44. Rothstein SN, Huber KD, Sluis-Cremer N, Little SR. In vitro characterization of a sustained-release formulation for enfuvirtide. Antimicrobial agents and chemotherapy. 2014;58(3):1797-9. PubMed PMID: 24366751. Pubmed Central PMCID: 3957899.

45. Ene L, Duiculescu D, Ruta S. How much do antiretroviral drugs penetrate into the central nervous system? Journal of medicine and life. 2011;4(4):432.

46. Ballabh P, Braun A, Nedergaard M. The blood-brain barrier: an overview: structure, regulation, and clinical implications. Neurobiology of disease. 2004 Jun;16(1):1-13. PubMed PMID: 15207256.

47. Varatharajan L, Thomas SA. The transport of anti-HIV drugs across blood-CNS interfaces: summary of current knowledge and recommendations for further research. Antiviral research. 2009 May;82(2):A99-109. PubMed PMID: 19176219. Pubmed Central PMCID: 2678986.

48. Abbott NJ, Ronnback L, Hansson E. Astrocyte-endothelial interactions at the blood-brain barrier. Nature reviews Neuroscience. 2006 Jan;7(1):41-53. PubMed PMID: 16371949.

49. Al-Ghananeem AM, Smith M, Coronel ML, Tran H. Advances in brain targeting and drug delivery of anti-HIV therapeutic agents. Expert opinion on drug delivery. 2013 Jul;10(7):973-85. PubMed PMID: 23510097.

50. Yilmaz A, Price RW, Gisslen M. Antiretroviral drug treatment of CNS HIV-1 infection. The Journal of antimicrobial chemotherapy. 2012 Feb;67(2):299-311. PubMed PMID: 22160207.

51. Pajouhesh H, Lenz GR. Medicinal chemical properties of successful central nervous system drugs. NeuroRx : the journal of the American Society for Experimental NeuroTherapeutics. 2005 Oct;2(4):541-53. PubMed PMID: 16489364. Pubmed Central PMCID: 1201314.

52. Lipinski CA, Lombardo F, Dominy BW, Feeney PJ. Experimental and computational approaches to estimate solubility and permeability in drug discovery and development settings. Advanced drug delivery reviews. 2001 Mar 1;46(1-3):3-26. PubMed PMID: 11259830.

53. Ghosh C, Gonzalez-Martinez J, Hossain M, Cucullo L, Fazio V, Janigro D, et al. Pattern of P450 expression at the human blood-brain barrier: roles of epileptic condition and laminar flow. Epilepsia. 2010 Aug;51(8):1408-17. PubMed PMID: 20074231. Pubmed Central PMCID: 3386640.

54. Gibbs JE, Gaffen Z, Thomas SA. Nevirapine uptake into the central nervous system of the Guinea pig: an in situ brain perfusion study. The Journal of pharmacology and experimental therapeutics. 2006 May;317(2):746-51. PubMed PMID: 16424147.

55. Blaney SM, Daniel MJ, Harker AJ, Godwin K, Balis FM. Pharmacokinetics of lamivudine and BCH-189 in plasma and cerebrospinal fluid of nonhuman primates. Antimicrobial agents and

chemotherapy. 1995 Dec;39(12):2779-82. PubMed PMID: 8593019. Pubmed Central PMCID: 163029.

56. Shen DD, Artru AA, Adkison KK. Principles and applicability of CSF sampling for the assessment of CNS drug delivery and pharmacodynamics. Advanced drug delivery reviews. 2004 Oct 14;56(12):1825-57. PubMed PMID: 15381336.

57. Best BM, Koopmans PP, Letendre SL, Capparelli EV, Rossi SS, Clifford DB, et al. Efavirenz concentrations in CSF exceed IC50 for wild-type HIV. The Journal of antimicrobial chemotherapy. 2011 Feb;66(2):354-7. PubMed PMID: 21098541. Pubmed Central PMCID: 3019085.

58. Antinori A, Perno CF, Giancola ML, Forbici F, Ippolito G, Hoetelmans RM, et al. Efficacy of cerebrospinal fluid (CSF)-penetrating antiretroviral drugs against HIV in the neurological compartment: different patterns of phenotypic resistance in CSF and plasma. Clinical infectious diseases : an official publication of the Infectious Diseases Society of America. 2005 Dec 15;41(12):1787-93. PubMed PMID: 16288405.

59. Capparelli EV, Holland D, Okamoto C, Gragg B, Durelle J, Marquie-Beck J, et al. Lopinavir concentrations in cerebrospinal fluid exceed the 50% inhibitory concentration for HIV. Aids. 2005 Jun 10;19(9):949-52. PubMed PMID: 15905676.

60. Best BM, Letendre SL, Koopmans P, Rossi SS, Clifford DB, Collier AC, et al. Low cerebrospinal fluid concentrations of the nucleotide HIV reverse transcriptase inhibitor, tenofovir. Journal of acquired immune

deficiency syndromes. 2012 Apr 1;59(4):376-81. PubMed PMID: 22217676. Pubmed Central PMCID: 3299895.

61. Letendre S. Central nervous system complications in HIV disease: HIV-associated neurocognitive disorder. Topics in antiviral medicine. 2011;19(4):137.

62. Williams DW, Calderon TM, Lopez L, Carvallo-Torres L, Gaskill PJ, Eugenin EA, et al. Mechanisms of HIV entry into the CNS: increased sensitivity of HIV infected CD14+CD16+ monocytes to CCL2 and key roles of CCR2, JAM-A, and ALCAM in diapedesis. PloS one. 2013;8(7):e69270. PubMed PMID: 23922698. Pubmed Central PMCID: 3724935.

63. Brew BJ, Gray L, Lewin S, Churchill M. Is specific HIV eradication from the brain possible or needed? Expert opinion on biological therapy. 2013 Mar;13(3):403-9. PubMed PMID: 23289898.

64. WHO WHO. Antiretroviral Therapy for HIV Infection in Adults and Adolescents: Recommendations for a Public Health Approach: 2010 Revision. WHO Guidelines Approved by the Guidelines Review Committee. Geneva2010.

65. Sanchez Martin A, Cabrera Figueroa S, Cruz Guerrero R, Hurtado LP, Hurle AD, Carracedo Alvarez A. Impact of pharmacogenetics on CNS side effects related to efavirenz. Pharmacogenomics. 2013 Jul;14(10):1167-78. PubMed PMID: 23859571.

66. Vrouenraets SM, Wit FW, van Tongeren J, Lange JM. Efavirenz: a review. Expert opinion on pharmacotherapy. 2007 Apr;8(6):851-71. PubMed PMID: 17425480.

67. Leutscher PD, Stecher C, Storgaard M, Larsen CS. Discontinuation of efavirenz therapy in HIV patients due to neuropsychiatric adverse effects. Scandinavian journal of infectious diseases. 2013 Aug;45(8):645-51. PubMed PMID: 23427878.

68. Jayaweera D, Dilanchian P. New therapeutic landscape of NNRTIs for treatment of HIV: a look at recent data. Expert opinion on pharmacotherapy. 2012 Dec;13(18):2601-12. PubMed PMID: 23176566.

69. Fumaz CR, Tuldra A, Ferrer MJ, Paredes R, Bonjoch A, Jou T, et al. Quality of life, emotional status, and adherence of HIV-1-infected patients treated with efavirenz versus protease inhibitor-containing regimens. Journal of acquired immune deficiency syndromes. 2002 Mar 1;29(3):244-53. PubMed PMID: 11873073.

70. Perez-Molina JA. Safety and tolerance of efavirenz in different antiretroviral regimens: results from a national multicenter prospective study in 1,033 HIV-infected patients. HIV clinical trials. 2002 Jul-Aug;3(4):279-86. PubMed PMID: 12187501.

71. Ogburn ET, Jones DR, Masters AR, Xu C, Guo Y, Desta Z. Efavirenz primary and secondary metabolism in vitro and in vivo: identification of novel metabolic pathways and cytochrome P450 2A6 as the principal catalyst of efavirenz 7-hydroxylation. Drug metabolism and disposition: the biological fate of chemicals. 2010 Jul;38(7):1218-29. PubMed PMID: 20335270. Pubmed Central PMCID: 2908985.

72. Wyen C, Hendra H, Siccardi M, Platten M, Jaeger H, Harrer T, et al. Cytochrome P450 2B6 (CYP2B6) and constitutive androstane receptor (CAR) polymorphisms are associated with early discontinuation of

efavirenz-containing regimens. The Journal of antimicrobial chemotherapy. 2011 Sep;66(9):2092-8. PubMed PMID: 21715435.

73. Tozzi V. Pharmacogenetics of antiretrovirals. Antiviral research. 2010 Jan;85(1):190-200. PubMed PMID: 19744523.

74. Marzolini C, Telenti A, Decosterd LA, Greub G, Biollaz J, Buclin T. Efavirenz plasma levels can predict treatment failure and central nervous system side effects in HIV-1-infected patients. Aids. 2001 Jan 5;15(1):71-5. PubMed PMID: 11192870.

75. Haas D, Ribaudo H, Kim R, Tierney C, Wilkinson G, Gulick R, et al. Pharmacogenetics of efavirenz and central nervous system side effects: an Adult AIDS Clinical Trials Group study. Aids. 2004;18(18):2391.

76. Takahashi M, Ibe S, Kudaka Y, Okumura N, Hirano A, Suzuki T, et al. No observable correlation between central nervous system side effects and EFV plasma concentrations in Japanese HIV type 1-infected patients treated with EFV containing HAART. AIDS research and human retroviruses. 2007;23(8):983-7.

77. Ramana LN, Anand AR, Sethuraman S, Krishnan UM. Targeting strategies for delivery of anti-HIV drugs. Journal of controlled release : official journal of the Controlled Release Society. 2014 Oct 28;192:271-83. PubMed PMID: 25119469.

78. Moss DM, Siccardi M, Murphy M, Piperakis MM, Khoo SH, Back DJ, et al. Divalent metals and pH alter raltegravir disposition in vitro. Antimicrobial agents and chemotherapy. 2012 Jun;56(6):3020-6. PubMed PMID: 22450971. Pubmed Central PMCID: 3370743.

79. Owen A, Pirmohamed M, Khoo SH, Back DJ. Pharmacogenetics of HIV therapy. Pharmacogenetics and genomics. 2006 Oct;16(10):693-703. PubMed PMID: 17001288.

80. Ssemwanga D, Lihana RW, Ugoji C, Abimiku A, Nkengasong J, Dakum P, et al. Update on HIV-1 Acquired and Transmitted Drug Resistance in Africa. AIDS reviews. 2014 Nov 27;17(1). PubMed PMID: 25427100.

81. Rosenbloom DI, Hill AL, Rabi SA, Siliciano RF, Nowak MA. Antiretroviral dynamics determines HIV evolution and predicts therapy outcome. Nature medicine. 2012 Sep;18(9):1378-85. PubMed PMID: 22941277. Pubmed Central PMCID: 3490032.

82. Luber AD. Genetic barriers to resistance and impact on clinical response. MedGenMed : Medscape general medicine. 2005;7(3):69. PubMed PMID: 16369295. Pubmed Central PMCID: 1681671.

83. Cory TJ, Schacker TW, Stevenson M, Fletcher CV. Overcoming pharmacologic sanctuaries. Current opinion in HIV and AIDS. 2013 May;8(3):190-5. PubMed PMID: 23454865. Pubmed Central PMCID: 3677586.

84. Fletcher CV, Staskus K, Wietgrefe SW, Rothenberger M, Reilly C, Chipman JG, et al. Persistent HIV-1 replication is associated with lower antiretroviral drug concentrations in lymphatic tissues. Proceedings of the National Academy of Sciences. 2014 February 11, 2014;111(6):2307-12.

85. L'Homme R, Warris A, Gibb D, Burger D. Children with HIV are not small adults: what is different in pharmacology? Current opinion in HIV and AIDS. 2007 Sep;2(5):405-9. PubMed PMID: 19372919.

86. Calmy A, Hirschel B, Cooper DA, Carr A. A new era of antiretroviral drug toxicity. Antiviral therapy. 2009;14(2):165-79. PubMed PMID: 19430091.

87. Gresele P, Falcinelli E, Momi S, Francisci D, Baldelli F. Highly active antiretroviral therapy-related mechanisms of endothelial and platelet function alterations. Reviews in cardiovascular medicine. 2014;15 Suppl 1:S9-20. PubMed PMID: 24987863.

88. Fernandez-Montero JV, Eugenia E, Barreiro P, Labarga P, Soriano V. Antiretroviral drug-related toxicities - clinical spectrum, prevention, and management. Expert opinion on drug safety. 2013 Sep;12(5):697-707. PubMed PMID: 23730950.

89. Adkins JC, Noble S. Efavirenz. Drugs. 1998 Dec;56(6):1055-64; discussion 65-6. PubMed PMID: 9878993.

90. Baldanti F, Paolucci S, Maga G, Labo N, Hubscher U, Skoblov AY, et al. Nevirapine-selected mutations Y181I/C of HIV-1 reverse transcriptase confer cross-resistance to stavudine. Aids. 2003 Jul 4;17(10):1568-70. PubMed PMID: 12824799.

91. Cavalcante GI, Capistrano VL, Cavalcante FS, Vasconcelos SM, Macedo DS, Sousa FC, et al. Implications of efavirenz for neuropsychiatry: a review. The International journal of neuroscience. 2010 Dec;120(12):739-45. PubMed PMID: 20964556.

92. Siccardi M, Martin P, McDonald TO, Liptrott NJ, Giardiello M, Rannard S, et al. Nanomedicines for HIV therapy. Therapeutic delivery. 2013 Feb;4(2):153-6. PubMed PMID: 23343155.

93. Sharma P, Garg S. Pure drug and polymer based nanotechnologies for the improved solubility, stability, bioavailability and targeting of anti-HIV drugs. Advanced drug delivery reviews. 2010 Mar 18;62(4-5):491-502. PubMed PMID: 19931328.

94. Site BC. [04/12/2014]. Available from: https://tsrlinc.com/resources/services/.

95. Jain S, Sharma JM, Jain AK, Mahajan RR. Surface-stabilized lopinavir nanoparticles enhance oral bioavailability without coadministration of ritonavir. Nanomedicine. 2013 Oct;8(10):1639-55. PubMed PMID: 23351133.

96. Zhou S, Chan E, Lim LY, Boelsterli UA, Li SC, Wang J, et al. Therapeutic drugs that behave as mechanism-based inhibitors of cytochrome P450 3A4. Current drug metabolism. 2004 Oct;5(5):415-42. PubMed PMID: 15544435.

97. McDonald TO, Giardiello M, Martin P, Siccardi M, Liptrott NJ, Smith D, et al. Antiretroviral solid drug nanoparticles with enhanced oral bioavailability: production, characterization, and in vitro-in vivo correlation. Advanced healthcare materials. 2014 Mar;3(3):400-11. PubMed PMID: 23997027.

98. Penn C, Watermeyer J, Evans M. Why don't patients take their drugs? The role of communication, context and culture in patient adherence and the work of the pharmacist in HIV/AIDS. Patient education and counseling. 2011 Jun;83(3):310-8. PubMed PMID: 21474263.

99. Baert L, van 't Klooster G, Dries W, Francois M, Wouters A, Basstanie E, et al. Development of a long-acting injectable formulation

with nanoparticles of rilpivirine (TMC278) for HIV treatment. European journal of pharmaceutics and biopharmaceutics : official journal of Arbeitsgemeinschaft fur Pharmazeutische Verfahrenstechnik eV. 2009 Aug;72(3):502-8. PubMed PMID: 19328850.

100. R Verloes GvK, L Baert, F van Velsen, M-P Bouche, K Spittaels, J Leempoels, P Williams, G Kraus, P Wigerinck, editor TMC278 long acting - a parenteral nanosuspension formulation that provides sustained clinically relevant plasma concentrations in HIV-negative volunteers

. 17th International AIDS Conference

Mexico City; 2008; Mexico City.

101. Spreen WR, Margolis DA, Pottage JC, Jr. Long-acting injectable antiretrovirals for HIV treatment and prevention. Current opinion in HIV and AIDS. 2013 Nov;8(6):565-71. PubMed PMID: 24100877. Pubmed Central PMCID: 3815009.

102. W. Spreen SLF, S. Chen, E. Gould, D. Wilfret, D. Subich, T. Taishi, Z. Hong, editor Pharmacokinetics, safety and tolerability of the HIV integrase inhibitor S/GSK1265744 long acting parenteral nanosus-pension following single dose administration to healthy adults [Abstract no. TUPE040]. 19th International AIDS Conference; 2012; Washington, DC.

103. Moss DM, Siccardi M. Optimizing nanomedicine pharmacokinetics using physiologically based pharmacokinetics modelling. British journal of pharmacology. 2014 Sep;171(17):3963-79. PubMed PMID: 24467481. Pubmed Central PMCID: 4243971.

104. Bosgra S, van Eijkeren J, Bos P, Zeilmaker M, Slob W. An improved model to predict physiologically based model parameters and their inter-individual variability from anthropometry. Critical reviews in toxicology. 2012 Oct;42(9):751-67. PubMed PMID: 22954170.

105. Siccardi M, Almond L, Schipani A, Csajka C, Marzolini C, Wyen C, et al. Pharmacokinetic and pharmacodynamic analysis of efavirenz dose reduction using an in vitro-in vivo extrapolation model. Clinical pharmacology and therapeutics. 2012 Oct;92(4):494-502. PubMed PMID: 22805423.

106. Rajoli RK, Back DJ, Rannard S, Freel Meyers CL, Flexner C, Owen A, et al. Physiologically Based Pharmacokinetic Modelling to Inform Development of Intramuscular Long-Acting Nanoformulations for HIV. Clinical pharmacokinetics. 2015 Jun;54(6):639-50. PubMed PMID: 25523214. Pubmed Central PMCID: 4450126.

107. Jhansi K, Vanita P, Lavanya S, Satya V. A Review on Antidepressant Drugs. Adv Pharmacoepidemiol Drug Saf. 2014;3:R001.

108. Tan KR, Rudolph U, Luscher C. Hooked on benzodiazepines: GABAA receptor subtypes and addiction. Trends in neurosciences. 2011 Apr;34(4):188-97. PubMed PMID: 21353710. Pubmed Central PMCID: 4020178.

109. Pagel J. The neuropharmacology of nightmares. Sleep and Sleep Disorders: Springer; 2006. p. 241-50.

110. Gottesmann C. GABA mechanisms and sleep. Neuroscience. 2002;111(2):231-9.

111. Whiting PJ. GABA-A receptor subtypes in the brain: a paradigm for CNS drug discovery? Drug discovery today. 2003 May 15;8(10):445-50. PubMed PMID: 12801796.

112. Sigel E. Mapping of the benzodiazepine recognition site on GABA-A receptors. Current topics in medicinal chemistry. 2002;2(8):833-9.

113. Moch S. A perspective on Anxiolytics. SA Pharmaceutical Journal. 2009;76(7):20-4.

114. Sanacora G. Cortical inhibition, gamma-aminobutyric Acid, and major depression: there is plenty of smoke but is there fire? Biological psychiatry. 2010;67(5):397.

115. Sieghart W. GABAA receptors: ligand-gated Cl-ion channels modulated by multiple drug-binding sites. Trends in pharmacological sciences. 1992;13:446-50.

116. Arendt G, de Nocker D, von Giesen H, Nolting T. Neuropsychiatric side effects of efavirenz therapy. Expert Opin Drug Saf. 2007;6(2):147-54.

117. Curley P, Schipani A, Egan D, Siccardi M, Wyen C, Fätkenheuer G, et al., editors. Investigation of the potential interactions of efavirenz with the GABAa receptor. Brittish Pharmacological Society Winter Meeting; 2012; London: pA2 online.

118. Villafuerte S, Heitzeg MM, Foley S, Yau WY, Majczenko K, Zubieta JK, et al. Impulsiveness and insula activation during reward anticipation are associated with genetic variants in GABRA2 in a family sample enriched for alcoholism. Molecular psychiatry. 2012 May;17(5):511-9. PubMed PMID: 21483437. Pubmed Central PMCID: 3166450.

119. Lind PA, Macgregor S, Agrawal A, Montgomery GW, Heath AC, Martin NG, et al. The role of GABRA2 in alcohol dependence, smoking, and illicit drug use in an Australian population sample. Alcoholism, clinical and experimental research. 2008 Oct;32(10):1721-31. PubMed PMID: 18727688. Pubmed Central PMCID: 2575093.

120. Uhart M, Weerts EM, McCaul ME, Guo X, Yan X, Kranzler HR, et al. GABRA2 markers moderate the subjective effects of alcohol. Addiction biology. 2013 Mar;18(2):357-69. PubMed PMID: 22501025. Pubmed Central PMCID: 3402582.

121. Pun FW, Zhao C, Lo WS, Ng SK, Tsang SY, Nimgaonkar V, et al. Imprinting in the schizophrenia candidate gene GABRB2 encoding GABA(A) receptor beta(2) subunit. Molecular psychiatry. 2011 May;16(5):557-68. PubMed PMID: 20404824.

122. Balan S, Sathyan S, Radha SK, Joseph V, Radhakrishnan K, Banerjee M. GABRG2, rs211037 is associated with epilepsy susceptibility, but not with antiepileptic drug resistance and febrile seizures. Pharmacogenetics and genomics. 2013 Nov;23(11):605-10. PubMed PMID: 24061200.

123. Loh EW, Tang NL, Lee DT, Liu SI, Stadlin A. Association analysis of GABA receptor subunit genes on 5q33 with heroin dependence in a Chinese male population. American journal of medical genetics Part B, Neuropsychiatric genetics : the official publication of the International Society of Psychiatric Genetics. 2007 Jun 5;144B(4):439-43. PubMed PMID: 17440936.

124. Genomics L. KASP genotyping technology [cited 2015 29th July]. Available from: http://www.lgcgroup.com/LGCGroup/media/PDFs/Products/Genotyping/KASP-brochure.pdf?ext=.pdf.

125. Rodriguez S, Gaunt TR, Day IN. Hardy-Weinberg equilibrium testing of biological ascertainment for Mendelian randomization studies. American journal of epidemiology. 2009 Feb 15;169(4):505-14. PubMed PMID: 19126586. Pubmed Central PMCID: 2640163.

126. Dhoro M, Zvada S, Ngara B, Nhachi C, Kadzirange G, Chonzi P, et al. CYP2B6*6, CYP2B6*18, Body weight and sex are predictors of efavirenz pharmacokinetics and treatment response: population pharmacokinetic modeling in an HIV/AIDS and TB cohort in Zimbabwe. BMC pharmacology & toxicology. 2015;16:4. PubMed PMID: 25889207. Pubmed Central PMCID: 4405819.

127. Gatch MB, Kozlenkov A, Huang RQ, Yang W, Nguyen JD, Gonzalez-Maeso J, et al. The HIV antiretroviral drug efavirenz has LSD-like properties. Neuropsychopharmacology : official publication of the American College of Neuropsychopharmacology. 2013 Nov;38(12):2373-84. PubMed PMID: 23702798. Pubmed Central PMCID: 3799056.

128. Simen AA, Ma J, Svetnik V, Mayleben D, Maynard J, Roth A, et al. Efavirenz modulation of sleep spindles and sleep spectral profile. Journal of sleep research. 2015 Feb;24(1):66-73. PubMed PMID: 25113527.

129. Ebrahim O, Mazanderani AH. Recent Developments in Hiv Treatment and Their Dissemination in Poor Countries. Infectious disease

reports. 2013 Jun 6;5(Suppl 1):e2. PubMed PMID: 24470966. Pubmed Central PMCID: 3892621.

130. Raffi F, Pozniak AL, Wainberg MA. Has the time come to abandon efavirenz for first-line antiretroviral therapy? The Journal of antimicrobial chemotherapy. 2014 Mar 5. PubMed PMID: 24603962.

131. Romao PR, Lemos JC, Moreira J, de Chaves G, Moretti M, Castro AA, et al. Anti-HIV drugs nevirapine and efavirenz affect anxiety-related behavior and cognitive performance in mice. Neurotoxicity research. 2011 Jan;19(1):73-80. PubMed PMID: 20012242.

132. O'Mahony SM, Myint AM, Steinbusch H, Leonard BE. Efavirenz induces depressive-like behaviour, increased stress response and changes in the immune response in rats. Neuroimmunomodulation. 2005;12(5):293-8. PubMed PMID: 16166808.

133. Manfredi R, Calza L, Chiodo F. Efavirenz versus nevirapine in current clinical practice: a prospective, open-label observational study. Journal of acquired immune deficiency syndromes. 2004 Apr 15;35(5):492-502. PubMed PMID: 15021314.

134. Walf AA, Frye CA. The use of the elevated plus maze as an assay of anxiety-related behavior in rodents. Nature protocols. 2007;2(2):322-8. PubMed PMID: 17406592. Pubmed Central PMCID: 3623971.

135. Sumnall HR, O'Shea E, Marsden CA, Cole JC. The effects of MDMA pretreatment on the behavioural effects of other drugs of abuse in the rat elevated plus-maze test. Pharmacology, biochemistry, and behavior. 2004 Apr;77(4):805-14. PubMed PMID: 15099927.

136. Pellow S, Chopin P, File SE, Briley M. Validation of open:closed arm entries in an elevated plus-maze as a measure of anxiety in the rat. Journal of neuroscience methods. 1985 Aug;14(3):149-67. PubMed PMID: 2864480.

137. Cruz AP, Frei F, Graeff FG. Ethopharmacological analysis of rat behavior on the elevated plus-maze. Pharmacology, biochemistry, and behavior. 1994 Sep;49(1):171-6. PubMed PMID: 7816869.

138. Rodgers RJ, Johnson NJ. Factor analysis of spatiotemporal and ethological measures in the murine elevated plus-maze test of anxiety. Pharmacology, biochemistry, and behavior. 1995 Oct;52(2):297-303. PubMed PMID: 8577794.

139. Fernandes C, File SE. The influence of open arm ledges and maze experience in the elevated plus-maze. Pharmacology, biochemistry, and behavior. 1996 May;54(1):31-40. PubMed PMID: 8728536.

140. File SE. The interplay of learning and anxiety in the elevated plus-maze. Behavioural brain research. 1993 Dec 20;58(1-2):199-202. PubMed PMID: 8136046.

141. McDonald TO, Martin P, Patterson JP, Smith D, Giardiello M, Marcello M, et al. Multicomponent Organic Nanoparticles for Fluorescence Studies in Biological Systems. Adv Funct Mater. 2012 Jun 20;22(12):2469-78. PubMed PMID: WOS:000304860500002. English.

142. Tovar-y-Romo LB, Bumpus NN, Pomerantz D, Avery LB, Sacktor N, McArthur JC, et al. Dendritic spine injury induced by the 8-hydroxy metabolite of efavirenz. The Journal of pharmacology and experimental

therapeutics. 2012 Dec;343(3):696-703. PubMed PMID: 22984227. Pubmed Central PMCID: 3500535.

143. Brandmann M, Nehls U, Dringen R. 8-Hydroxy-efavirenz, the primary metabolite of the antiretroviral drug Efavirenz, stimulates the glycolytic flux in cultured rat astrocytes. Neurochemical research. 2013 Dec;38(12):2524-34. PubMed PMID: 24091996.

144. Food and Drug Administration F. Guidance for Industry Bioanalytical Method Validation 2013 [cited 2015 16th June]. Available from: http://www.fda.gov/downloads/drugs/guidancecomplianceregulatoryinformation/guidances/ucm368107.pdf.

145. Kailasa SK, Wu H-F. Rapid Quantification of Efavirenz in Human Plasma by Electrospray Ionization Tandem Mass Spectrometry. Journal of the Chinese Chemical Society. 2014;61(4):437-41.

146. Olagunju A, Siccardi M, Amara A, Jevtovic D, Kusic J, Owen A, et al. CYP2B6 516G>T (rs3745274) and smoking status are associated with efavirenz plasma concentration in a Serbian cohort of HIV patients. Therapeutic drug monitoring. 2014 Dec;36(6):734-8. PubMed PMID: 24831655.

147. Olagunju A, Bolaji OO, Amara A, Waitt C, Else L, Soyinka J, et al. Development, validation and clinical application of a novel method for the quantification of efavirenz in dried breast milk spots using LC-MS/MS. The Journal of antimicrobial chemotherapy. 2015 Feb;70(2):555-61. PubMed PMID: 25326089.

148. Tashima KT, Caliendo AM, Ahmad M, Gormley JM, Fiske WD, Brennan JM, et al. Cerebrospinal fluid human immunodeficiency virus type 1 (HIV-1) suppression and efavirenz drug concentrations in HIV-1-infected patients receiving combination therapy. The Journal of infectious diseases. 1999 Sep;180(3):862-4. PubMed PMID: 10438381.

149. Thompson CG, Bokhart MT, Sykes C, Adamson L, Fedoriw Y, Luciw PA, et al. Mass spectrometry imaging reveals heterogeneous efavirenz distribution within putative HIV reservoirs. Antimicrobial agents and chemotherapy. 2015 May;59(5):2944-8. PubMed PMID: 25733502. Pubmed Central PMCID: 4394831.

150. Liu X, Van Natta K, Yeo H, Vilenski O, Weller PE, Worboys PD, et al. Unbound drug concentration in brain homogenate and cerebral spinal fluid at steady state as a surrogate for unbound concentration in brain interstitial fluid. Drug metabolism and disposition: the biological fate of chemicals. 2009 Apr;37(4):787-93. PubMed PMID: 19116265.

151. Himmelsbach M. 10 years of MS instrumental developments--impact on LC-MS/MS in clinical chemistry. Journal of chromatography B, Analytical technologies in the biomedical and life sciences. 2012 Feb 1;883-884:3-17. PubMed PMID: 22177236.

152. EMA EMA. Guideline on bioanalytical method validation 2011 [cited 2015 16th June]. Available from: http://www.ema.europa.eu/docs/en_GB/document_library/Scientific_guideline/2011/08/WC500109686.pdf.

153. Winston A, Amin J, Clarke A, Else L, Amara A, Owen A, et al. Cerebrospinal fluid exposure of efavirenz and its major metabolites when

dosed at 400 mg and 600 mg once daily: a randomized controlled trial. Clinical infectious diseases : an official publication of the Infectious Diseases Society of America. 2015 Apr 1;60(7):1026-32. PubMed PMID: 25501988.

154. Owen A, Chandler B, Back DJ. The implications of P-glycoprotein in HIV: friend or foe? Fundamental & clinical pharmacology. 2005 Jun;19(3):283-96. PubMed PMID: 15910652.

155. Marchetti S, Mazzanti R, Beijnen JH, Schellens JH. Concise review: clinical relevance of drug–drug and herb–drug interactions mediated by the ABC transporter ABCB1 (MDR1, P-glycoprotein). The oncologist. 2007;12(8):927-41.

156. Leschziner GD, Andrew T, Pirmohamed M, Johnson MR. ABCB1 genotype and PGP expression, function and therapeutic drug response: a critical review and recommendations for future research. The pharmacogenomics journal. 2007 Jun;7(3):154-79. PubMed PMID: 16969364.

157. Janneh O, Chandler B, Hartkoorn R, Kwan WS, Jenkinson C, Evans S, et al. Intracellular accumulation of efavirenz and nevirapine is independent of P-glycoprotein activity in cultured CD4 T cells and primary human lymphocytes. The Journal of antimicrobial chemotherapy. 2009 Nov;64(5):1002-7. PubMed PMID: 19748977.

158. Peroni RN, Di Gennaro SS, Hocht C, Chiappetta DA, Rubio MC, Sosnik A, et al. Efavirenz is a substrate and in turn modulates the expression of the efflux transporter ABCG2/BCRP in the gastrointestinal

tract of the rat. Biochemical pharmacology. 2011 Nov 1;82(9):1227-33. PubMed PMID: 21803024.

159. Wai San Kwan DM, Ruben Hartkoorn, Enrique Salcedo-Sora, Pat Bray, Saye Khoo, David Back, Andrew Owen, editor Determining the substrate specificity of SLCO1B3 for antiretroviral drugs using a X. laevismodel. Brittish Pharmacological Society Winter Meeting; 2008; London: pA2 online; 2008.

160. Hartkoorn RC, Kwan WS, Shallcross V, Chaikan A, Liptrott N, Egan D, et al. HIV protease inhibitors are substrates for OATP1A2, OATP1B1 and OATP1B3 and lopinavir plasma concentrations are influenced by SLCO1B1 polymorphisms. Pharmacogenetics and genomics. 2010 Feb;20(2):112-20. PubMed PMID: 20051929.

161. Wong HL, Bendayan R, Rauth AM, Xue HY, Babakhanian K, Wu XY. A mechanistic study of enhanced doxorubicin uptake and retention in multidrug resistant breast cancer cells using a polymer-lipid hybrid nanoparticle system. The Journal of pharmacology and experimental therapeutics. 2006 Jun;317(3):1372-81. PubMed PMID: 16547167.

162. Mukherjee S, Ghosh RN, Maxfield FR. Endocytosis. Physiological reviews. 1997 Jul;77(3):759-803. PubMed PMID: 9234965.

163. Canton I, Battaglia G. Endocytosis at the nanoscale. Chemical Society reviews. 2012 Apr 7;41(7):2718-39. PubMed PMID: 22389111.

164. Cleal K, He L, Watson PD, Jones AT. Endocytosis, intracellular traffic and fate of cell penetrating peptide based conjugates and nanoparticles. Current pharmaceutical design. 2013;19(16):2878-94. PubMed PMID: 23140451.

165. Dickens D, Owen A, Alfirevic A, Giannoudis A, Davies A, Weksler B, et al. Lamotrigine is a substrate for OCT1 in brain endothelial cells. Biochemical pharmacology. 2012 Mar 15;83(6):805-14. PubMed PMID: 22227272.

166. Leite DF, Echevarria-Lima J, Calixto JB, Rumjanek VM. Multidrug resistance related protein (ABCC1) and its role on nitrite production by the murine macrophage cell line RAW 264.7. Biochemical pharmacology. 2007 Mar 1;73(5):665-74. PubMed PMID: 17169333.

167. Hayer-Zillgen M, Bruss M, Bonisch H. Expression and pharmacological profile of the human organic cation transporters hOCT1, hOCT2 and hOCT3. British journal of pharmacology. 2002 Jul;136(6):829-36. PubMed PMID: 12110607. Pubmed Central PMCID: 1573414.

168. Gupta A, Dai Y, Vethanayagam RR, Hebert MF, Thummel KE, Unadkat JD, et al. Cyclosporin A, tacrolimus and sirolimus are potent inhibitors of the human breast cancer resistance protein (ABCG2) and reverse resistance to mitoxantrone and topotecan. Cancer chemotherapy and pharmacology. 2006 Sep;58(3):374-83. PubMed PMID: 16404634.

169. Alfirevic A, Durocher J, Elati A, Leon W, Dickens D, Radisch S, et al. Misoprostol-induced fever and genetic polymorphisms in drug transporters SLCO1B1 and ABCC4 in women of Latin American and European ancestry. Pharmacogenomics. 2015 Jun;16(9):919-28. PubMed PMID: 26122863.

170. Kirchhausen T, Macia E, Pelish HE. Use of dynasore, the small molecule inhibitor of dynamin, in the regulation of endocytosis. Methods

in enzymology. 2008;438:77-93. PubMed PMID: 18413242. Pubmed Central PMCID: 2796620.

171. Yumoto R, Nishikawa H, Okamoto M, Katayama H, Nagai J, Takano M. Clathrin-mediated endocytosis of FITC-albumin in alveolar type II epithelial cell line RLE-6TN. American journal of physiology Lung cellular and molecular physiology. 2006 May;290(5):L946-55. PubMed PMID: 16361359.

172. Yao W, Li K, Liao K. Macropinocytosis contributes to the macrophage foam cell formation in RAW264.7 cells. Acta biochimica et biophysica Sinica. 2009 Sep;41(9):773-80. PubMed PMID: 19727526.

173. MacLean-Fletcher S, Pollard TD. Mechanism of action of cytochalasin B on actin. Cell. 1980 Jun;20(2):329-41. PubMed PMID: 6893016.

174. Liptrott NJ, Giardiello M, Hunter JW, Tatham L, Tidbury LR, Siccardi M, et al. Flow cytometric analysis of the physical and protein-binding characteristics of solid drug nanoparticle suspensions. Nanomedicine. 2015 May;10(9):1407-21. PubMed PMID: 25055247.

175. Riss TL, Moravec RA, Niles AL, Benink HA, Worzella TJ, Minor L, et al. Cell Viability Assays. In: Sittampalam GS, Coussens NP, Nelson H, Arkin M, Auld D, Austin C, et al., editors. Assay Guidance Manual. Bethesda (MD)2004.

176. Moss DM, Liptrott NJ, Siccardi M, Owen A. Interactions of antiretroviral drugs with the SLC22A1 (OCT1) drug transporter. Frontiers in pharmacology. 2015;6:78. PubMed PMID: 25914645. Pubmed Central PMCID: 4392609.

177. Neumeyer A, Bukowski M, Veith M, Lehr CM, Daum N. Propidium iodide labeling of nanoparticles as a novel tool for the quantification of cellular binding and uptake. Nanomedicine. 2011 Aug;7(4):410-9. PubMed PMID: 21215331.

178. Weksler B, Romero IA, Couraud PO. The hCMEC/D3 cell line as a model of the human blood brain barrier. Fluids and barriers of the CNS. 2013;10(1):16. PubMed PMID: 23531482. Pubmed Central PMCID: 3623852.

179. Stanimirovic DB, Bani-Yaghoub M, Perkins M, Haqqani AS. Blood-brain barrier models: in vitro to in vivo translation in preclinical development of CNS-targeting biotherapeutics. Expert opinion on drug discovery. 2015 Feb;10(2):141-55. PubMed PMID: 25388782.

180. Cucullo L, Couraud PO, Weksler B, Romero IA, Hossain M, Rapp E, et al. Immortalized human brain endothelial cells and flow-based vascular modeling: a marriage of convenience for rational neurovascular studies. Journal of cerebral blood flow and metabolism : official journal of the International Society of Cerebral Blood Flow and Metabolism. 2008 Feb;28(2):312-28. PubMed PMID: 17609686.

181. Weidner LD, Zoghbi SS, Lu S, Shukla S, Ambudkar SV, Pike VW, et al. The Inhibitor Ko143 Is Not Specific for ABCG2. The Journal of pharmacology and experimental therapeutics. 2015 Sep;354(3):384-93. PubMed PMID: 26148857.

182. Ivanov AI. Pharmacological inhibition of endocytic pathways: is it specific enough to be useful? Methods in molecular biology. 2008;440:15-33. PubMed PMID: 18369934.

183. Takeshita H, Kusuzaki K, Ashihara T, Gebhardt MC, Mankin HJ, Hirasawa Y. Actin organization associated with the expression of multidrug resistant phenotype in osteosarcoma cells and the effect of actin depolymerization on drug resistance. Cancer letters. 1998 Apr 10;126(1):75-81. PubMed PMID: 9563651.

184. NJ Liptrott PM, M Giardiello, T McDonald, S Rannard, A Owen, editor Solid Drug Nanoparticle Dispersions for Improved delivery of Efavirenz to Macrophages. British Pharmacological Society Winter Meeting; 2012; London, UK.

185. Theys K, Camacho RJ, Gomes P, Vandamme AM, Rhee SY, Portuguese HIVRSG. Predicted residual activity of rilpivirine in HIV-1 infected patients failing therapy including NNRTIs efavirenz or nevirapine. Clinical microbiology and infection : the official publication of the European Society of Clinical Microbiology and Infectious Diseases. 2015 Jun;21(6):607 e1-8. PubMed PMID: 25704446.

186. Westerhout J, Ploeger B, Smeets J, Danhof M, de Lange EC. Physiologically based pharmacokinetic modeling to investigate regional brain distribution kinetics in rats. The AAPS journal. 2012 Sep;14(3):543-53. PubMed PMID: 22588644. Pubmed Central PMCID: 3385827.

187. Kalvass JC, Maurer TS. Influence of nonspecific brain and plasma binding on CNS exposure: implications for rational drug discovery. Biopharmaceutics & drug disposition. 2002 Nov;23(8):327-38. PubMed PMID: 12415573.

188. Poulin P, Theil FP. Prediction of pharmacokinetics prior to in vivo studies. 1. Mechanism-based prediction of volume of distribution. Journal

of pharmaceutical sciences. 2002 Jan;91(1):129-56. PubMed PMID: 11782904.

189. Almond LM, Hoggard PG, Edirisinghe D, Khoo SH, Back DJ. Intracellular and plasma pharmacokinetics of efavirenz in HIV-infected individuals. The Journal of antimicrobial chemotherapy. 2005 Oct;56(4):738-44. PubMed PMID: 16141277.

190. Avery LB, Sacktor N, McArthur JC, Hendrix CW. Protein-free efavirenz concentrations in cerebrospinal fluid and blood plasma are equivalent: applying the law of mass action to predict protein-free drug concentration. Antimicrobial agents and chemotherapy. 2013 Mar;57(3):1409-14. PubMed PMID: 23295919. Pubmed Central PMCID: 3591913.

191. Liu X, Tu M, Kelly RS, Chen C, Smith BJ. Development of a computational approach to predict blood-brain barrier permeability. Drug metabolism and disposition: the biological fate of chemicals. 2004 Jan;32(1):132-9. PubMed PMID: 14709630.

192. Pardridge WM. Drug and gene delivery to the brain: the vascular route. Neuron. 2002 Nov 14;36(4):555-8. PubMed PMID: 12441045.

193. Yilmaz A, Watson V, Dickinson L, Back D. Efavirenz pharmacokinetics in cerebrospinal fluid and plasma over a 24-hour dosing interval. Antimicrobial agents and chemotherapy. 2012 Sep;56(9):4583-5. PubMed PMID: 22687515. Pubmed Central PMCID: 3421893.

194. Sanchez A, Cabrera S, Santos D, Valverde MP, Fuertes A, Dominguez-Gil A, et al. Population pharmacokinetic/pharmacogenetic

model for optimization of efavirenz therapy in Caucasian HIV-infected patients. Antimicrobial agents and chemotherapy. 2011 Nov;55(11):5314-24. PubMed PMID: 21896912. Pubmed Central PMCID: 3195031.

195. Csajka C, Marzolini C, Fattinger K, Decosterd LA, Fellay J, Telenti A, et al. Population pharmacokinetics and effects of efavirenz in patients with human immunodeficiency virus infection. Clinical pharmacology and therapeutics. 2003 Jan;73(1):20-30. PubMed PMID: 12545140.

196. Chang CY, Ke DS, Chen JY. Essential fatty acids and human brain. Acta neurologica Taiwanica. 2009 Dec;18(4):231-41. PubMed PMID: 20329590.

197. Kalvass JC, Maurer TS, Pollack GM. Use of plasma and brain unbound fractions to assess the extent of brain distribution of 34 drugs: comparison of unbound concentration ratios to in vivo p-glycoprotein efflux ratios. Drug metabolism and disposition: the biological fate of chemicals. 2007 Apr;35(4):660-6. PubMed PMID: 17237155.

198. Siccardi M, Olagunju A, Seden K, Ebrahimjee F, Rannard S, Back D, et al. Use of a physiologically-based pharmacokinetic model to simulate artemether dose adjustment for overcoming the drug-drug interaction with efavirenz. In silico pharmacology. 2013;1:4. PubMed PMID: 25505649. Pubmed Central PMCID: 4230487.

199. Zimmermann C, van de Wetering K, van de Steeg E, Wagenaar E, Vens C, Schinkel AH. Species-dependent transport and modulation properties of human and mouse multidrug resistance protein 2 (MRP2/Mrp2, ABCC2/Abcc2). Drug Metabolism and Disposition. 2008;36(4):631-40.

200. Pushpakom SP, Owen A, Vilar FJ, Castro H, Dunn DT, Back DJ, et al. Adipogenic gene variants in patients with HIV-associated lipodystrophy. Pharmacogenetics and genomics. 2011 Feb;21(2):76-83. PubMed PMID: 21178827.

201. Popovic M, Shenton J, Chen J, Baban A, Tharmanathan T, Mannargudi B, et al. Nevirapine hypersensitivity. Adverse Drug Reactions. 2010:437-51.

202. Janneh O, Jones E, Chandler B, Owen A, Khoo SH. Inhibition of P-glycoprotein and multidrug resistance-associated proteins modulates the intracellular concentration of lopinavir in cultured CD4 T cells and primary human lymphocytes. The Journal of antimicrobial chemotherapy. 2007 Nov;60(5):987-93. PubMed PMID: 17890284.